Enhancement of immunostimulatory effect of CpG oligodeoxynucleotide by using boron nitride nanospheres

（窒化ホウ素ナノ粒子を用いたCpGオリゴデオキシヌクレオチドの免疫活性化能の向上）

Huijie Zhang

A dissertation submitted in fulfillment of the requirement for the degree of

Doctor of Science

Graduate School of Life Science

Hokkaido University

北海道大学

September 2013

CONTENTS

Chapter 1 Background

1.1 Immune system

We are surrounded by billions of pathogenic microorganisms (bacteria, virus, fungi, and parasites). They threaten us continuously, luckily for us, getting into the human body is not an easy task, because we are equipped with powerful defense mechanisms, the immune system. Our immune system is made up of a complex and vital network of cells and organs that protect the body from infection. It works in a two-step process against the invading pathogenic microorganisms: innate immunity halts the infection, and adaptive immunity subsequently clears it (Figure 1.1).

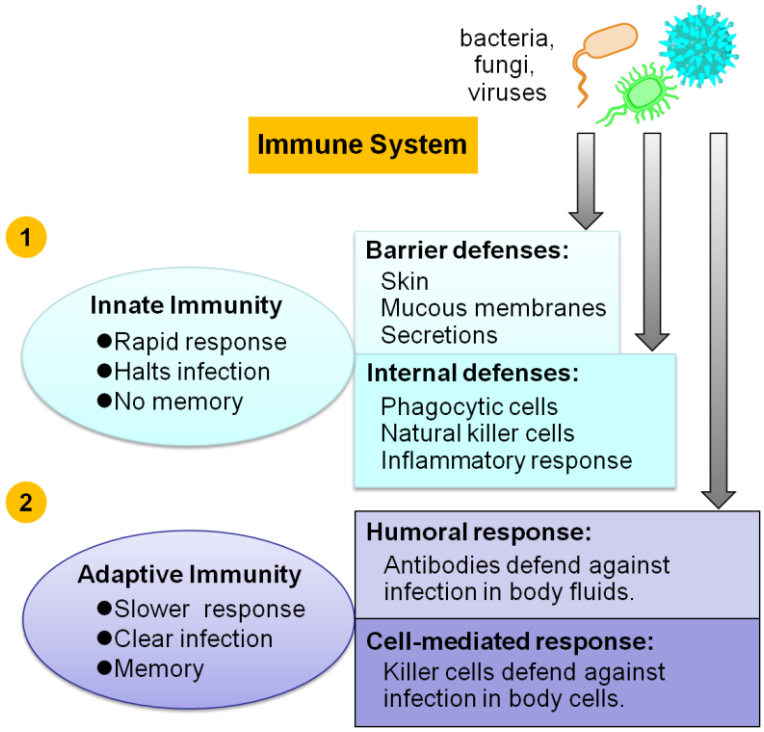

Figure 1.1 The immune system is composed of two major subdivisions, the innate immune system and the adaptive immune system. These two immune systems have different composition and distinct functions during a microorganisms infection.

The first line of defense is innate immunity, which comprises the cells and mechanisms that defend the host from infection by other microorganisms in a non-specific manner. The innate immunity is activated by exposure to pathogen-associated molecular patterns (PAMPs) expressed by a diverse group of infectious microorganisms.[1] Our skin, mucous membranes, and their secretions make up the first line of protection,

which forms a formidable physical barrier to most microorganisms. If the microorganisms penetrate this barrier, the white blood cells are called into action. White blood cells, including phagocytes, macrophages, and natural killer cells, are one of the most important features of innate immunity. They serve the innate immune system by triggering inflammation that eliminating pathogenic threats. [2-3] They can also kill bacteria and viruses. However, the innate immunity does not confer long-lasting or protective immunity to the host but only provides immediate defense against infection.

If microorganisms break through the innate immune system, adaptive immunity starts to work. With its T and B cells, it produces high-affinity antibodies and killer cells that destroy infected cells. After combating the infection, our adaptive immune system maintains an immunologic memory that allows a more rapid and powerful mobilization of defense forces next time the same microorganism attacks. These two defense lines of the immune system provide good protection against infections.

1.2 CpG ODNs

The initial sensing of invading microorganisms is mediated by innate pattern recognition receptors (PRRs) which can recognize the PAMPs.[4] Toll-like receptors (TLRs) are the first identified and best characterized receptors among the PRRs, which recognize a wide range of PAMPs.[5-8] Bacterial DNA containing unmethylated cytosine-phosphate-guanosine (CpG) motifs activate host defense mechanisms leading to innate and adaptive immune responses. These unmethylated CpG motifs are primarily responsible for the immunostimulatory property of bacterial DNA. However, vertebrate DNA lacks this property, as most of the CpG motifs in their DNA are methylated at position 5 of cytosine.[9-10] The innate immune system detects these unmethylated motifs using TLR 9.[11-13] Unmethylated CpG DNA released during an infection provides a ‘danger signal’ to the innate immune system, triggering a protective immune response that improves the ability of the host to eliminate the pathogen.[14] Synthetic Short, single-stranded oligodeoxynucleotides (ODNs) containing unmethylated CpG motifs mimic the bacterial DNA and possess similar immunostimulatory effects. CpG ODNs are stable, inexpensive and easy to produce. This makes them an attractive model to study innate immunity and immunoprotection.[15] The binding of CpG ODNs with TLR 9 initiates an immunostimulatory cascade that induce the maturation, differentiation, and proliferation of multiple immune cells including B and T lymphocytes, natural killer (NK) cells, and

monocytes/macrophage.[16-17] This further triggers cell signaling pathways including mitogen activated protein kinases (MAPKs) and NFκB, subsequently results in the induction of multiple proinflammatory cytokines and chemokines and modulates the cellular inflammatory response.[13,18] These abilities enable CpG ODNs to act as promising immune adjuvant, as well as immunotherapeutic agents against allergy/asthma, cancer, and infectious diseases.[18-21]

1.2.1 CpG ODNs-TLR 9 interaction and cell signaling

While the majority of TLRs recognize PAMPs on the cell surface, the TLR 9 that interacts with CpG ODNs are mainly found intracellularly in the endosome.[22-23] For immunostimulation, CpG ODNs must be internalized intracellularly and be co-localized with TLR 9 in endosome.[24-26] The mechanisms of CpG ODNs uptake in cells remain uncertain. It has been observed that CpG ODNs are taken up into the cell via receptor mediated endocytosis independent of the sequence motif. Furthermore, phosphatidylinositol-3 kinase (PI3K) facilitates this internalization of CpG ODNs into endosomal vesicles where they interacts directly with the TLR 9.[14] The interaction between CpG ODNs and TLR 9 triggers an intracytoplasmic activation signal (Figure 1.2). This signal initiates the recruitment of myeloid differentiation primary response gene 88 (MyD88).[14] MyD88 recruits interleukin (IL)-1 receptor-associated kinase (IRAK) to TLR 9 through interaction of the death domains of both molecules, followed by activation of the IRAK-tumor necrosis factor (TNF) receptor-associated factor (TRAF)-6 complex. TRAF6 activates transforming growth factor-β -activated kinase (TAK) 1. This leads to mitogen-activated protein kinase (MAPK) and inhibitor of nuclear factor (NF)-κB kinase (IKK) complexes, resulting in the upregulation of transcription factors, including NF-κB and activator protein-1 (AP1), which in turn activate production of pro-inflammatory cytokine genes. In pDCs, TRAF activates interferon (IFN) regulatory factor (IRF)-7, which activates type I IFN gene transcription. [27-29]

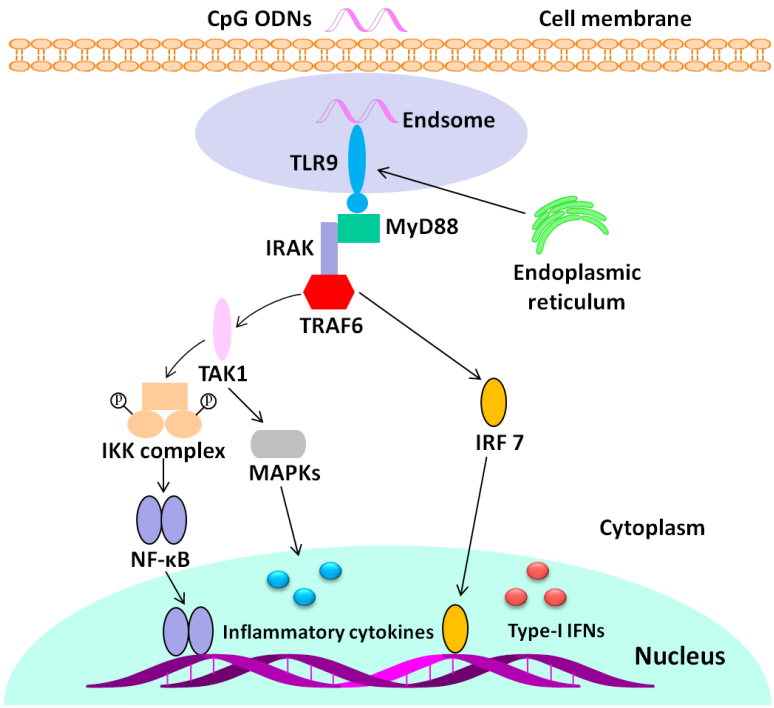

Figure 1.2 CpG ODNs-TLR 9 interaction and cell signaling. CpG ODNs are internalized into endosome and interact with TLR 9. This interaction triggers a MyD88-dependent pathway, leading to the upregulation of NF-κB and IRF-7, which respectively activates production of pro-inflammatory cytokine genes and type I IFN gene.

1.2.2 Immunostimulatory effect of CpG ODNs

The immune system recognizes CpG ODNs using TLR 9. B cells and plasmacytoid dendritic cells (pDCs) are the main human cell types that express TLR 9 and respond directly to CpG ODNs stimulation. CpG ODNs activate these cells and facilitate innate and adaptive immune responses (Figure 1.3). CpG ODNs induce B cells to enter G1 phase of the cell cycle and secrete IL-6, IL-10 and IL-12 through NF-κB and other signal transduction pathways in a few hours.[5,30-33] These cytokines are important to the innate immune system. IL-6 induced by CpG ODNs is required for the B cells to proceed to secrete antibodies.[30] As a result, the production of antibodies is enhanced.[34-35] IL-6 and IL-12 secreted by B cells also play important role in adaptive immune response.

CpG ODNs activate pDCs to secrete cytokines involved in innate immune response, including type I IFN and TNF-α.[36] These pDCs also improve the function of professional antigen-presenting cells (APCs).[14] Furthermore, pDCs activated by CpG ODNs secrete IL-12 and promote the differentiation of T helper (Th) 0 into Th1, as well as inducing Th1 to migrate to B cells.[37-40] CpG ODNs can also induce pDCs to increase the expression of costimulatory molecules CD40, CD80 and CD86.[13,41] B cells that interact with Th1 differentiate into plasma cells, which possess the ability to produce antibodies, playing a central role in adaptive immunity. Also, IFN-α promotes CD8-positive cytotoxic T lymphocyte response.[42-43]

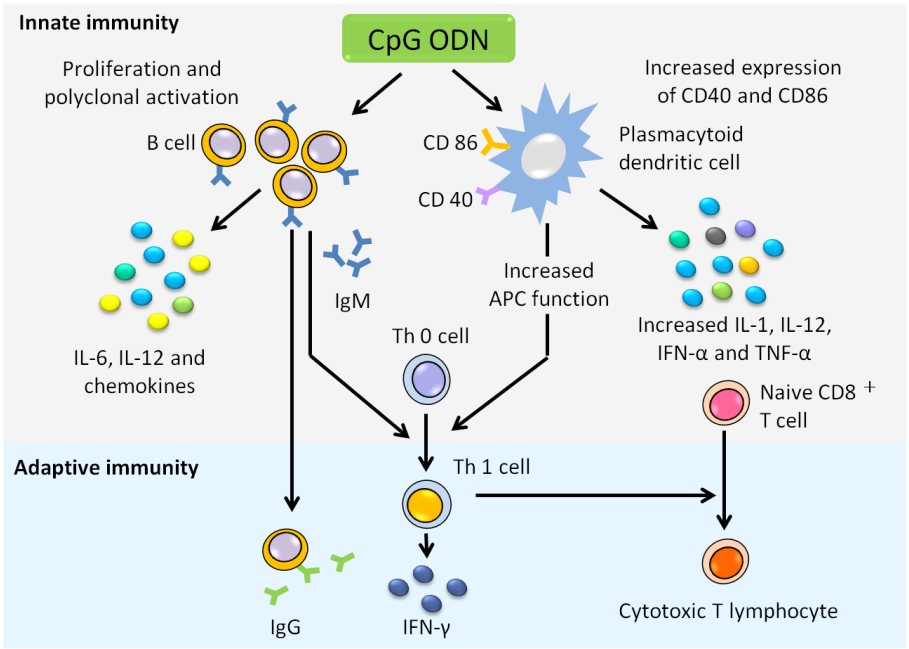

Figure 1.3 Immunostimulatory effect of CpG ODNs. CpG ODNs directly activate human B cells and pDCs, creating an immune milieu that is rich in pro-inflammatory and T helper 1 (Th1)-type cytokines. This innate immune response forms a foundation on which antigen-specific adaptive immunity is based. In particular, by improving the function of professional antigen-presenting cells (APCs), CpG ODNs facilitate the generation of humoral and cellular vaccine-specific immunity. IFN, interferon; IL, interleukin; TNF, tumor-necrosis factor.[14]

1.2.3 Therapeutic applications of CpG ODNs

As described above, CpG ODNs mimic the bacterial CpG DNA and activate both the innate and

adaptive immune systems. This immunostimulatory effect of CpG ODNs provides them with various potential immunotherapeutic applications. To date, four major applications of CpG ODNs have been developed (Figure 1.4).[13-14,19-20,44-45] When combined with allergen, CpG ODNs stimulate an antigen-specific Th1-cell response that inhibits the development of Th2-cell-mediated allergic asthma.[14-15] The innate immune response stimulated by CpG ODNs has developed to protect the host from infectious pathogens. Therefore, CpG ODNs might be used as stand-alone agents to reduce susceptibility to infection.[14,20] The immune cascade elicited by CpG ODNs results in the activation of natural killer (NK) cells and cytotoxic T lymphocytes (CTLs) that facilitates (alone or in combination with other therapies) the treatment of cancer.[13-14] CpG ODNs improve the function of APCs, and create a cytokine/chemokine milieu that is good for the development of an adaptive immune response to co-administered vaccines.[14,19]

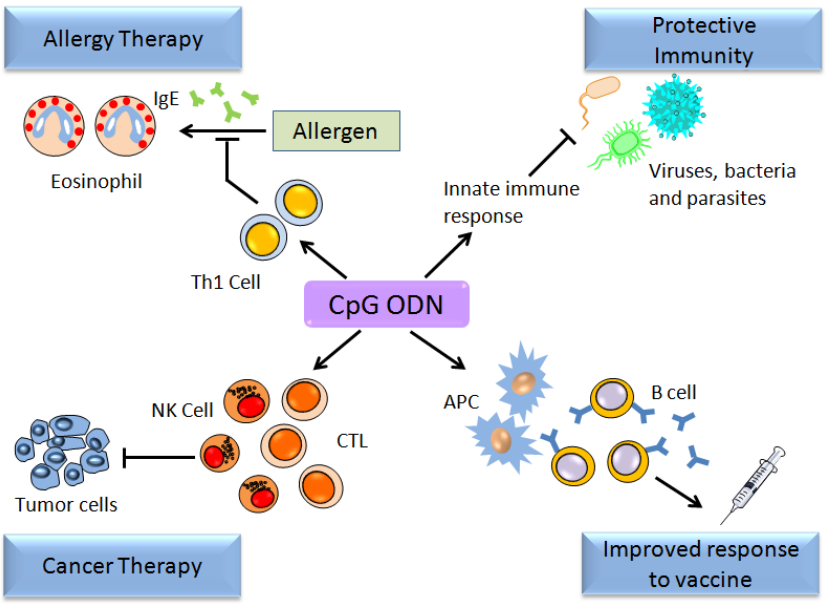

Figure 1.4 Potential immunostimulatory applications of CpG ODNs.[14]

1.2.4 Class of CpG ODNs

Free CpG ODNs containing only a phosphodiester backbone are not stable and prone to nuclease degradation. This severely limits their applications. Substituting the oxygen in the phosphate group with sulfur generates a phosphorothioate CpG ODNs, which are more resistant to nuclease degradation and possess a better immunostimulatory effect.[46-47] To date, at least four classes of such chemically modified synthetic CpG ODNs have been defined based on their different ability to stimulate cells that expressing

TLR 9 (Figure 1.5 and Figure 1.6).[48-51] Class A (also known as type D) CpG ODNs are composed of a mixed phosphodiester/phosphorothioate backbone, as well as palindromic CpG motifs at the center of their sequence.[13,49,52-53] Poly-G sequences on phosphorothioate backbones are attached to the 3′ and 5 ends, which lead to the aggregation of CpG ODNs into large complexes, a process that is thought to enhance cellular uptake.[52] This class of CpG ODNs is notable in its ability to activates pDCs and induce large amounts of IFN-α. However, it is weak stimulator of B cells which leads to the secretion of proinflammatory cytokines such as IL-6 and IL-12.[48-49] The entire sequence of class B (also referred to type K) CpG ODNs consist entirely of a stabilized phosphorothioate backbone without a poly-G tail.[13,52-54] This class of CpG ODNs strongly induces the proliferation and activation of B cells. However, its ability to induce IFN-α from pDCs is low.[54] Class C CpG ODNs includes one or two CpG motifs with a phosphodiester backbone at the 5′ end, and contains a palindromic sequence on a phosphorothioate backbone at the 3′ end. This class of CpG ODNs shows an intermediate immune property between class A and class B CpG ODNs, that it has the ability to induce the proliferation of B cells and the production of IFN-α *via* pDCs.[50-51] Also, novel class P CpG ODNs was reported, which contains two palindromic motifs on phosphorothioate backbones. It shows a high potential to produce IFN-α and activate NF-κB.[55-56]

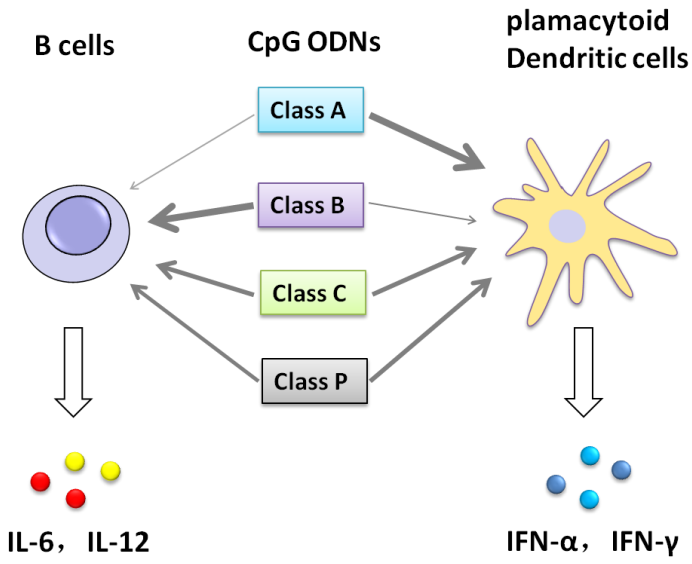

Figure 1.5 Distinct classed of CpG ODNs. Four classes of such chemically modified synthetic CpG ODNs have been defined based on their different ability to stimulate cells that expressing TLR 9 as well as their structures.

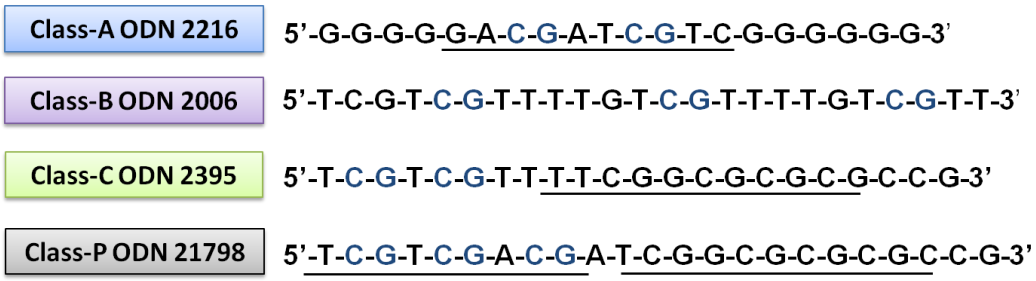

Figure 1.6 Distinct classes of CpG ODNs. Palindromic sequence is underlined.

1.3 Enhancement of the immunostimulatory effect of CpG ODNs

CpG ODNs have shown strong immunostimulatory effect and significant potential use as immunotherapeutic agents against a wide variety of diseases. However, the biologic activity of natural CpG ODNs is often transient, and their rapid degradation and inefficient delivery to target cells or tissues can be a major limitation. Chemical modification of the CpG ODNs backbone may be an effective method to enhance the biologic activity of CpG ODNs, however, several severe side effects are concerned. In this regard, there has been great interest in developing strategies for enhancing the immunostimulatory effect of CpG ODNs. Some of the possible mechanisms are listed below. it is likely that more than one mechanism may be involved at any one time, and some may act synergistically, further enhancing the immunostimulatory effect of CpG ODNs.

1.3.1 Increasing the half-time of CpG ODNs

Phosphodiester CpG ODNs are not stable, and are rapidly degraded after injection with a half-life of about 5 min.[57] This resulted in a rapid clearance of CpG ODNs from the site of administration to the systemic circulation, which severely limit their therapeutic application. Therefore, increasing the half-life of CpG ODNs would be an efficient approach to sustain their activity. Chemical modification by substituting the oxygen with sulphur creates phosphorothioate CpG ODNs, which significantly reduced degradation by nucleases and achieved a half-life of 30–60 min in plasma.[57-58] Meng et al discovered linear-structured ODNs

consisting only of a phosphodiester backbone with crosslinked CpG motifs possess high TLR 9 activation capacity.[59] And the immunostimulatory effect of these class B CpG ODNs is most optimal when there are two to four CpG motifs. When four or more CpG motifs were linked, ODNs consisting only of a phosphodiester backbone greatly improved its resistance against DNase. The ODNs contained nine or more CpG motifs remained largely intact without being degraded in serum for more than 24 hours, and possessed high TLR 9 activation capacity even in low concentrations.

1.3.2 Increasing cellular uptake of CpG ODNs

After endocytosis, CpG ODNs in the endosome or lysosome can activate the TLR 9. This initiates the induction of multiple cytokines and chemokines, further modulates the immune responses. Therefore, cellular uptake of CpG ODNs is important for triggering immune response through interaction with TLR 9. Free CpG ODNs were negatively charged, which was difficult for them to bind to a negatively charged cell surface. This electrostatic repulsion is believed to limit the efficiency of free CpG ODNs uptake. One of the reasons that CpG ODNs adsorbed into nanoparticles or with encapsulated phosphorothioate backbone show greater TLR 9 activity than free CpG ODNs is that the cellular uptake efficiency of CpG ODNs is improved. The cellular uptake efficiency of CpG ODNs is being studied using fluorescently labeled CpG ODNs. When fluorescently labeled free CpG ODNs were added to cultured 293XL-TLR 9 cells, fluorescence was not observed inside the cells. In contrast, strong fluorescence was observed when CpG ODNs are delivered by mesoporous silica nanoparticles and boron nitride nanoparticles.[60-61] Zhao et al and Bianco et al also reported that carbon nanotube can potentiate CpG ODNs immunostimulatory effect by enhancing their delivery into antigen-presenting cells.[62-63] Therefore, methods that enhance CpG ODNs internalization by APCs may enhance their immunostimulatory effect.

1.3.3 Enhancing delivery to endolysosome

Besides the *in vivo* instability of CpG ODNs, the difficulty in delivery to the intracellular compartments where TLR 9 localizes also limits the applications of CpG ODNs. After taken up my immune cells, CpG ODNs may accumulate within the endosomal compartment where they interact with TLR 9.[26] Therefore,

enhancing the endosomal release of CpG ODNs, such as delivery of CpG ODNs in cationic liposomes, the use of endosome-disrupting agents may potentiate their immunostimulatory effect.[64-66] However, how endosomal release of CpG ODNs enhance their immunostimulatory effect is unclear and requires further investigations. In addition, compounds such as monensin and choloroquin could inhibit the immunostimulatory effect of CpG ODNs by affecting the endosomal acidification and/or maturation, that is why they can be used as therapeutic agents for many autoimmune disease like rheumatoid arthritis and systemic lupus erythematosus.[13]

1.3.4 Increasing TLR 9 expression

CpG ODNs stimulate immune systems through the activation of TLR 9. Therefore, enhancement of TLR 9 expression would be a rational approach for a better immunostimulatory effect of CpG ODNs in cells. Bernasconi et al reported that BCR triggering is required for CpG ODNs-induced differentiation of naive B cells, which rapidly up-regulate TLR 9 expression in human naive B cells.[67] It was found that TLR 9 gene expression was up-regulated upon LPS stimulation.[68] The up-regulated TLR 9 is thought to respond to CpG ODNs more effectively and enhance the immunostimulatory effect of CpG ODNs.

1.3.5 Sustained release of CpG ODNs

The increase in uptake efficiency of CpG ODNs and their retention in the endolysosome and lysosome decrease the dosage of CpG ODNs needed for a robust immune responses. Accordingly, the sustained release of CpG ODNs may also result in decreased dosage and continuous effects. Formulating the CpG ODNs in a delivery vehicle could retain the CpG ODNs locally at the site of administration and protect them from nuclease degradation, which result in a slow release of CpG ODNs. Zhu et al reported an enzyme-triggered sustainable release system for CpG ODNs.[69] CpG ODNs were mixed with poly(L-lysine) and hollow mesoporous silica nanoparticles and formed a layer-by-layer complexes. The complexes exhibited a enzyme-triggered controlled release of CpG ODNs in the α-chymotrypsin solution. The release rates of CpG ODNs could also be controlled by changing the enzyme concentration. By controlling the release of CpG ODNs, side effects including autoimmunity and lymphoid architectural damage that occur when CpG ODNs

is given in large amounts can be decreased.[70]

1.3.6 Local cellular recruitment and activation

The immunostimulatory effect of CpG ODNs could be enhanced by combination with cytokines or chemokines which recruit immune cells such as dendritic cells to a local site where they can be activated by CpG ODNs.[71] Nichani et al reported that emulsigen induces local inflammation associated with local cellular infiltration at the site of injection.[72] And this cellular infiltration is enhanced when emulsigen is mixed with CpG ODNs. These localized cell recruitment and activation may contribute to the immunostimulatory effect of CpG ODNs.

1.4 Carriers-based delivery of CpG ODNs

The application of CpG ODNs as an adjuvant has been shown to be effective for treating infectious diseases, cancers, and allergies. In recent years, a large number of delivery systems have been evaluated to determine if they can enhance the biologic activity of CpG ODNs. In particular, various vehicles have been developed as carriers for delivery of CpG ODNs. Lipid-based delivery systems have been used extensively for delivery of protein and drugs, as well as DNA and CpG ODNs.[73-76] Liposomes enhance the biologic activity of ODNs in many ways. Zhang et al reported that cationic liposomes greatly increased cellular uptake and intracellular delivery of ODNs into the cytoplasm. Liposomes could also protect the ODNs from nuclease degradation and thus increased their half-life *in vivo*.[77-78] Besides the ability to enhance the activity of ODNs, liposomes have also been demonstrated as an effective delivery vehicle for CpG ODNs. Stabilized cationic liposomes enhanced the serum stability of CpG ODNs and facilitated their uptake by B cells, dendritic cells, and macrophages.[65] Suzuki et al reported that CpG ODNs encapsulated in cationic liposomes (CpG ODNs-liposomes) improved their incorporation into CD11c(+) dendritic cells and induces enhanced serum IL-12 levels.[76] Furthermore, compared to unmodified CpG ODNs, CpG ODNs-liposomes had a much stronger ability to activate NK cells and NKT cells to produce IFN-gamma.[76] All of these studies suggested that formulation of CpG ODNs in liposomes was more effective than free CpG ODNs in inducing immune responses. Many studies have reported on systems that incorporate CpG ODNs and antigens in biodegradable nanoparticles. Poly(lactide-co-glycolide) (PLGA) microspheres possess immunological

adjuvant properties, which have been used extensively as delivery vehicles for protein drug and CpG ODNs.[79-80] Singh et al reported that CpG ODNs loaded PLGA microparticles co-administered with HIV-1 env gp 120 recombinant protein significantly enhanced serum IgG antibody responses.[81] Demento et al minimized the release rate of CpG ODNs by using biotin-avidin binding to attach CpG ODNs to the surface of biodegradable PLGA nanoparticles.[82] They also found that immunization with CpG ODNs-modified nanoparticles resulted in a greater number of circulating effector T cells and greater activity of Ag-specific lymphocytes than unmodified nanoparticles or aluminum hydroxide. Besides, many inorganic nanoparticles were also chosen as carriers for the delivery of CpG ODNs. Zhao et al reported that carbon nanotubes can potentiate CpG ODNs immunopotency by enhancing their delivery into tumor-associated inflammatory cells.[62] Gold nanoparticles have also been used as a vehicle for the intracellular delivery of CpG ODNs.[83] While these methods have significantly improved the application of CpG ODNs in biological studies and even clinical trials. It is still highly demanding to develop a simple and better delivery system that can simultaneously address the challenges including efficiency of cellular uptake, stability against nuclease degradation, and potential cellular toxicity upon complexation with transfection agents.

1.5 Boron nitride nanospheres

With its novel properties and structural similarity to carbon materials, hexagonal boron nitride has received considerable scientific attention. Profiting from the layerd structure, it has various morphologies, including sheet,[84-85] tubes,[86] spheres[87] etc. Almost all of the structures have superb antioxidation ability, high thermal conductivity, excellent stability, and great mechanical properties despite of different morphologies.[88] These make BN an interesting material for many applications ranging from composite materials to electrical and optical devices working under hazardous environments.[86,89-91] Recently, it has been revealed that BN nanomaterials possess good biocompatibility, much better than that of carbon materials.[92-93] Chen et al. demonstrated that BN nanotubes (BNNT) are noncytotoxic and can be surface functionalized with biologicall epitopes such as proteins, DNA and RNA, they also showed that BNNT could delivery DNA oligomer to the interior of cells with no apparent toxicity.[92] Ciofani et al. reported that BNNT are highly internalized by C2C12 cells, which neither decreased the C2C12 myoblast viability nor significantly affected the myotube formation.[94]

BN nanospheres (BNNS) may have better biocompatibility, unlike other BN morphologies, as spheres are considered to possess easier cell uptake and lower structure-induced toxicity.[95-96] Furthermore, BNNS with very small size would greatly improve the particle dispersion, which is a crucial factor for their biomedical applications.[87] Taken together, with their unique nanostructure and unusual properties, BNNS have great potential for the development of novel nanovectors for cell therapy, drug, and gene delivery, and for other biomedical and clinical applications. BNNS used in this study were synthesized by a chemical vapor deposition method.[87] The as-prepared BNNS have a uniform spherical shape with an average diameter of about 150 nm (Figure 1.7a). In addition, well orderd channels could be clearly seen from the high-resolution transmission electron microscopy image of the BNNS (Figure 1.7b).

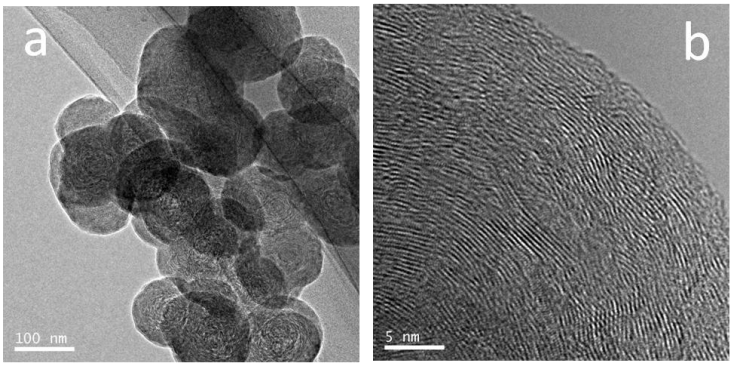

Figure 1.7 Typical transmission electron microscopy image of the BNNS. (a) Low-resolution image. (b) High-resolution image.

1.6 Objectives of this study

Bacterial and viral DNA containing unmethylated CpG motifs stimulate the mammalian innate immune system. This process is mediated by the activation of TLR 9, a member of Toll-like receptor family. Synthetic ODNs containing unmethylated CpG motifs are like those found in bacterial DNA and possess similar immunostimulatory effects. The activation of TLR 9 initiates an immunostimulatory cascade that induce the maturation, differentiation, and proliferation of multiple immune cells including B and T lymphocytes, NK cells, and monocytes/macrophage. This further triggers cell signaling pathways including MAPKs and NFκB, subsequently results in the induction of multiple proinflammatory cytokines and chemokines that modulating the cellular inflammatory response. As such, CpG ODNs have potential for treatment of infectious diseases, allergies, and cancers. However, the immunostimulatory effects are often limited by the poor stability and cellular uptake of natural CpG ODNs. Therefore, there has been great interest in developing approaches to optimize the stimulatory activity of CpG ODNs. Chemical modification of CpG ODNs backbone is an effective technique to protect against degradation by nucleases. However, there is concern over several severe side effects. Since CpG ODNs are negatively charged, it is difficult for them to bind to the negatively charged cell surface. This electrostatic repulsion is believed to limit the efficiency of CpG ODNs uptake and their immunostimulatory effect. Evidence is accumulating indicates that both the stability and cellular uptake of natural CpG ODNs can be enhanced by using nanoparticles as carriers. Therefore, delivery of unmodified CpG ODNs using nanoparticles maybe an good approach to improve their immunostimulatory effect, and make it possible to use naturally occurring CpG ODNs in clinical applications.

In this regard, the objective of this study is to enhance the immunostimulatory effect of CpG ODNs by developing novel delivery systems based on BNNS.

1.7 Dissertation organization

The main contexts of each chapter in this thesis are organized as follows:

In chapter 1, a general introduction of this study was given, including the mechanism of human immune system, the interaction between CpG ODNs and TLR 9, therapeutic potential of CpG ODNs, mechanisms for enhancing the immunostimulatory effect of CpG ODNs, and the BNNS.

In chapter 2, a novel CpG ODNs delivery system based on a BNNS-binding peptide has been developed. Firstly, a 12-amino acid peptide, designated as BP7, which had specific affinity for BNNS, was indentified using phage display technique. BNNS that bound BP7 (BNNS/BP7) were taken up into cells and showed no cytotoxicity. Using BP7 as a linker, the loading capacity of CpG ODNs on BNNS increased 5-fold compared to the direct binding of CpG ODNs to BNNS. Then we used the BP7–CpG ODNs conjugates–loaded BNNS to stimulate the peripheral blood mononuclear cells (PBMCs) and measured the cytokine productions. BP7–CpG ODNs conjugates–loaded BNNS had a greater capacity to induce IL-6 and TNF-α production from PBMCs than that of CpG ODNs directly loaded on BNNS. However, it could not induce IFN-α from PBMCs. The higher amount of cytokine induction from BP7–CpG ODNs conjugates–loaded BNNS may be attributed to a higher loading capacity and stronger binding to BNNS with the linker BP7. Thus, the BNNS-binding peptide provide a promising strategy for enhancing the immunostimulatory effect of CpG ODNs.

In chapter 3, another CpG ODNs delivery system using cationic polymer-functionalized BNNS has been developed. Polyethyleneimine (PEI) was coated on the surface of BNNS to achieve a positive surface charge, which facilitated the loading of negatively-charged CpG ODNs onto the BNNS. BNNS/PEI complexes greatly improved the cellular uptake efficiency of CpG ODNs. This further resulted in a enhanced IL-6 and TNF-α production from PBMCs compared to that of CpG ODNs directly loaded on BNNS. Most importantly, B class CpG ODNs loaded on BNNS/PEI complexes induced IFN-α, while neither free CpG ODNs nor CpG ODNs loaded directly on BNNS had this potential. It is thought that when the class B CpG ODNs were loaded onto the positively charged BNNS-PEI complexes, they formed the higher-order multimeric structure similar to class A CpG ODNs, and acquired the ability to induce the IFN-α.

In chapter 4, chitosan coated BNNS were used as carrier for the delivery of CpG ODNs. BNNS/CS complexes had positive zeta potential and exhibited a better dispersity and stability in aqueous solution than BNNS due to the CS coating. The BNNS/CS complexes greatly improved the loading capacity and cellular uptake efficiency of CpG ODNs due to their positive surface charge. The loading capacity of the CpG ODNs depend on the molecular weight (MW) of CS, which affected the positive charge density on the surface of BNNS. CpG ODNs loaded on BNNS/CS complexes significantly enhanced the IL-6 and TNF-α productions from PBMCs compared to that of CS/CpG ODNs complexes and CpG ODNs directly loaded on BNNS. We also found that molecular weight of the CS used for BNNS coating affected the cytokines induction through varying the strength of the condensation of the CpG ODNs. Surprisingly, different from PEI-functionalized BNNS, CpG ODNs loaded on BNNS/CS could not induce IFN-α production from PBMCs. We also found that CS had a suppressive effect on TLR 9 mediated IFN-α induction. However, the mechanism remains unclear and further investigation is under way.

Chapter 5 is a summary. In this study, we have successfully developed several delivery systems for CpG ODNs based on BNNS, These delivery systems improved the loading capacity and cellular uptake of CpG ODNs, and are proved to be effective in enhancing the immunostimulatory effect of CpG ODNs. We also found that CS had a suppressive effect on TLR 9 mediated IFN-α induction. However, the mechanism remains unknown. Future work will be focused on the mechanisms of this effect and its possible therapeutic applications in immunological disorder diseases.

1.8 References

1. Medzhitov R, Janeway CA. Innate immunity: The virtues of a nonclonal system of recognition. *Cell.* 1997;91(3):295-298.
2. Lemaitre B, Nicolas E, Michaut L, Reichhart JM, Hoffmann JA. The dorsoventral regulatory gene cassette spatzle/Toll/cactus controls the potent antifungal response in Drosophila adults. *Cell.* 1996;86(6):973-983.
3. Poltorak A, He XL, Smirnova I, et al. Defective LPS signaling in C3H/HeJ and C57BL/10ScCr mice: Mutations in Tlr4 gene. *Science.* 1998;282(5396):2085-2088.
4. Janeway CA, Medzhitov R. Innate immune recognition. *Annu. Rev. Immunol.* 2002;20:197-216.
5. Akira S, Uematsu S, Takeuchi O. Pathogen recognition and innate immunity. *Cell.* 2006;124(4):783-801.
6. Beutler BA. TLRs and innate immunity. *Blood.* 2009;113(7):1399-1407.
7. Hoffmann JA. The immune response of Drosophila. *Nature.* 2003;426(6962):33-38.
8. Kawai T, Akira S. Toll-like Receptors and Their Crosstalk with Other Innate Receptors in Infection and Immunity. *Immunity.* 2011;34(5):637-650.
9. Jain VV, Kitagaki K, Kline JN. CpG DNA and immunotherapy of allergic airway diseases. *Clin. Exp. Allergy.* 2003;33(10):1330-1335.
10. Krieg AM. Mechanisms and applications of immune stimulatory CpG oligodeoxynucleotides. *Bba-Gene Struct Expr.* 1999;1489(1):107-116.
11. Hemmi H, Takeuchi O, Kawai T, et al. A Toll-like receptor recognizes bacterial DNA. *Nature.* 2000;408(6813):740-745.
12. Bauer S, Kirschning CJ, Häcker H, et al. Human TLR9 confers responsiveness to bacterial DNA via species-specific CpG motif recognition. *Proc. Natl. Acad. Sci. U. S. A.* 2001;98(16):9237-9242.
13. Krieg AM. CpG motifs in bacterial DNA and their immune effects. *Annu. Rev. Immunol.* 2002;20:709-760.
14. Klinman DM. Immunotherapeutic uses of CpG oligodeoxynucleotides. *Nat. Rev. Immunol.*

2004;4(4):248-257.

15. Wilson HL, Dar A, Napper SK, Marianela Lopez A, Babiuk LA, Mutwiri GK. Immune mechanisms and therapeutic potential of CpG oligodeoxynucleotides. *Int. Rev. Immunol.* 2006;25(3-4):183-213.

16. Stacey KJ, Sweet MJ, Hume DA. Macrophages ingest and are activated by bacterial DNA. *J. Immunol.* 1996;157(5):2116-2122.

17. Sun SQ, Zhang XH, Tough DF, Sprent J. Type I interferon-mediated stimulation of T cells by CgG DNA. *J. Exp. Med.* 1998;188(12):2335-2342.

18. Fonseca DE, Kline JN. Use of CpG oligonucleotides in treatment of asthma and allergic disease. *Adv. Drug Delivery. Rev.* 2009;61(3):256-262.

19. Klinman DM, Klaschik S, Sato T, Tross D. CpG oligonucleotides as adjuvants for vaccines targeting infectious diseases. *Adv. Drug Delivery. Rev.* 2009;61(3):248-255.

20. Krieg AM. Therapeutic potential of Toll-like receptor 9 activation. *Nat. Rev. Drug Discov.* 2006;5(6):471-484.

21. Murad YM, Clay TM. CpG Oligodeoxynudeofides as TLR9 Agonists Therapeutic Applications in Cancer. *BioDrugs*. 2009;23(6):361-375.

22. Rutz M, Metzger J, Gellert T, et al. Toll-like receptor 9 binds single-stranded CpG-DNA in a sequence- and pH-dependent manner. *Eur. J. Immunol.* 2004;34(9):2541-2550.

23. Hacker H, Mischak H, Miethke T, et al. CpG-DNA-specific activation of antigen-presenting cells requires stress kinase activity and is preceded by non-specific endocytosis and endosomal maturation. *EMBO J.* 1998;17(21):6230-6240.

24. Guiducci C, Ott G, Chan JH, et al. Properties regulating the nature of the plasmacytoid dendritic cell response to Toll-like receptor 9 activation. *J. Exp. Med.* 2006;203(8):1999-2008.

25. Zhao QY, Waldschmidt T, Fisher E, Herrera CJ, Krieg AM. Stage-Specific Oligonucleotide Uptake in Murine Bone-Marrow B-Cell Precursors. *Blood.* 1994;84(11):3660-3666.

26. Latz E, Schoenemeyer A, Visintin A, et al. TLR9 signals after translocating from the ER to CpG DNA in the lysosome. *Nat. Immunol.* 2004;5(2):190-198.

27. Gupta GK, Agrawal DK. CpG Oligodeoxynucleotides as TLR9 Agonists Therapeutic Application in Allergy and Asthma. *BioDrugs.* 2010;24(4):225-235.

28. Blasius AL, Beutler B. Intracellular Toll-like Receptors. *Immunity.* 2010;32(3):305-315.

29. Kumar H, Kawai T, Akira S. Toll-like receptors and innate immunity. *Biochem. Biophys. Res. Commun.* 2009;388(4):621-625.

30. Yi AK, Klinman DM, Martin TL, Matson S, Krieg AM. Rapid immune activation by CpG motifs in bacterial DNA. Systemic induction of IL-6 transcription through an antioxidant-sensitive pathway. *J. Immunol.* 1996;157(12):5394-5402.

31. Redford TW, Yi AK, Ward CT, Krieg AM. Cyclosporin A enhances IL-12 production by CpG motifs in bacterial DNA and synthetic oligodeoxynucleotides. *J. Immunol.* 1998;161(8):3930-3935.

32. Krieg AM, Yi AK, Matson S, et al. CpG motifs in bacterial DNA trigger direct B-cell activation. *Nature.* 1995;374(6522):546-549.

33. Klinman DM, Yi AK, Beaucage SL, Conover J, Krieg AM. CpG motifs present in bacterial DNA rapidly induce lymphocytes to secrete interleukin 6, interleukin 12, and interferon gamma. *Proc. Natl. Acad. Sci. U. S. A.* 1996;93(7):2879-2883.

34. Jung J, Yi AK, Zhang X, Choe J, Li L, Choi YS. Distinct response of human B cell subpopulations in recognition of an innate immune signal, CpG DNA. *J. Immunol.* 2002;169(5):2368-2373.

35. Bernasconi NL, Traggiai E, Lanzavecchia A. Maintenance of serological memory by polyclonal activation of human memory B cells. *Science.* 2002;298(5601):2199-2202.

36. Asselin-Paturel C, Brizard G, Chemin K, et al. Type I interferon dependence of plasmacytoid dendritic cell activation and migration. *J. Exp. Med.* 2005;201(7):1157-1167.

37. Napolitani G, Rinaldi A, Bertoni F, Sallusto F, Lanzavecchia A. Selected Toll-like receptor agonist combinations synergistically trigger a T helper type 1-polarizing program in dendritic cells. *Nat. Immunol.* 2005;6(8):769-776.

38. Roman M, MartinOrozco E, Goodman S, et al. Immunostimulatory DNA sequences function as T helper-1-promoting adjuvants. *Nat. Med.* 1997;3(8):849-854.

39. Hartmann G, Weiner GJ, Krieg AM. CpG DNA: A potent signal for growth, activation, and maturation of human dendritic cells. *Proc. Natl. Acad. Sci. U. S. A.* 1999;96(16):9305-9310.

40. Vollmer J, Jurk M, Samulowitz U, et al. CpG oligodeoxynucleotides stimulate IFN-gamma-inducible protein-10 production in human B cells. *J. Endotoxin Res.* 2004;10(6):431-438.

41. Krug A, Towarowski A, Britsch S, et al. Toll-like receptor expression reveals CpG DNA as a unique microbial stimulus for plasmacytoid dendritic cells which synergizes with CD40 ligand to induce high amounts of IL-12. *Eur. J. Immunol.* 2001;31(10):3026-3037.

42. Schwarz K, Storni T, Manolova V, et al. Role of Toll-like receptors in costimulating cytotoxic T cell responses. *Eur. J. Immunol.* 2003;33(6):1465-1470.

43. Heit A, Maurer T, Hochrein H, et al. Toll-like receptor 9 expression is not required for CpG DNA-aided cross-presentation of DNA-conjugated antigens but essential for cross-priming of CD8 T cells. *J. Immunol.* 2003;170(6):2802-2805.

44. Klinman DM. Use of CpG oligodeoxynucleotides as immunoprotective agents. *Expert Opin. Biol. Ther.* 2004;4(6):937-946.

45. Klinman DM, Currie D, Gursel I, Verthelyi D. Use of CpG oligodeoxynucleotides as immune adjuvants. *Immunol. Rev.* 2004;199(1):201-216.

46. Mutwiri GK, Nichani AK, Babiuk S, Babiuk LA. Strategies for enhancing the immunostimulatory effects of CpG oligodeoxynucleotides. *J. Control. Release.* 2004;97(1):1-17.

47. Hanagata N. Structure-dependent immunostimulatory effect of CpG oligodeoxynucleotides and their delivery system. *Int. J. Nanomedicine.* 2012;7:2181-2195.

48. Verthelyi D, Ishii KJ, Gursel M, Takeshita F, Klinman DM. Human peripheral blood cells differentially recognize and respond to two distinct CpG motifs. *J. Immunol.* 2001;166(4):2372-2377.

49. Krug A, Rothenfusser S, Hornung V, et al. Identification of CpG oligonucleotide sequences with high induction of IFN-alpha/beta in plasmacytoid dendritic cells. *Eur. J. Immunol.* 2001;31(7):2154-2163.

50. Hartmann G, Battiany J, Poeck H, et al. Rational design of new CpG oligonucleotides that combine B cell activation with high IFN-alpha induction in plasmacytoid dendritic cells. *Eur. J. Immunol.* 2003;33(6):1633-1641.

51. Marshall JD, Fearon K, Abbate C, et al. Identification of a novel CpG DNA class and motif that optimally stimulate B cell and plasmacytoid dendritic cell functions. *J. Leukoc. Biol.* 2003;73(6):781-792.

52. Barbalat R, Ewald SE, Mouchess ML, Barton GM. Nucleic acid recognition by the innate immune system. *Annu. Rev. Immunol.* 2011;29:185-214.

53. Gursel M, Verthelyi D, Gursel I, Ishii KJ, Klinman DM. Differential and competitive activation of human immune cells by distinct classes of CpG oligodeoxynucleotide. *J. Leukoc. Biol.* 2002;71(5):813-820.

54. Hartmann G, Weeratna RD, Ballas ZK, et al. Delineation of a CpG phosphorothioate oligodeoxynucleotide for activating primate immune responses in vitro and in vivo. *J. Immunol.* 2000;164(3):1617-1624.

55. Samulowitz U, Weber M, Weeratna R, et al. A Novel Class of Immune-Stimulatory CpG Oligodeoxynucleotides Unifies High Potency in Type I Interferon Induction with Preferred Structural Properties. *Oligonucleotides.* 2010;20(2):93-101.

56. Donhauser N, Helm M, Pritschet K, et al. Differential effects of P-Class versus other CpG oligodeoxynucleotide classes on the impaired innate immunity of plasmacytoid dendritic cells in HIV type 1 infection. *AIDS Res. Hum. Retrovir.* 2010;26(2):161-171.

57. Sands H, Goreyferet LJ, Ho SP, et al. Biodistribution and metabolism of internally 3H-labeled oligonucleotides. II. 3',5'-blocked oligonucleotides. *Mol. Pharmacol.* 1995;47(3):636-646.

58. Agrawal S, Zhao QY. Antisense therapeutics. *Curr. Opin. Chem. Biol.* 1998;2(4):519-528.

59. Meng WJ, Yamazaki T, Nishida Y, Hanagata N. Nuclease-resistant immunostimulatory phosphodiester CpG oligodeoxynucleotides as human Toll-like receptor 9 agonists. *BMC Biotechnol.* 2011;11:88.

60. Zhu Y, Meng W, Li X, Gao H, Hanagata N. Design of mesoporous silica/cytosine−phosphodiester−guanine oligodeoxynucleotide complexes to enhance delivery efficiency. *J. Phys. Chem. C.* 2010;115(2):447-452.

61. Zhi CY, Meng WJ, Yamazaki T, et al. BN nanospheres as CpG ODN carriers for activation of toll-like receptor 9. *J. Mater. Chem.* 2011;21(14):5219-5222.

62. Zhao DC, Alizadeh D, Zhang LY, et al. Carbon nanotubes enhance CpG uptake and potentiate antiglioma immunity. *Clin. Cancer Res.* 2011;17(4):771-782.

63. Bianco A, Hoebeke J, Godefroy S, et al. Cationic carbon nanotubes bind to CpG

oligodeoxynucleotides and enhance their immunostimulatory properties. *J. Am. Chem. Soc.* 2004;127(1):58-59.

64. Yamamoto T, Yamamoto S, Kataoka T, Tokunaga T. Lipofection of synthetic oligodeoxyribonucleotide having a palindromic sequence of AACGTT to murine splenocytes enhances interferon production and natural killer activity. *Microbiol. Immunol.* 1994;38(10):831-836.

65. Gursel I, Gursel M, Ishii KJ, Klinman DM. Sterically stabilized cationic liposomes improve the uptake and immunostimulatory activity of CpG oligonucleotides. *J. Immunol.* 2001;167(6):3324-3328.

66. Krieg AM, Tonkinson J, Matson S, et al. Modification of antisense phosphodiester oligodeoxynucleotides by a 5' cholesteryl moiety increases cellular association and improves efficacy. *Proc. Natl. Acad. Sci. U. S. A.* 1993;90(3):1048-1052.

67. Bernasconi NL, Onai N, Lanzavecchia A. A role for Toll-like receptors in acquired immunity: up-regulation of TLR9 by BCR triggering in naive B cells and constitutive expression in memory B cells. *Blood.* 2003;101(11):4500-4504.

68. An HZ, Xu HM, Yu YZ, et al. Up-regulation of TLR9 gene expression by LPS in mouse macrophages via activation of NF-kappa B, ERK and p38 MAPK signal pathways. *Immunol. Lett.* 2002;81(3):165-169.

69. Zhu YF, Meng WJ, Gao H, Hanagata N. Hollow Mesoporous Silica/Poly(L-lysine) Particles for Codelivery of Drug and Gene with Enzyme-Triggered Release Property. *J. Phys. Chem. C.* 2011;115(28):13630-13636.

70. Foged C, Brodin B, Frokjaer S, Sundblad A. Particle size and surface charge affect particle uptake by human dendritic cells in an in vitro model. *Int. J. Pharm.* 2005;298(2):315-322.

71. Ahlers JD, Belyakov IM, Berzofsky JA. Cytokine, chemokine, and costimulatory molecule modulation to enhance efficacy of HIV vaccines. *Curr. Mol. Med.* 2003;3(3):285-301.

72. Nichani AK, Kaushik RS, Mena A, et al. CpG oligodeoxynucleotide induction of antiviral effector molecules in sheep. *Cell. Immunol.* 2004;227(1):24-37.

73. Kim D, Rhee JW, Kwon S, et al. Enhancement of immunomodulatory activity by liposome-encapsulated natural phosphodiester bond CpG-DNA in a human B cell line. *Bmb Reports.*

2010;43(4):250-256.

74. Zheng L, Huang L, Huang XL, et al. Liposome mediated delivery of proteins into human dendritic cells for antigen presentation. *J. Leukoc. Biol.* 1998;S2:73-73.

75. Li P, Liu DH, Sun XL, Liu CX, Liu YJ, Zhang N. A novel cationic liposome formulation for efficient gene delivery via a pulmonary route. *Nanotechnology.* 2011;22(24):245104.

76. Suzuki Y, Wakita D, Chamoto K, et al. Liposome-encapsulated CpG oligodeoxynucleotides as a potent adjuvant for inducing type 1 innate immunity. *Cancer Res.* 2004;64(23):8754-8760.

77. De Oliveira MC, Boutet V, Fattal E, et al. Improvement of in vivo stability of phosphodiester oligonucleotide using anionic liposomes in mice. *Life Sci.* 2000;67(13):1625-1637.

78. Yu RZ, Geary RS, Leeds JM, et al. Pharmacokinetics and tissue disposition in monkeys of an antisense oligonucleotide inhibitor of Ha-ras encapsulated in stealth liposomes. *Pharm. Res.* 1999;16(8):1309-1315.

79. Rafati A, Boussahel A, Shakesheff KM, et al. Chemical and spatial analysis of protein loaded PLGA microspheres for drug delivery applications. *J. Control. Release.* 2012;162(2):321-329.

80. Mueller M, Reichardt W, Koerner J, Groettrup M. Coencapsulation of tumor lysate and CpG-ODN in PLGA-microspheres enables successful immunotherapy of prostate carcinoma in TRAMP mice. *J. Control. Release.* 2012;162(1):159-166.

81. Singh M, O'Hagan DT. Recent advances in vaccine adjuvants. *Pharm. Res.* 2002;19(6):715-728.

82. Demento SL, Bonafe N, Cui WG, et al. TLR9-targeted biodegradable nanoparticles as immunization vectors protect against west nile encephalitis. *J. Immunol.* 2010;185(5):2989-2997.

83. Wei M, Chen N, Li J, et al. Polyvalent immunostimulatory nanoagents with self-assembled CpG oligonucleotide-conjugated gold nanoparticles. *Angew. Chem. Int. Ed.* 2012;51(5):1202-1206.

84. Zhi CY, Bando Y, Tang CC, Kuwahara H, Golberg D. Large-scale fabrication of boron nitride nanosheets and their utilization in polymeric composites with improved thermal and mechanical properties. *Adv. Mater.* 2009;21(28):2889-2893.

85. Han W-Q, Wu L, Zhu Y, Watanabe K, Taniguchi T. Structure of chemically derived mono- and few-atomic-layer boron nitride sheets. *Appl. Phys. Lett.* 2008;93(22):223103.

86. Chopra NG, Luyken RJ, Cherrey K, et al. Boron nitride nanotubes. *Science.*

1995;269(5226):966-967.

87. Tang CC, Bando Y, Huang Y, Zhi CY, Golberg D. Synthetic routes and formation mechanisms of spherical boron nitride nanoparticles. *Adv. Funct. Mater.* 2008;18(22):3653-3661.

88. Zhi CY, Bando Y, Tang CC, Golberg D. Boron nitride nanotubes. *Mater. Sci. Eng., R.* 2010;70(3-6):92-111.

89. Zhi CY, Bando Y, Tang CC, Xie RG, Sekiguchi T, Golberg D. Perfectly dissolved boron nitride nanotubes due to polymer wrapping. *J. Am. Chem. Soc.* 2005;127(46):15996-15997.

90. Gao ZH, Zhi CY, Bando Y, Golberg D, Serizawa T. Isolation of individual boron nitride nanotubes via peptide wrapping. *J. Am. Chem. Soc.* 2010;132(14):4976-4977.

91. Golberg D, Bando Y, Tang CC, Zhi CY. Boron nitride nanotubes. *Adv. Mater.* 2007;19(18):2413-2432.

92. Chen X, Wu P, Rousseas M, et al. Boron nitride nanotubes are noncytotoxic and can be functionalized for interaction with proteins and cells. *J. Am. Chem. Soc.* 2009;131(3):890-891.

93. Ciofani G, Danti S, Nitti S, Mazzolai B, Mattoli V, Giorgi M. Biocompatibility of boron nitride nanotubes: an up-date of in vivo toxicological investigation. *Int. J. Pharm.* 2013;444(1-2):85-88.

94. Ciofani G, Ricotti L, Danti S, et al. Investigation of interactions between poly-L-lysine-coated boron nitride nanotubes and C2C12 cells: up-take, cytocompatibility, and differentiation. *Int. J. Nanomedicine.* 2010;5:285-298.

95. Jonsson E, Simonsen L, Karlsson M, Larsson R. The hollow fiber model: a new method for in vivo-evaluation of antitumor effect, toxicity and pharmacokinetics of new anticancer drugs. *Ann. Oncol.* 1998;9(S2):44-44.

96. Waritz RS, Ballantyne B, Clary JJ. Subchronic inhalation toxicity of 3.5-mu m diameter carbon fibers in rats. *J. Appl. Toxicol.* 1998;18(3):215-223.

Chapter 2 Identification of a specific binding peptide to BNNS for the intracellular delivery of CpG ODNs

2.1 Introduction

Bacterial and viral DNA containing unmethylated CpG dinucleotides stimulate the mammalian innate immune system.[1-4] This process is mediated by the activation of TLR 9, a member of Toll-like receptor family.[1,5-6] CpG ODNs are short, synthetic, single-stranded DNA sequences containing CpG motifs, which possess a similar immunostimulatory property to bacterial DNA.[3,7] As such, CpG ODNs delivery has potential for clinical applications in the treatment of infectious diseases, allergies, and cancers.[8-11] However, the immunostimulatory effects are often limited by the poor stability and cellular uptake of CpG ODNs. Chemical modification of nucleotides is an effective technique to protect against degradation by nucleases.[12-14] Nuclease-resistant CpG ODNs consisting of phosphorothioate backbones have been developed by modifying the phosphate group of the nucleic acid targeted by nucleases, replacing the oxygen with sulfur. However, there is concern over undesirable side effects associated with the use of CpG ODNs with a phosphorothioate backbone.[15-17] Since CpG ODNs are negatively charged, it is difficult for them to bind to the negatively charged cell surface. This electrostatic repulsion is believed to limit the efficiency of CpG ODNs uptake. Delivery of unmodified CpG ODNs using carrier nanoparticles is, therefore, one strategy to improve stability and to enhance cellular uptake.[18-22]

With its novel properties and structural similarity to carbon, BN has received considerable scientific interest, with applications ranging from composite materials to electrical and optical devices.[23-26] Furthermore, BN has the advantage of a high biocompatibility, with easier cellular uptake and lower toxicity than carbon.[27-29] Chen et al. demonstrated passive adsorption of single-stranded DNA oligomers onto the surface of BNNT and cellular uptake of BNNT loaded with the DNA.[27] We previously studied the effect of unmodified CpG ODNs delivery using 150-nm BNNS, synthesized by chemical vapor deposition,[30] on TLR 9 activation.[31] BNNS had no cytotoxicity, and protected unmodified CpG ODNs from degradation by serum nucleases. In addition, BNNS taken up by cells localized to endolysosomes, and this localization was maintained even after cell division. This was particularity advantageous, since TLR 9 also localizes to

endolysosomes. However, the loading capacity of CpG ODNs on the surface of BNNS was not sufficient to induce a robust cytokine response. In addition, a burst release of CpG ODNs from BNNS was observed. It is possible that these effects are due to the weak interaction between CpG ODNs and the surface of BNNS.

To ameliorate these problems, in this chapter, we screened peptides that have an affinity for BNNS and used the candidate peptide as a linker molecule to bind CpG ODNs to BNNS, which have a chemically inert and structurally stable surface.[30] Phage display has emerged recently as a powerful approach for identifying peptide motifs that possess high affinity and specificity against a particular target, including various inorganic nanomaterials,[32-33] metals,[34-36] semiconductors,[37-38] and polymers.[39] Using this technique, we identified a peptide with selective affinity for BNNS, and characterized the intracellular delivery and response to CpG ODNs indirectly bound to BNNS through the linker peptide (Figure 2.1). An enhanced immunostimulatory effect of CpG ODNs was achieved and discussed in detail.

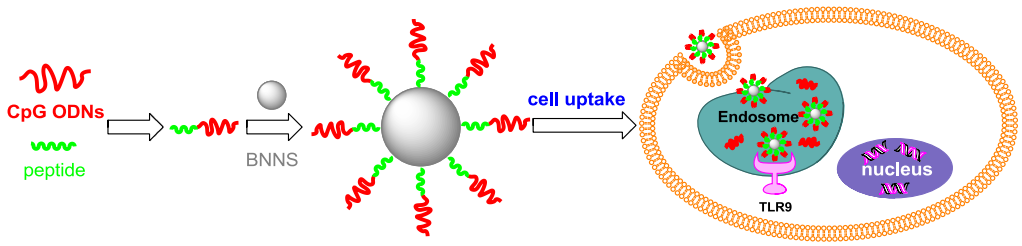

Figure 2.1 Schematic illustration of using a BNNS-binding peptide for the intracellular delivery of CpG ODNs.

2.2 Materials and methods

2.2.1 Materials

Highly pure BNNS, with an average size of approximately 150 nm, were synthesized by a chemical vapor deposition method as previously reported.[30] Fluorescein isothiocyanate-labeled peptides were purchased from Thermo Fisher Scientific (Germany). Phosphodiester-based class-B CpG ODNs, referred to as CpG ODNs 2006x3-PD,[41] were purchased from Fasmac, Inc. (Kanagawa, Japan). CpG ODNs were diluted in sterile water and stored at -20 ℃.

2.2.2 Screening of BNNS-binding peptides using phage display

The detailed procedures of screening of BNNS-binding peptides were summarized in Figure 2.2. BNNS (1 mg/mL) were suspended by sonication in Tris-HCl–buffered saline (50 mM HCl, 150 mM NaCl, pH 7.5) containing 0.1% Tween-20 (TBS-T). The Ph.D.-12 phage library (New England Biolabs, Beverly, MA, USA) containing 1×10^{11} pfu was added to 1 mL BNNS solution. After incubation for 1 h at room temperature with gentle agitation, the BNNS were washed 10 times with TBS-T to remove any unbound phages. Bound phages were then eluted by incubation for 10 min at room temperature in 1 mL of 0.2 M glycine-HCl (pH 2.2). The eluted phages were immediately neutralized by adding 150 μL of 1 M Tris-HCl (pH 9.1), and the number of phages was estimated by infecting Escherichia coli strain ER2738. The eluted phages were amplified in E. coli and subjected to the next round of panning, which was repeated 5 times. By the fifth panning, the phage recovery ratio (output phage:input phage) was high enough to pick 96 individual clones, which were then characterized by sequencing with the universal primer 96 g III (5′-3′CCCTCATAGTTAGCGTAACG) purchased from Fasmac, Inc. (Kanagawa, Japan).

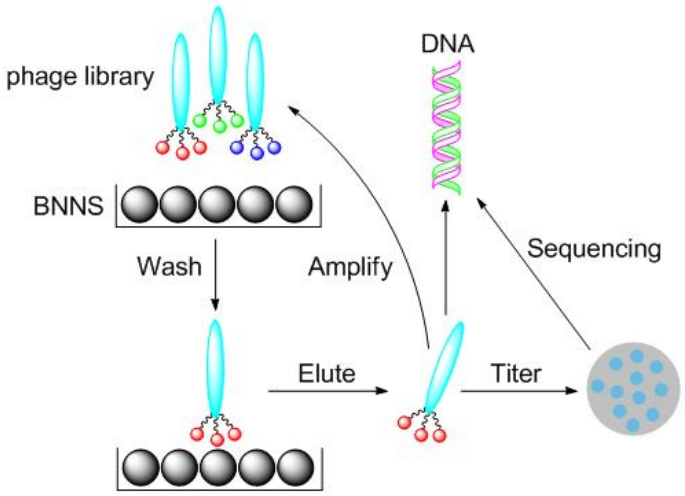

Figure 2.2 Schematic illustration of screening of BNNS-binding peptides using phage display.

2.2.3 Determination of peptide to BNNS affinity

FITC-labeled peptides were dissolved in TBS-T at 10 μg/mL. For direct binding studies, 500 μL of FITC-labeled peptide was added to an equal volume BNNS solution and incubated for 1 h at room temperature. The BNNS mixture was then washed 6 times with TBS-T to remove unbound phages. 10 μL of

peptide-bound BNNS suspension was placed on a glass slide, visualized by fluorescence microscopy (DM2500, Leica, Germany), and quantified with Image J software (written by Wayne Rasband). Binding affinities are expressed as the average fluorescence intensity of the images. In the control group, the BNNS were incubated without peptides.

2.2.4 Determination of peptide to BNNS specificity

Five-hundred microliters of FITC-labeled BP1 or BP7 (1 μg/mL in TBS-T) were incubated with 500 μg of BNNS or other nanomaterials for 1 h with gentle rotation. The mixture was then centrifuged and the supernatant was collected. Fluorescence intensities (FI) of the supernatants were measured by a microplate reader (MTP-880 Lab, Corona). The binding specificity of BP1 and BP7 to each nanomaterial was calculated as the percentage of each peptide that bound to it.

2.2.5 Characterization of peptides and BNNS

Circular dichroism (CD) spectra were obtained using a J-725 spectrophotometer (JASCO, Japan) at room temperature. Fluorescence spectra were analyzed by a F-7000 spectrofluorometer (Hitachi, Japan) with an excitation of 260 nm and a scanning rate of 240 nm/min. UV/vis absorption spectra were measured with a U-2900 spectrophotometer (Hitachi, Japan) at room temperature. Zeta potential measurements were conducted using a LEZA-600 electrophoresis zeta potential analyzer (Otsuka, Japan).

2.2.6 Cell culture

HeLa cells, a cervical cancer–derived cell line, were maintained in Eagle's minimum essential medium (MEM) (Life Technologies, Carlsberg, CA, USA) containing 10% v/v fetal bovine serum (FBS) and penicillin/streptomycin (100 mg/L medium). HEK293XL/null cells, a human embryonic kidney cell line, were purchased from InvivoGen (San Diego, CA, USA) and grown in Dulbecco's modified Eagle medium (DMEM) (Sigma-Aldrich, St. Louis, MO, USA) containing 10% (v/v) FBS and penicillin/streptomycin (100 mg/L). Frozen peripheral blood mononuclear cells (PBMCs) were purchased from Cellular Technology Limited (Shaker Heights, OH, USA) and thawed according to the manufacturer's protocol. All cell lines were incubated at 37 ℃ with 5% CO_2.

2.2.7 Cytotoxicity assay

Cytotoxicity of BNNS and the BNNS/BP7 complex was investigated using a water-soluble tetrazolium salt assay (CCK-8). A total of 4000 cells were seeded in a 96-well plate for 24 h to allow the cells to adhere, after which the cells were exposed to serial dilutions of BNNS, BNNS/BP7 complex, or medium (control). After a 24 h incubation at 37 ℃ with 5% CO_2, 10 μL of CCK-8 solution was added to each well and incubated for another 3 h. Next, the absorbance was measured at a wavelength of 450 nm. Cytotoxicity was expressed as the percentage of cell viability compared to that of untreated control cells.

2.2.8 Cellular uptake

HeLa or HEK293XL/null cells (4×10^4) were seeded in a 35-mm petri dish with a glass bottom and incubated for 24 h at 37 ℃ with 5% CO_2. BNNS/BP7 complex was then added to the dish at a final concentration of 50 μg/mL. After incubation for 24 h, the cells were washed twice with PBS and fixed with 3.7% (v/v) paraformaldehyde. The fixed cells were visualized using confocal laser scanning microscopy (SP5; CLSM, Leica, Germany).

2.2.9 Preparation of BP7–CpG ODNs conjugates

BP7–CpG ODNs conjugates were prepared using a protein–protein crosslinking kit (Molecular Probes, Invitrogen, CA, USA) according to the manufacturer's instructions. Briefly, a thiol-reactive maleimide group was introduced on the lysine residue of BP7 by incubation with excess trans-4-(maleimidylmethyl)cyclohexane-1-carboxylate. The BP7-maleimide was then incubated with thiol-labeled CpG ODNs to form a stable thioester bond between BP7 and CpG ODNs. The conjugates were confirmed by native polyacrylamide gel electrophoresis and ethidium bromide staining.

2.2.10 CpG ODNs loading

CpG ODNs and BP7–CpG ODNs conjugates were incubated with 40 μL of BNNS solution (2 mg/mL in PBS at pH 7.4) at a final concentration of 100 ng/mL for 1 h, followed by centrifugation to remove unbound material in the supernatant. Supernatant CpG ODNs concentration was measured by a Nano Drop

2000 spectrophotometer (Thermo Scientific). Loading capacity was defined as the amount of CpG ODNs per 1 mg BNNS. The CpG ODNs and BP7–CpG ODNs conjugates–loaded BNNS were resuspended by adding 46 μL PBS and used for cytokine induction. The microstructures of the BP7–CpG ODNs conjugates–loaded BNNS were observed by 3000F high-resolution field emission transmission electron microscopy (JEOL, Japan) operated at an acceleration voltage of 300 kV.

2.2.11 CpG ODNs release assay

One milliliter PBS (adjusted to pH 5.0 with HCl) was added to 1 mg CpG ODNs or BP7–CpG ODNs conjugates–loaded BNNS and stirred at room temperature. At regular intervals, the solution was centrifuged, and aliquots of PBS (200 μL) were removed to measure the concentration of released CpG ODNs. A total of 200 μL fresh PBS was added to the solution for each aliquot removed.

2.2.12 Cytokine assay

PBMCs were seeded in RPMI 1640 medium supplemented with 10% FBS, at a density of 5×10^6 cells/mL. Cells were immediately stimulated with CpG ODNs or BP7–CpG ODNs conjugates–loaded BNNS. The final concentration of BNNS was about 87 μg/mL. Free BP7–CpG ODNs conjugates were used at a final concentration of 1 μg/mL, corresponding to the concentration of the BNNS-loaded conjugates. After 24h and 8h of incubation respectively at 37℃, cell supernatants were collected for further analysis. The concentration of IL-6, TNF-α and IFN-α in the media was determined by enzyme-linked immunosorbent assay (ELISA) using the Ready-SET-Go! Human IL-6 kit (eBiosciences, CA, USA), Human TNF-α kit (eBiosciences, CA, USA) and Human IFN-alpha-Module set (eBioscience, Vienna, Austria), as per manufacturer's protocol.

2.2.13 Statistical analysis

Statistical analysis was performed using Student's t-test. Data are presented as mean ± SD. Differences were considered statistically significant for $*p < 0.05$ and $**p < 0.01$.

2.3 Results and discussion

2.3.1. Screening for BNNS-specific peptides

We used a randomized 12-mer peptide phage library (Ph.D.-12, New England Biolabs), which are commonly used for screening peptide aptamers against various targets. Phages were incubated with highly pure BNNS synthesized using chemical vapor deposition. The ratio of output to input phages increased continuously for 5 rounds of panning against BNNS (Figure 2.3), demonstrating that phages with higher affinities had been successfully concentrated in the phage pool. We randomly picked 96 individual clones from the phage pool. DNA sequence analysis revealed that the clones consisted of 8 different peptides (Table 2.1). Of these clones, LLADTTHHRPWT (referred to as BP1), had the highest frequency (58%).

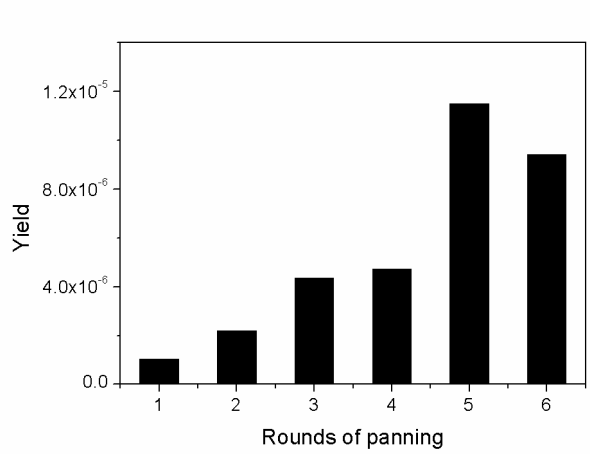

Figure 2.3 Yield (output phages /input phages) against the rounds of panning.

Table 2.1 Selected peptides with affinity for BNNS.

Name	Sequences	Frequency (%)	pI[a]
BP1	LLADTTHHRPWT	58.3	6.92
BP2	APLQPRSDNPFR	8.3	9.64
BP3	SATTPLIFPQTT	6.3	5.24
BP4	YPAPQPLVTKTS	6.3	8.59
BP5	ERSWTLDSALSM	5.2	4.37
BP6	QHSAAHYSTRLS	3.1	8.76
BP7	VDAQSKSYTLHD	3.1	5.39
BP8	SFHQLPARSPLP	2.1	9.49

[a] pI = isoelectric point. Values are calculated using online software (http://au.expasy.org/).

Similar to carbon nanotube (CNT)-binding peptides reported previously,[42] the BNNS-binding peptides were significantly rich in aromatic residues, including histidine (H) and tryptophan (W), compared to the original phage library (Figure 2.4). However, we could not find a consensus amino acid sequence or shared features in the selected peptides, suggesting that each peptide might have their own binding site and BNNS-binding mechanism.

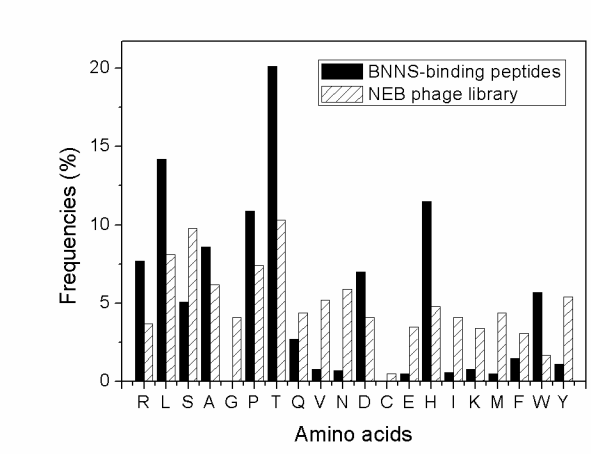

Figure 2.4 Amino acid frequencies in the BNNS-binding peptide sequence.

To further investigate the BNNS-binding affinities and specificities of the peptides, we labeled the peptides with fluorescein isothiocyanate. Fluorescent image analysis confirmed that all of the selected peptides bound to BNNS (Figure 2.5, Figure 2.6). Of them, 2 peptide sequences, LLADTTHHRPWT (BP1) and VDAQSKSYTLHD (BP7), showed a higher affinity for BNNS (Figure 2.5, Figure 2.6).

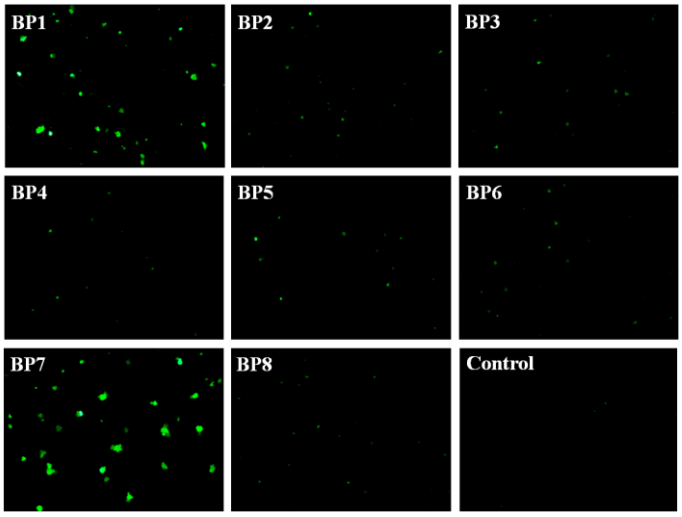

Figure 2.5 Fluorescence microscopy images of the FITC-labeled peptides binding to BNNS. In the control group, the BNNS were incubated without peptides.

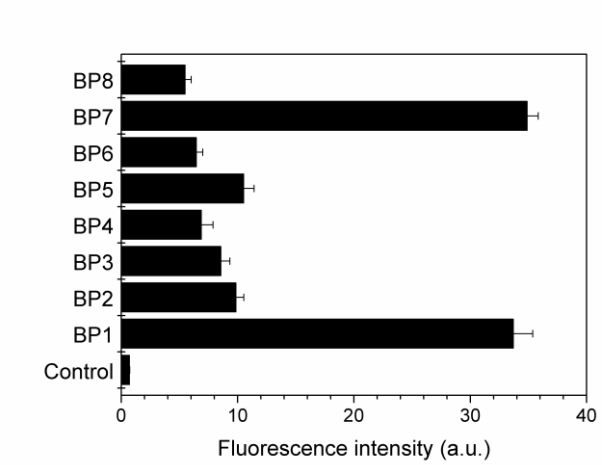

Figure 2.6 Binding affinities of the peptides for BNNS. FITC-labeled peptide was incubated with BNNS for 1 h, washed, and visualized. Binding affinity was determined by averaging the fluorescence intensity of the images.

We next examined the binding specificities of these 2 peptides with BNNS and 8 other types of nanomaterials. Although BP1 showed cross-affinity to various types of nanomaterials such as CNT, gold (Au) nanoparticles, and copper oxide (CuO) nanoparticles, as observed by other researchers,[33,42-43] BP7 specifically bound to BNNS (Figure 2.7). In addition, BP7 binding notably improved the solubility of BNNS in aqueous solution. The solubility and dispersion of BNNS are crucial characteristics for potential applications in drug delivery systems.

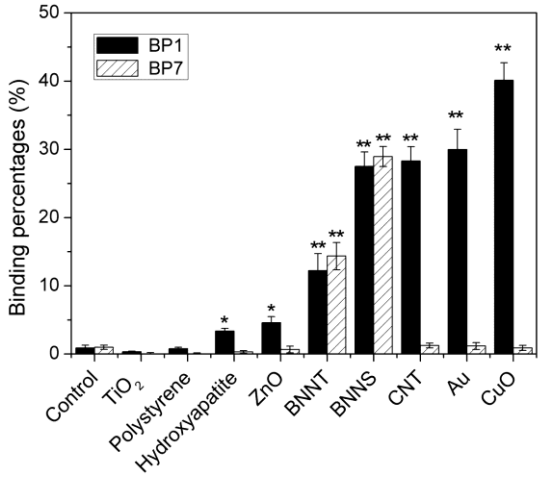

Figure 2.7 Binding specificities of the peptides for BNNS. FITC-labeled BP1 and BP7 were incubated with BNNS or other nanomaterials for 1 h. Solutions were centrifuged and unbound peptide was determined by the fluorescence intensity of supernatant. Binding specificities were calculated as the percentage of peptide that bound to each nanomaterial. Data are presented as mean ± SD (n = 3); *$p < 0.05$, **$p < 0.01$.

2.3.2 BP7 to BNNS binding properties

To identify key amino acid residues involved in the binding of BP7 to BNNS, we constructed a series of FITC-labeled BP7 variants in which specific amino acids were substituted by alanine (A) residues or terminal sequences were deleted. Replacing valine (V), tyrosine (Y), and leucine (L) at the first (V1), eighth (Y8), and tenth (L10) positions from the N-terminus of BP7 impaired BNNS binding (Figure. 2.8). In addition, the deletion of 3 residues from either terminus of BP7 also reduced the affinity. In particular, the mutation of tyrosine (Y8A) significantly affected the binding affinity for BNNS, suggesting that Y8 is essential for binding. Substitution of the remaining 4 amino acid residues with alanine (D2A, K6A, H11A, and D12A) had little effect on the binding. Tyrosine is an aromatic amino acid that is expected to form π–π interactions, while valine and leucine are nonpolar residues that easily form hydrophobic interactions. These interactions have been reported to be important for CNT and BNNT binding peptides.[25,32,44]

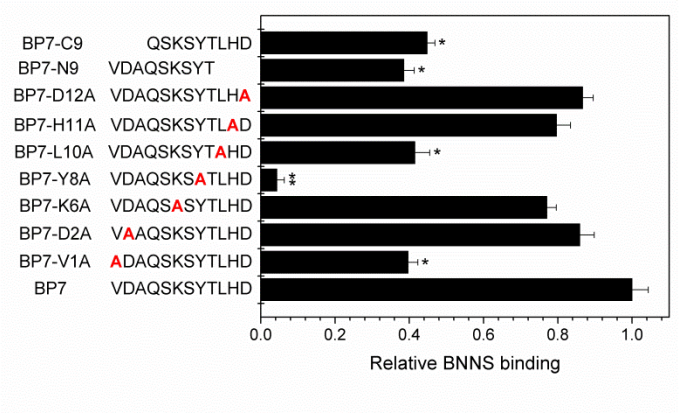

Figure 2.8 Binding affinity of BP7 mutants for BNNS. Terminal sequence deletion and Ala scanning (i.e., the substitution of alanine residues (A) for amino acids within the peptide) were used to determine key amino acids for BP7 binding. Binding affinity was determined as previously described and normalized to BP7 binding. Data are presented as mean ± SD (n = 3). *$p < 0.05$, **$p < 0.01$.

To characterize the conformational features of BP7, we measured the CD spectrum of free BP7 in the presence and absence of BNNS. Molecular conformation plays an important role in determining the binding strength of peptides to a target.[44-45] As shown in Figure 2.9, BP7 had a peak at around 200 nm in solution, which is a typical random coil spectrum. However, the spectrum dramatically changed when bound to BNNS, suggesting a conformational change of BP7 on the surface of BNNS. Such a conformational change from a

random coil is also reported in BP1 (also known as UW-1), which was identified as a binding peptide to single-walled CNT.[42] According to molecular dynamic simulation, peptides are believed to change their conformation and spatial arrangement on nanomaterials, depending on the surface energy of the nanomaterial and charge balance between peptide and material.[44]

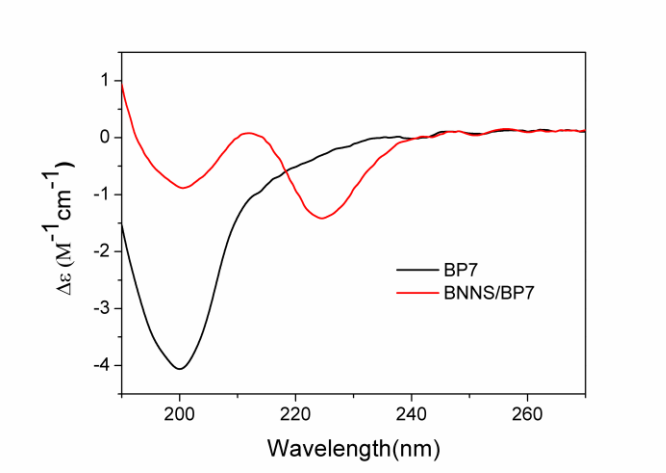

Figure 2.9 CD spectra of BP7 and the BNNS/BP7 complex measured between 190 nm and 270 nm with a scanning speed of 20 nm/min and a bandwidth of 0.5 nm.

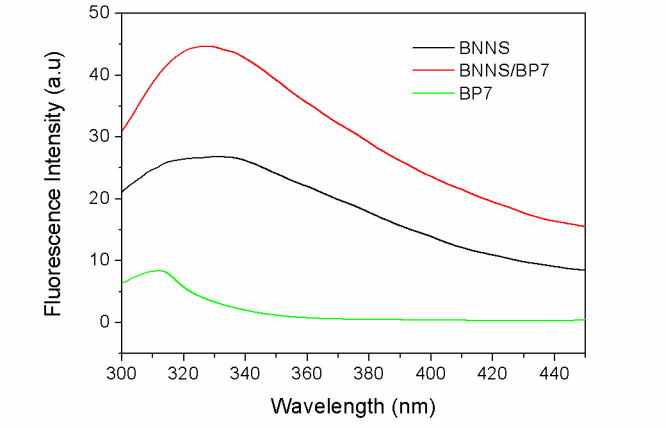

Figure 2.10 Fluorescence emission spectra of BNNS, BP7 and BNNS/BP7 complex in TBS buffer.

To gain further insight into the mechanism of the π–π interactions between BNNS and BP7, we investigated the fluorescence spectra of pure BNNS, pure BP7, and the BNNS/BP7 complex (Figure 2.10). The peak corresponding to tyrosine residues appeared at 313 nm in pure BP7 and shifted to 328 nm in the BNNS/BP7 complex. This result implies that a charge transfer occurred between BNNS and BP7 due to the strong π–π interactions, similar to the CNT-binding peptide reported previously.[42] Such charge transfer is also observed between CNT and polymers.[46] The UV/vis absorption spectra showed that the sharp peak assigned to pure BNNS appeared at 202 nm and shifted to 196 nm in the BNNS/BP7 complex (Figure. 2.11). This

observation suggests that the electronic structure of BNNS was affected by the charge transfer between BNNS and BP7 from the π–π interaction. However, the detailed mechanisms of this π–π interaction remain unclear.

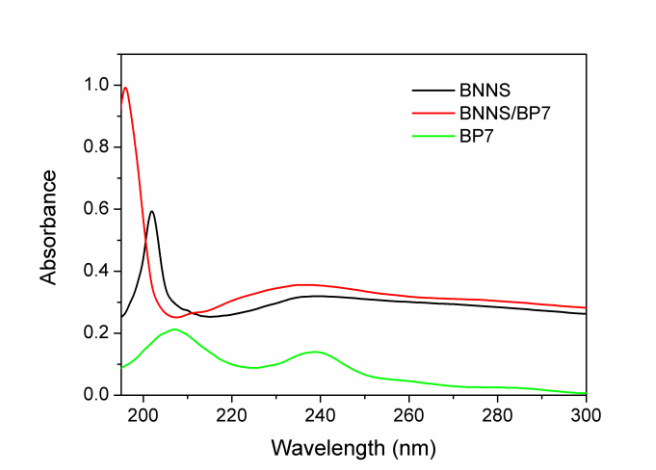

Figure 2.11 UV/vis absorption spectra of BNNS, BP7, and the BNNS/BP7 complex.

2.3.3 Cytotoxicity and cellular uptake of the BNNS/BP7 complex

Biological safety is a critical criterion in the application of nanomaterials as carriers for drug delivery.[47] Although BNNS and BNNT have been reported to be suitable materials for drug delivery, [27,31] the safety of the BNNS/BP7 complex warranted investigation. Similar to BNNS, the BNNS/BP7 complex showed no apparent decrease in cellular viability of human PBMCs and HEK293 cells (Figure 2.12), even at a concentration of 100 μg/mL, suggesting no cytotoxic effect of BP7 on the safety of BNNS.

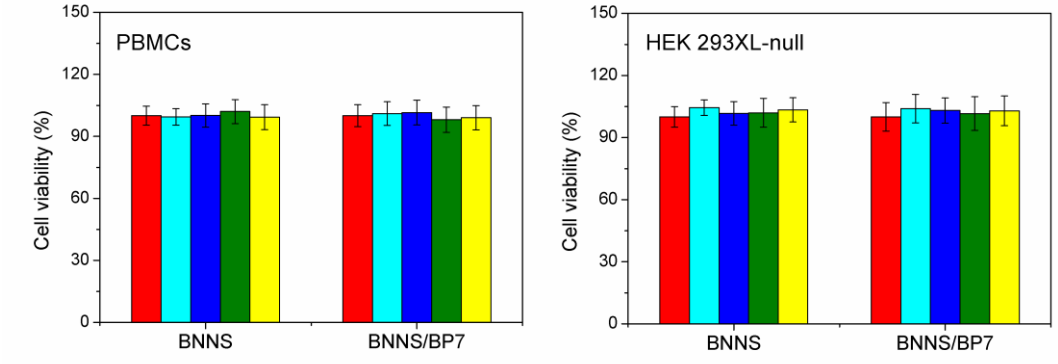

Figure 2.12 Cytotoxicity of BNNS and the BNNS/BP7 complex. Cells were incubated with increasing concentrations of BNNS or the BNNS/BP7 complex, and cell viability was measured by a water-soluble tetrazolium salt assay. Concentrations of the nanospheres: 0 μg/mL (Red), 25 μg/mL (Cyan), 50 μg/mL (Blue), 75 μg/mL (Olive), 100 μg/mL (Yellow). Data are presented as mean ± SD (n = 5).

Cellular uptake is another important criterion for the application of nanomaterials as an intracellular delivery system. When cells were incubated for 24 h with 50 μg/mL BNNS loaded with FITC-labeled BP7, we observed intracellular FITC fluorescence (Figure 2.13). This implies that BP7 was carried into the cells by BNNS. Moreover, compared to our previous cellular uptake investigation of the pure BNNS, no distinct enhancement by BP7 was observed in this study, both of the BNNS and the BNNS/BP7 complex showed good cellular uptake behavior. These results suggest that the BNNS/BP7 complex is an efficient carrier for intracellular delivery of CpG ODNs.

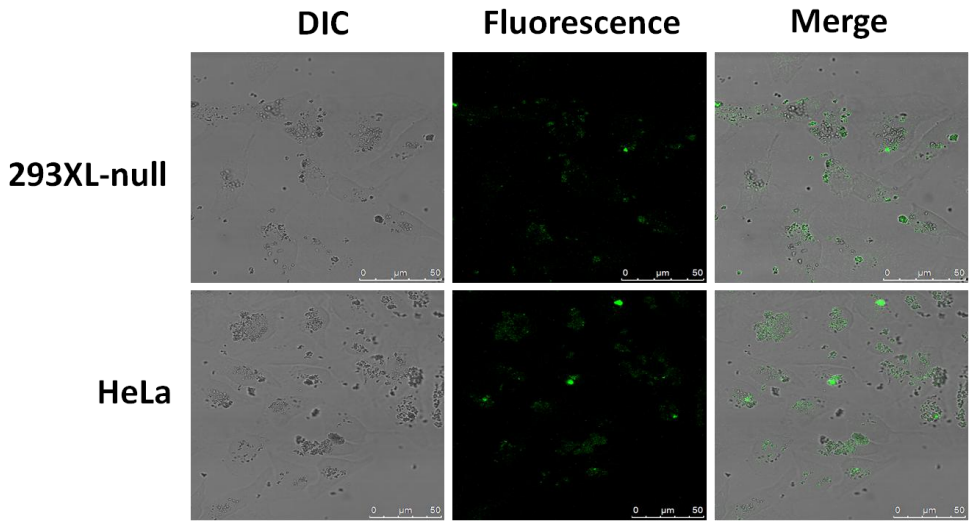

Figure 2.13 Cellular uptake of BNNS/BP7 complexes in HEK293XL-null and Hela cells.

2.3.4 Loading capacity of CpG ODNs on BNNS

We modified the lysine of BP7 with a thiol-reactive maleimide and thiolated the 3′ end of class-B CpG ODNs. The thiolated CpG ODNs were crosslinked with the maleimide-modified BP7, resulting in the formation of a BP7–CpG ODNs conjugates. The conjugates were then loaded on BNNS, with BP7 serving as a linker. The maximum loading capacity of CpG ODNs was dramatically increased when BP7 was used as a linker, to approximately 5-fold higher than CpG ODNs loaded directly onto BNNS (Figure 2.14). However, when we used another two BP7 mutants (BP7-Y8A and BP7-L10A) as linkers, which had the reduced affinity for BNNS, the loading capacity of their conjugates with CpG ODNs on BNNS significantly decreased compared to that of BP7 (Figure 2.14). These results suggest that the higher loading capacity of BP7–CpG ODNs is due to the high binding affinity of BP7 to BNNS.

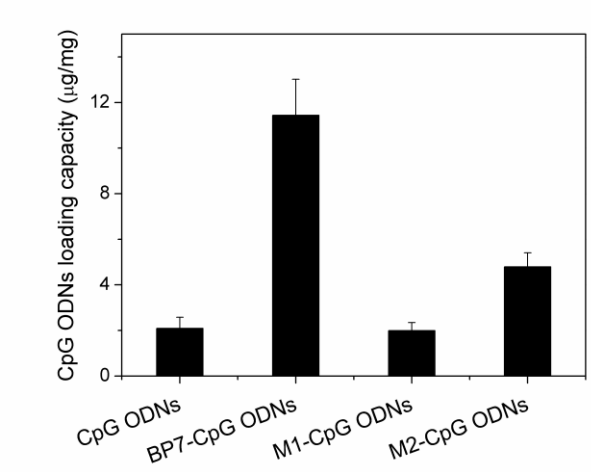

Figure 2.14 Loading capacity of CpG ODNs, BP7-CpG ODNs and BP7 mutants–CpG ODNs conjugates on BNNS, denoted as μg CpG ODNs loaded on 1 mg BNNS. M1 (BP7-Y8A) and M2 (BP7-L10A) are mutants of BP7 whose tyrosine (Y8) and leucine (L10) at eighth and tenth positions from N-terminal were replaced by alanine (A), respectively. Data presented as mean ± SD (n = 3).

We then examined the morphology of BP7–CpG ODNs conjugates on BNNS using a transmission electron microscope. An amorphous-like layer was clearly observed on the surface of BNNS (Figure 2.15), indicating the bound BP7–CpG ODNs conjugates. However, the conjugates were not uniformly distributed on the surface. This irregular binding may be attributed to the heterogeneity of the BNNS surface. Oxygen impurities might affect the affinity of BP7–CpG ODNs for the surface of BNNS, due to the irregular distribution of oxygen impurities during the formation of BNNS.[30]

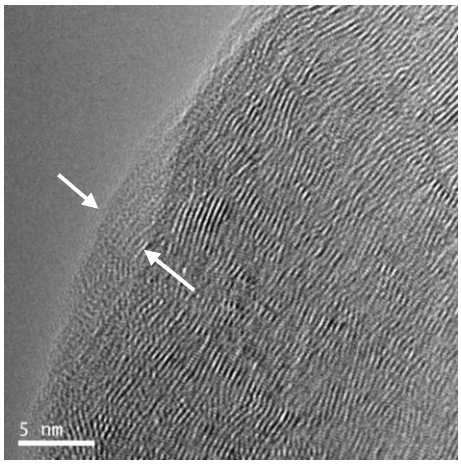

Figure 2.15 TEM image of BP7–CpG ODNs conjugate–loaded BNNS. The white arrows indicate the bound layer of BP7–CpG ODNs conjugate.

Next, we tested the release of the BP7–CpG ODNs conjugates from the surface of BNNS under acidic conditions that correspond to the physiological environment in a TLR 9-localized endolysosome. Approximately 65% of CpG ODNs directly bound to BNNS was quickly released from BNNS within 12 h, while only 30% of the BP7–CpG ODNs conjugates were released within 24 h (Figure 2.16). After 48 h, almost no further release of the BP7–CpG ODNs conjugates could be observed. This suggests CpG ODNs could not be easily released from BNNS surface because of the stronger binding of the BP7–CpG ODNs conjugates to BNNS than direct binding of CpG ODNs.

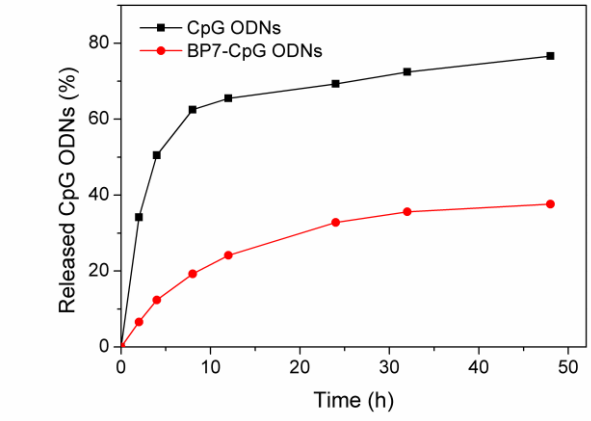

Figure 2.16 Release profile of CpG ODNs and the BP7–CpG ODNs conjugate loaded on BNNS at pH 5.

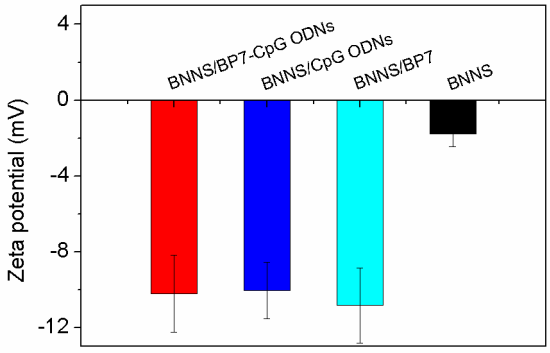

Figure 2.17 Zeta potentials of BNNS, BNNS/BP7, BNNS/CpG ODNs, BNNS/BP7-CpG ODNs complexs in TBS buffer (pH 7.4). Data presented as mean ± SD (n =6).

Zeta potential showed that BNNS have a slight negative surface charge density (Figure 2.17), suggesting that the lower loading capacity of negatively charged, free CpG ODNs may be due to the negative surface charge of BNNS. However, the BNNS/BP7 complex showed a higher negative charge density compared to BNNS, implying that BP7 also has a negative charge. This is in accordance with our theoretical prediction (Table 1), that BP7 had a predicted isoelectric point of 5.39. However, BP7 was still able to bind

to the negatively charged BNNS, suggesting that the strong π–π interaction and hydrophobic interaction between BNNS and BP7 can overcome the electrostatic repulsion.

2.3.5 Cytokine induction by BP7-CpG ODNs conjugates delivered by BNNS

Though the class-B CpG ODNs used in this study activates TLR 9 and induces IL-6 and TNF-α, it does not potently induce IFN-α to the extent of class-A CpG ODNs.[48-52] However, Kerkmann et al. reported that class-B CpG ODNs loaded on cationic polystyrene nanoparticles with a diameter of 180 nm induced IFN-α to a greater degree than did free class-A CpG ODNs.[53]

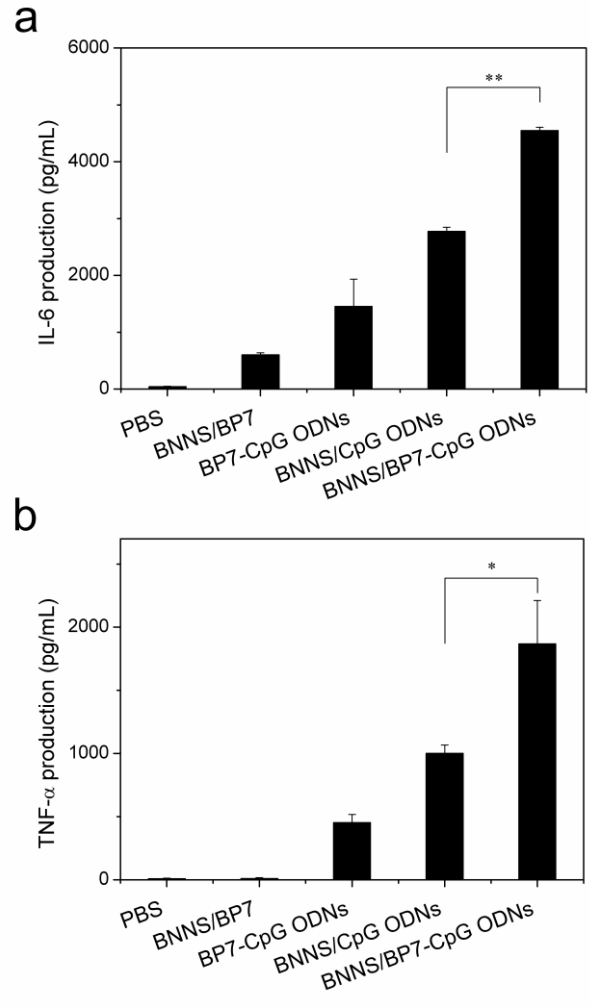

Figure 2.18 Cytokine induction in PBMCs stimulated by BP7–CpG ODNs conjugate–loaded BNNS. Loaded BNNS (87 μg/mL) or a corresponding concentration of free BP7–CpG ODNs conjugate (1 μg/mL) was incubated with PBMCs for 8h (TNF-α) and 24h (IL-6) respectively. (a) IL-6 production. (b) TNF-α production. Data are presented as mean ± SD (n = 3); *$p < 0.05$, **$p < 0.01$.

The BP7–CpG ODNs induced IL-6 and TNF-α (Figure 2.18), but not IFN-α (Figure 2.19). CpG ODNs loaded directly on BNNS induced about twice the amount of IL-6 and TNF-α than the free BP7–CpG ODNs conjugate (Figure 2.18). This was mainly due to the improved cellular uptake efficiency of CpG ODNs by the BNNS carrier. In our previous work, when fluorescein labeled free CpG ODNs was added to cultured 239XL-TLR 9 cells, fluorescence was not observed inside the cells. In contrast, strong fluorescence was observed in CpG ODNs when delivered by BNNS.[31] As expected, BP7–CpG ODNs conjugates loaded BNNS induced the highest level of IL-6 and TNF-α (Figure 2.18). However, when we used another two BP7 mutants (BP7-Y8A and BP7-L10A)–CpG ODNs conjugates loaded BNNS to stimulate the PBMCs, the level of IL-6 and TNF-α induction significantly decreased compared to that of BP7 (Figure 2.20). This indicates that the higher IL-6 and TNF-α induction of BP7–CpG ODNs conjugates loaded BNNS should be attributed to the higher loading capacity of BP7–CpG ODNs on BNNS.

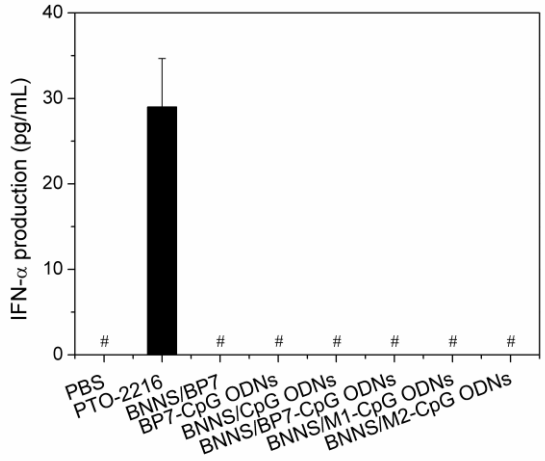

Figure 2.19 IFN-α induction from PBMCs stimulated by CpG ODNs. M1 (BP7-Y8A) and M2 (BP7-L10A) are mutants of BP7 whose tyrosine (Y8) and leucine (L10) at eighth and tenth positions from N-terminal were replaced by alanine (A), respectively. The concentration of the BNNS was about 87μg/mL. PTO-2216 CpG ODNs are positive control. Data presented as mean ± SD (n =3). The symbol # means not detectable (below detection limit).

IL-6 and TNF-α induction is thought to be mainly by BP7–CpG ODNs on BNNS, but not free BP7–CpG ODNs released from BNNS. BP7–CpG ODNs without BNNS and BP7–CpG ODNs loaded on BNNS were used at the same concentration. Therefore, since only 30% of the BP7–CpG ODNs conjugates were released from BNNS within 24 h, IL-6 and TNF-α induction by released BP7-CpG ODNs alone would

have resulted in less IL-6 and TNF-α than that induced by free BP7–CpG ODNs.

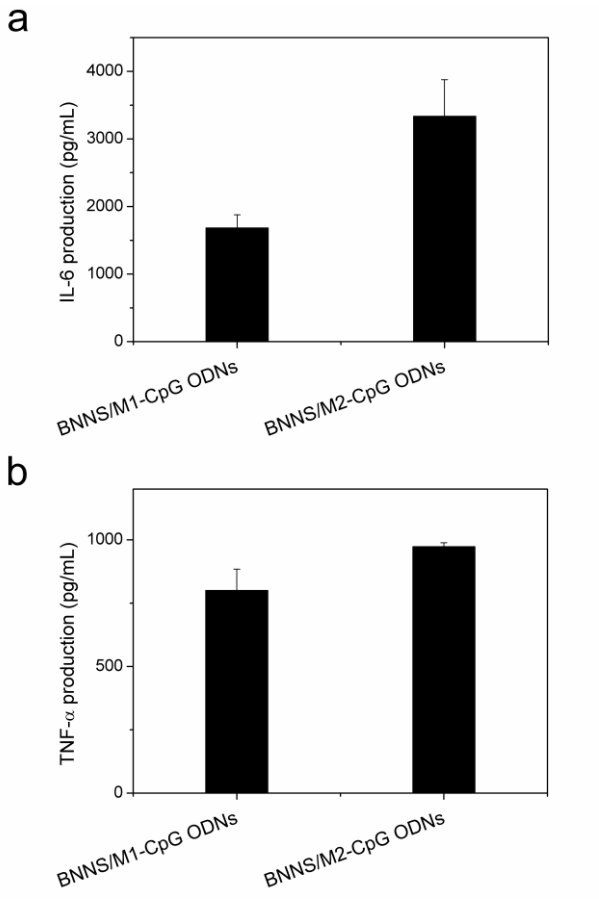

Figure 2.20 Cytokine induction from PBMCs stimulated by BP7 mutants–CpG ODNs conjugate–loaded BNNS. (a) IL-6 production. (b) TNF-α production. Loaded BNNS (87 μg/mL) was incubated with PBMCs for 8 h (TNF-α) and 24 h (IL-6) respectively, M1 (BP7-Y8A) and M2 (BP7-L10A) are mutants of BP7 whose tyrosine (Y8) and leucine (L10) at eighth and tenth positions from N-terminal were replaced by alanine (A), respectively. Data are presented as mean ± SD (n = 3).

Structure of the CpG ODNs plays an important role in their immunostimulatory effect.[54] Class A CpG ODNs induce the production of IFN-α, as they form a higher-order structures. However, such higher-order structures are not observed in class B CpG ODNs, they form a linear structures.[55] Although unmodified class-B CpG ODNs do not have the potential to induce IFN-α, it has been reported that class-B CpG ODNs electrostatically adsorbed onto polystyrene and silica nanoparticles induce IFN-α.[53] However, BP7-CpG ODNs loaded on BNNS, like free CpG-ODNs, were not capable of inducing IFN-α. The polystyrene nanoparticles used in the studies had surfaces coated with cations for electrostatic binding of CpG ODNs.[53]

Because of this, it is possible that all of the nucleotides in CpG ODNs bound to the cationic surface of the nanoparticles, since the negatively charged phosphate group of the nucleotides was involved in the electrostatic binding. In contrast, in BP7–CpG ODNs conjugates, only 1 terminus (3′ end) of a CpG ODNs indirectly binds to the surface of BNNS through the linker peptide BP7, since the 3′ end of CpG ODNs is thiolated for crosslinking with maleimide-modified BP7. Therefore, the method of binding for BP7–CpG ODNs on BNNS differs from CpG ODNs binding on polystyrene nanoparticles. This difference in binding method may affect the activation of TLR 9 and further influence the potential for cytokine induction.

2.4 Conclusion

The peptide BP7 (VDAQSKSYTLHD) was identified from a combinatorial phage display library and was found to exhibit a highly specific binding to BNNS. The tyrosine residue (Y8) of BP7 was critical to maintain high affinity for BNNS. Attractive π–π interactions are considered to be the main driving force for the binding of BP7 to BNNS, although hydrophobic interactions may also be involved in the binding, which leads to a conformational change of BP7 on the surface of BNNS. The BNNS/BP7 complex was easily taken up by cells, and showed no cytotoxicity. By using BP7 as a linker molecule, BNNS were capable of delivering CpG ODNs to immune cells. BP7–CpG ODNs conjugates loaded on BNNS improved the capacity of IL-6 and TNF-α induction from PBMCs compared to that of CpG ODNs directly loaded on BNNS. The higher potential for cytokine induction in the BP7–CpG ODNs conjugates–loaded BNNS may be attributed to a higher loading capacity and stronger binding to BNNS. We anticipate that these findings will open a new avenue for the functionalization of BNNS with peptides and pave the way for the application of BNNS in the delivery of nucleic acid therapies, such as CpG ODNs and small interfering RNA.

2.5 References

1. Klinman DM. Immunotherapeutic uses of CpG oligodeoxynucleotides. *Nat. Rev. Immunol.* 2004;4(4):248-257.
2. Wagner H. Bacterial CpG DNA activates immune cells to signal infectious danger. *Adv. Immunol.* 1999;73:329-368.
3. Krieg AM, Yi AK, Matson S, et al. CpG motifs in bacterial DNA trigger direct B-cell activation. *Nature.* 1995;374(6522):546-549.
4. Vollmer J, Krieg AM. Immunotherapeutic applications of CpG oligodeoxynucleotide TLR9 agonists. *Adv. Drug Delivery. Rev.* 2009;61(3):195-204.
5. Hemmi H, Takeuchi O, Kawai T, et al. A Toll-like receptor recognizes bacterial DNA. *Nature.* 2000;408(6813):740-745.
6. Bauer S, Kirschning CJ, Häcker H, et al. Human TLR9 confers responsiveness to bacterial DNA via species-specific CpG motif recognition. *Proc. Natl. Acad. Sci. U. S. A.* 2001;98(16):9237-9242.
7. Klinman DM, Yi AK, Beaucage SL, Conover J, Krieg AM. CpG motifs present in bacterial DNA rapidly induce lymphocytes to secrete interleukin 6, interleukin 12, and interferon gamma. *Proc. Natl. Acad. Sci. U. S. A.* 1996;93(7):2879-2883.
8. Krieg AM. Therapeutic potential of Toll-like receptor 9 activation. *Nat. Rev. Drug Discov.* 2006;5(6):471-484.
9. Murad YM, Clay TM. CpG Oligodeoxynudeofides as TLR9 Agonists Therapeutic Applications in Cancer. *BioDrugs.* 2009;23(6):361-375.
10. Fonseca DE, Kline JN. Use of CpG oligonucleotides in treatment of asthma and allergic disease. *Adv. Drug Delivery. Rev.* 2009;61(3):256-262.
11. Klinman DM, Klaschik S, Sato T, Tross D. CpG oligonucleotides as adjuvants for vaccines targeting infectious diseases. *Adv. Drug Delivery. Rev.* 2009;61(3):248-255.
12. Agrawal S, Zhao QY. Antisense therapeutics. *Curr. Opin. Chem. Biol.* 1998;2(4):519-528.
13. Mutwiri GK, Nichani AK, Babiuk S, Babiuk LA. Strategies for enhancing the immunostimulatory effects of CpG oligodeoxynucleotides. *J. Controlled Release.* 2004;97(1):1-17.

14. Kurreck J. Antisense technologies - Improvement through novel chemical modifications. *Eur. J. Biochem.* 2003;270(8):1628-1644.

15. Sheehan JP, Lan HC. Phosphorothioate oligonucleotides inhibit the intrinsic tenase complex. *Blood.* 1998;92(5):1617-1625.

16. Levin AA. A review of issues in the pharmacokinetics and toxicology of phosphorothioate antisense oligonucleotides. *Biochim. Biophys. Acta, Gene Struct. Expression.* 1999;1489(1):69-84.

17. Henry SP, Beattie G, Yeh G, et al. Complement activation is responsible for acute toxicities in rhesus monkeys treated with a phosphorothioate oligodeoxynucleotide. *Int. Immunopharmacol.* 2002;2(12):1657-1666.

18. Wilson KD, de Jong SD, Tam YK. Lipid-based delivery of CpG oligonucleotides enhances immunotherapeutic efficacy. *Adv. Drug Delivery. Rev.* 2009;61(3):233-242.

19. Bianco A, Hoebeke J, Godefroy S, et al. Cationic carbon nanotubes bind to CpG oligodeoxynucleotides and enhance their immunostimulatory properties. *J. Am. Chem. Soc.* 2004;127(1):58-59.

20. Standley SM, Mende I, Goh SL, et al. Incorporation of CpG oligonucleotide ligand into protein-loaded particle vaccines promotes antigen-specific CD8 T-cell immunity. *Bioconjugate Chem.* 2006;18(1):77-83.

21. Rattanakiat S, Nishikawa M, Funabashi H, Luo D, Takakura Y. The assembly of a short linear natural cytosine-phosphate-guanine DNA into dendritic structures and its effect on immunostimulatory activity. *Biomaterials.* 2009;30(29):5701-5706.

22. Zhu Y, Meng W, Li X, Gao H, Hanagata N. Design of mesoporous silica/cytosine−phosphodiester−guanine oligodeoxynucleotide complexes to enhance delivery efficiency. *J. Phys. Chem. C.* 2010;115(2):447-452.

23. Chopra NG, Luyken RJ, Cherrey K, et al. Boron-nitride nanotubes. *Science.* 1995;269(5226):966-967.

24. Zhi CY, Bando Y, Tang CC, Xie RG, Sekiguchi T, Golberg D. Perfectly dissolved boron nitride nanotubes due to polymer wrapping. *J. Am. Chem. Soc.* 2005;127(46):15996-15997.

25. Gao ZH, Zhi CY, Bando Y, Golberg D, Serizawa T. Isolation of individual boron nitride nanotubes

via peptide wrapping. *J. Am. Chem. Soc.* 2010;132(14):4976-4977.

26. Golberg D, Bando Y, Tang CC, Zhi CY. Boron nitride nanotubes. *Adv. Mater.* 2007;19(18):2413-2432.

27. Chen X, Wu P, Rousseas M, et al. Boron nitride nanotubes are noncytotoxic and can be functionalized for interaction with proteins and cells. *J. Am. Chem. Soc.* 2009;131(3):890-891.

28. Jonsson E, Simonsen L, Karlsson M, Larsson R. The hollow fiber model: A new method for in vivo-evaluation of antitumor effect, toxicity and pharmacokinetics of new anticancer drugs. *Ann. Oncol.* 1998;9(S2):44-44.

29. Waritz RS, Ballantyne B, Clary JJ. Subchronic inhalation toxicity of 3.5-μm diameter carbon fibers in rats. *J. Appl. Toxicol.* 1998;18(3):215-223.

30. Tang CC, Bando Y, Huang Y, Zhi CY, Golberg D. Synthetic routes and formation mechanisms of spherical boron nitride nanoparticles. *Adv. Funct. Mater.* 2008;18(22):3653-3661.

31. Zhi CY, Meng WJ, Yamazaki T, et al. BN nanospheres as CpG ODN carriers for activation of toll-like receptor 9. *J. Mater. Chem.* 2011;21(14):5219-5222.

32. Wang SQ, Humphreys ES, Chung SY, et al. Peptides with selective affinity for carbon nanotubes. *Nat. Mater.* 2003;2(3):196-200.

33. Roy MD, Stanley SK, Amis EJ, Becker ML. Identification of a highly specific hydroxyapatite-binding peptide using phage display. *Adv. Mater.* 2008;20(10):1830-1836.

34. Sano K-I, Shiba K. A hexapeptide motif that electrostatically binds to the surface of Titanium. *J. Am. Chem. Soc.* 2003;125(47):14234-14235.

35. Sarikaya M, Tamerler C, Jen AKY, Schulten K, Baneyx F. Molecular biomimetics: nanotechnology through biology. *Nat. Mater.* 2003;2(9):577-585.

36. Cui Y, Kim SN, Jones SE, Wissler LL, Naik RR, McAlpine MC. Chemical functionalization of graphene enabled by phage displayed peptides. *Nano Lett.* 2010;10(11):4559-4565.

37. Goede K, Busch P, Grundmann M. Binding specificity of a peptide on semiconductor surfaces. *Nano Lett.* 2004;4(11):2115-2120.

38. Whaley SR, English DS, Hu EL, Barbara PF, Belcher AM. Selection of peptides with semiconductor binding specificity for directed nanocrystal assembly. *Nature.* 2000;405(6787):665-668.

39. Serizawa T, Sawada T, Matsuno H. Highly specific affinities of short peptides against synthetic polymers. *Langmuir.* 2007;23(22):11127-11133.

40. Yu RZ, Geary RS, Leeds JM, et al. Pharmacokinetics and tissue disposition in monkeys of an antisense oligonucleotide inhibitor of Ha-ras encapsulated in stealth liposomes. *Pharm. Res.* 1999;16(8):1309-1315.

41. Meng WJ, Yamazaki T, Nishida Y, Hanagata N. Nuclease-resistant immunostimulatory phosphodiester CpG oligodeoxynucleotides as human Toll-like receptor 9 agonists. *BMC Biotechnol.* 2011;11:88.

42. Su ZD, Leung T, Honek JF. Conformational selectivity of peptides for single-walled carbon nanotubes. *J. Phys. Chem. B.* 2006;110(47):23623-23627.

43. Ejima H, Matsuno H, Serizawa T. Biological identification of peptides that specifically bind to poly(phenylene vinylene) surfaces: recognition of the branched or linear structure of the conjugated polymer. *Langmuir.* 2010;26(22):17278-17285.

44. Slocik JM, Naik RR. Probing peptide-nanomaterial interactions. *Chem. Soc. Rev.* 2010;39(9):3454-3463.

45. Hnilova M, Oren EE, Seker UOS, et al. Effect of molecular conformations on the adsorption behavior of gold-binding peptides. *Langmuir.* 2008;24(21):12440-12445.

46. Chen J, Liu H, Weimer WA, Halls MD, Waldeck DH, Walker GC. Noncovalent engineering of carbon nanotube surfaces by rigid, functional conjugated polymers. *J. Am. Chem. Soc.* 2002;124(31):9034-9035.

47. Zhu YF, Ikoma T, Hanagata N, Kaskel S. Rattle-type Fe_3O_4@SiO_2 hollow mesoporous spheres as carriers for drug delivery. *Small.* 2010;6(3):471-478.

48. Krieg AM. CpG motifs in bacterial DNA and their immune effects. *Annu. Rev. Immunol.* 2002;20:709-760.

49. Gursel M, Verthelyi D, Gursel I, Ishii KJ, Klinman DM. Differential and competitive activation of human immune cells by distinct classes of CpG oligodeoxynucleotide. *J. Leukocyte Biol.* 2002;71(5):813-820.

50. Hartmann G, Krieg AM. Mechanism and function of a newly identified CpG DNA moth in human

primary B cells. *J. Immunol.* 2000;164(2):944-952.

51. Hartmann G, Weeratna RD, Ballas ZK, et al. Delineation of a CpG phosphorothioate oligodeoxynucleotide for activating primate immune responses in vitro and in vivo. *J. Immunol.* 2000;164(3):1617-1624.

52. Krug A, Towarowski A, Britsch S, et al. Toll-like receptor expression reveals CpG DNA as a unique microbial stimulus for plasmacytoid dendritic cells which synergizes with CD40 ligand to induce high amounts of IL-12. *Eur. J. Immunol.* 2001;31(10):3026-3037.

53. Kerkmann M, Costa LT, Richter C, et al. Spontaneous formation of nucleic acid-based nanoparticles is responsible for high interferon-α induction by CpG-A in plasmacytoid dendritic cells. *J. Biol. Chem.* 2005;280(9):8086-8093.

54. Hanagata N. Structure-dependent immunostimulatory effect of CpG oligodeoxynucleotides and their delivery system. *Int. J. Nanomedicine.* 2012;7:2181-2195.

55. Klein DCG, Latz E, Espevik T, Stokke BT. Higher order structure of short immunostimulatory oligonucleotides studied by atomic force microscopy. *Ultramicroscopy.* 2010;110(6):689-693.

Chapter 3 Polyethyleneimine-functionalized BNNS as an efficient carrier for enhancing the immunostimulatory effect of CpG ODNs

3.1 Introduction

Bacterial DNA has been known for its immunostimulatory effect, which activates host defense system leading to innate and adaptive immune responses.[1-4] The specific sequence present in bacterial DNA that is responsible for those effects is the unmethylated CpG motif.[1,5] Synthetic ODNs containing unmethylated CpG motifs are like those found in bacterial DNA and possess similar immunostimulatory effects.[1,6] After taken up by immune cells, CpG ODNs bind to intracellular TLR 9 in the endosomes of B cells and plasmacytoid dendritic cells.[2-3,7] The binding initiates an immunostimulatory cascade that induce the maturation, differentiation, and proliferation of multiple immune cells including B and T lymphocytes, NK cells, and monocytes/macrophage.[8-9] This further triggers cell signaling pathways including MAPKs and NFκB, subsequently results in the induction of multiple proinflammatory cytokines and chemokines and modulates the cellular inflammatory response.[10-11] These abilities enable CpG ODNs to act as promising immune adjuvants, as well as immunotherapeutic agents against allergy/asthma, cancer, and infectious diseases.[11-14] However, the biologic activity of CpG ODNs is reported to be transient, furthermore, the extreme susceptibility to nuclease degradation in serum and poor cellular uptake of natural CpG ODNs severely limits their therapeutic applications.[15-16] Therefore, there has been great interest in developing approaches to optimize the stimulatory activity of CpG ODNs. Many strategies are involved in chemical modification of the CpG ODNs backbone. For instance, substituting the oxygen with sulfur generates a phosphorothioate CpG ODNs, which are more resistant to nuclease degradation and possess a better immunostimulatory effect.[16-17] However, several severe side effects caused by the modification of CpG ODNs backbone has been reported.[18-19] In this regard, many research has been conducted on searching for delivery systems to improve the stimulatory activity of CpG ODNs. Evidence is accumulating indicates that both the innate and adaptive immune responses induced by CpG ODNs can be significantly enhanced by using various nanoparticles as carriers.[16-17] Therefore, using nanoparticles as carriers may make it possible to

use naturally occurring CpG ODNs in clinical applications.

Nowadays, increasing attention has been paid to BN thanks to its outstanding properties and structural similarity with carbon.[20-21] BN also possess the advantage of easier cellular uptake and lower cytotoxicity than carbon materials.[22-23] Therefore, BN has found many applications ranging from composite materials to electrical and optical devices.[21,24] Furthermore, biomedical application of the BN nanomaterials has also been reported. Both *in vitro* and *in vivo* experiments suggested that BNNT had the optimal biocompatibility, indicating their potential biomedical applications.[25-27] We previously used BNNS as carrier for the delivery of unmodified CpG ODNs on activation of TLR 9.[28] BNNS exhibited no cytotoxicity and protected unmodified CpG ODNs from nuclease degradation. Furthermore, BNNS delivered CpG ODNs into lysosome compartments of the immune cells and stimulated an enhanced immune response compared to free CpG ODNs. However, since CpG ODNs and BNNS are both negatively charged, the loading capacity and cellular uptake efficiency of CpG ODNs is thought to be limited by the electrostatic repulsion and could not induce a robust cytokine response. Furthermore, B class CpG ODNs loaded on BNNS only induced the IL-6 and TNF-α, but could not induce IFN-α. However, high amount of IFN-α induction was reported when class-B CpG ODNs were adsorbed electrostatically onto polystyrene nanoparticles.[29] We hypothesized that methods which enhance the CpG ODNs internalization by immune cells may potentiate their immunostimulatory effect. And if the class-B CpG ODNs are loaded electrostatically onto BNNS, they may acquire the ability to induce IFN-α.

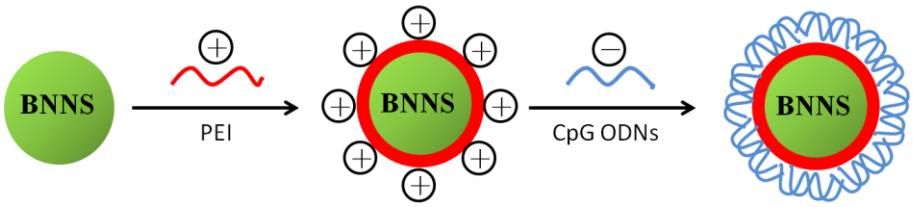

Figure 3.1 Schematic illustration of the process for preparation of the PEI-functionalized BNNS as an efficient CpG ODNs carrier.

In this chapter, we developed a novel CpG ODNs delivery system based on polyethyleneimine (PEI)-functionalized BNNS (Figure 3.1). PEI has been recognized as the ‘golden standard’ cationic polymer for nucleic acid delivery, either used alone or used for surface coating of nanoparticles to bind negatively charged nucleic acid drug.[30-31] Furthermore, PEI with low molecular weight are reported to be less toxic, and

more effective as a coating material for nanoparticles to enhance the immunostimulatory effect of CpG ODNs.[32] The loading capacity and the cellular uptake of CpG ODNs loaded on BNNS-PEI were investigated. The enhanced immunostimulatory effect of CpG ODNs by using PEI-functionalized BNNS as carrier was also studied and discussed in detail.

3.2 Materials and methods

3.2.1 Materials

Branched PEI with average molecular weight of 600 Da was purchased from Wako Pure Chemicals (Osaka, Japan). Phosphodiester-based class-B CpG ODNs, referred to as CpG ODNs 2006x3-PD,[33] were obtained from Fasmac, Inc. (Kanagawa, Japan) and diluted in sterile water at a concentration of 100 μM then stored at -20 ℃. Frozen PBMCs were purchased from Cellular Technology Limited (OH, USA) and thawed according to the manufacturer's protocol. RPMI-1640 medium and fetal bovine serum (FBS) were obtained form Gibco (NY, USA). Cell Counting Kit-8 (CCK-8) was purchased from Dojindo (Kumamoto, Japan).

3.2.2 Preparation of BNNS-PEI complexes

BNNS with high purity were synthesized by a chemical vapor deposition method as previously reported.[34] PEI was diluted with Milli-Q water to a concentration of 10 % (v/v) prior to use. Working solutions were prepared from the stock by dilution with Milli-Q water. For the functionalization of the BNNS, 1 mg of the BNNS was suspended in 1 mL PEI solution and stirred at room temperature for 2 hours. Then the PEI-functionalized BNNS were washed five times with Milli-Q water by centrifugation and re-dispersed in phosphate-buffered saline.

3.2.3 Characterizations

Fourier transform infrared (FTIR) spectra were performed on a Spectrum GX spectrophotometer (Perkin Elmer, USA) at 4 cm^{-1} resolution with 32 scans. Transmission electron microscopy were conducted by a 3000F high-resolution field emission transmission electron microscopy (JEOL, Japan) operated at an acceleration voltage of 300 kV. Dynamic light scattering (DLS) measurements were obtained using a Photal

DLS-6000DL instrument (Otsuka, Japan). Zeta potential measurements were carried out using a LEZA-600 electrophoresis zeta potential analyzer (Otsuka, Japan). Thermogravimetric analysis were conducted on an SII TG/DTA 6200 system using a heating rate of 5℃ per minute with an open alumina cell.

3.2.4 Cell culture and in vitro cytotoxicity assay

Frozen human PBMCs were thawed according to the manufacturer's protocol. The cytotoxicity of BNNS and the BNNS-PEI complexes to PBMCs were evaluated using a CCK-8 assay. PBMCs were seeded into 96-well plate at a density of 50000 cells per well. After 24 h incubation at 37℃ with 5% CO_2 until the cells adhered to the plate, a series concentrations of BNNS, BNNS-PEI complexes were added into the cell culture. After another 24 h incubation, 10 μL of CCK-8 solution was added to each well and incubated for an additional 3 h. Finally, the absorbance at 450 nm was measured using the microplate reader to determine the relative cell viability.

3.2.5 Preparation of BNNS-PEI/CpG ODNs complexes

25 μL of CpG ODNs solution was added to equal volume of BNNS-PEI solution (2 mg/mL in PBS at pH 7.4) and shaken at room temperature for 1 h. The mixture was then centrifuged at 15000 rpm for 15 minutes to collect the BNNS-PEI/CpG ODNs complexes. Binding of the CpG ODNs to the BNNS-PEI was further confirmed by the gel electrophoresis using a 10-20% gel. BNNS-PEI were incubated with CpG ODNs at various weight ratio (BNNS-PEI/CpG ODNs) from 5 to 100, then the mixture was centrifuged and the supernatant was collected for gel electrophoresis. CpG ODNs in the gel were visualized by ethidium bromide using a Dolphin-Doc UV transilluminator (Kurabo, Japan). Loading capacity was calculated from the concentration of the unloaded CpG ODNs in the supernatant measured by a NanoDrop 2000 spectrophotometer (Thermo Scientific). The BNNS-PEI/CpG ODNs complexes were resuspended by adding 50 μL PBS and used for the following cytokine stimulation.

3.2.6 Uptake of CpG ODNs by human PBMCs

Human PBMCs (8×10^4) were seeded in a 35-mm petri dish with a glass bottom and incubated for 24 h at 37℃ with 5% CO_2. BNNS/FITC-CpG ODNs and BNNS-PEI/FITC-CpG ODNs complexes were then

added to the dish at a final concentration of 50 μg/mL, free FITC-CpG ODNs and BNNS were used as control. After incubation for 24 h, the cells were washed twice with cold PBS to terminate the uptake and then fixed with 3.7% (v/v) paraformaldehyde. Fuorescence in the fixed cells were visualized using an SP5 confocal laser scanning microscopy (Leica, Germany) with a 63× oil immersion objective.

3.2.7 Cytokine assay

Human PBMCs were seeded at a density of 5×10^6 cells/mL in RPMI 1640 medium supplemented with 10% FBS, and then immediately stimulated with BNNS/CpG ODNs and BNNS-PEI/CpG ODNs complexes. After 48 h and 8 h of incubation at 37℃ respectively, cell supernatants were collected for further analysis. The concentrations of IL-6, IFN-α, and TNF-α in the medium were determined by ELISA using the Ready-SET-Go! Human IL-6 kit (eBioscience, CA, USA), Human TNF-α kit (eBioscience, CA, USA) and Human IFN-alpha-Module set (eBioscience, Vienna, Austria) as per manufacturer's protocol.

3.2.8 Statistical analysis

Statistical analysis was performed using Student's t-test. Data are presented as mean ± SD.

3.3 Results and discussion

3.3.1 Preparation and characterization of BNNS-PEI complexes

BNNS were synthesized by a chemical vapor deposition method.[34] To obtain the positively-charged surface and facilitate the loading of CpG ODNs onto the BNNS, we used PEI to functionalize the surface of BNNS. Figure 3.1 shows the schematic illustration of the preparation route. BNNS were non-covalently functionalized by PEI polymers firstly, forming positively charged BNNS-PEI complexes. Then the negatively charged CpG ODNs were loaded onto the BNNS-PEI complexes *via* electrostatic interactions. Zeta potential measurements confirmed the successful functionalization of the BNNS with PEI. Coating of the PEI greatly increased the zeta potential of BNNS from -5 mV to +40 mV for BNNS-PEI complexes (Figure 3.2). In addition, a rise in the surface charge of BNNS-PEI complexes was observed when increasing the starting concentration of the PEI solution during the functionalization of the BNNS. This is thought to be

due to the increased amino groups coated on the surface of BNNS. PEI concentrations were optimized to 5% in order to achieve a highest positive zeta potential and were used in the following studies. Therefore, the positive charge that BNNS-PEI complexes bears can facilitate the loading of the negatively charged CpG ODNs through the electrostatic interaction and enhance the cellular uptake of the complexes.

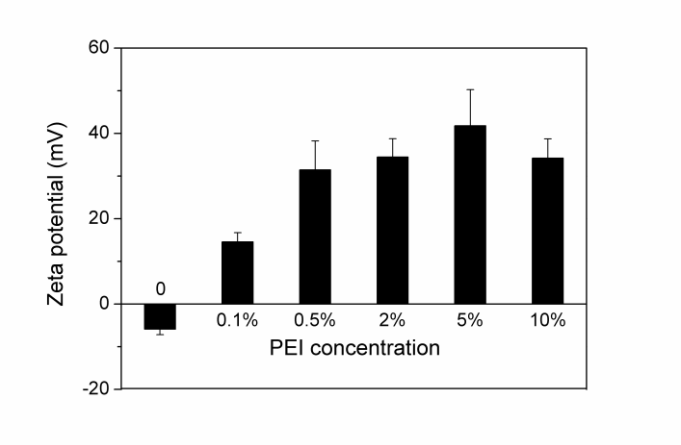

Figure 3.2 Zeta potentials of BNNS and series BNNS-PEI complexes at different starting concentration of PEI.

TGA, a convenient technique to reveal the composition and change in the thermal stability of the complexes, was used here to determine the amount of the PEI coated on the surface of BNNS, As shown in Figure 3.3, BNNS had only a little mass loss (<5%) due to its superb structural stability and anti-oxidation ability. In contrast, a much higher weight loss (22%) was observed for BNNS-PEI complexes. Thus, the weight ratio of PEI in the BNNS-PEI complexes was calculated to be around 17%, which are thought to facilitate the CpG ODNs loading on the BNNS.

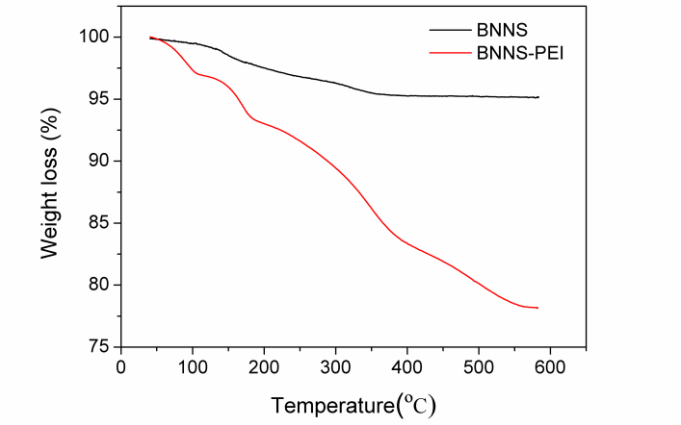

Figure 3. 3. Thermal gravimetric analysis of the BNNS and BNNS-PEI complexes.

Further measurement of the size distributions showed that PEI coating did not result in a significant increase in the mean particle of the BNNS-PEI complexes, which exhibited a relatively narrow size distribution in PBS compared to that of BNNS (Figure 3.4). This indicates that BNNS-PEI complexes may have good dispersity in PBS. Taken together, BNNS-PEI complexes are considered promising as carrier for CpG ODNs delivery.

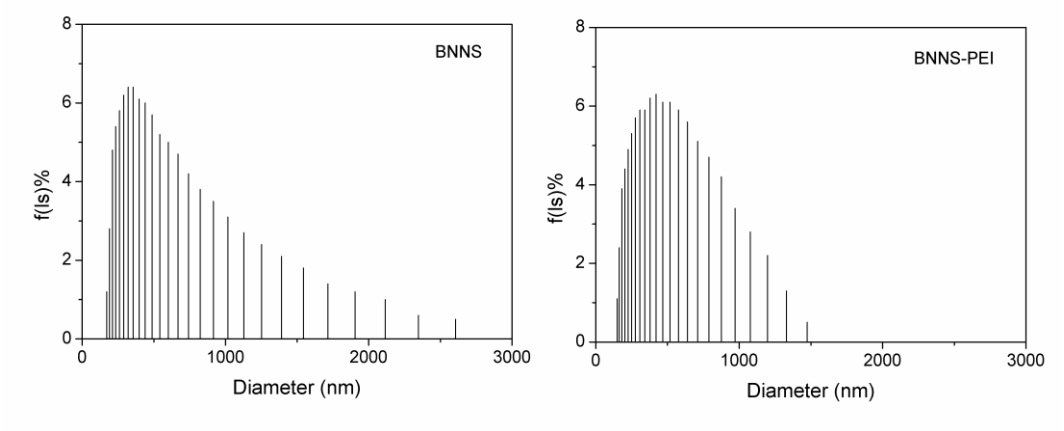

Figure 3.4 Hydrodynamic diameters distribution of BNNS and BNNS-PEI complexes.

3.3.2 *In vitro* cytotoxicity

The cytotoxicity of a carrier is critical for its application in drug delivery system.[36] Here, the in vitro cytotoxicity of the BNNS-PEI complexes was evaluated with human PBMCs by a water-soluble tetrazolium cell proliferation assay. Although PEI have been widely used as non-viral gene delivery carriers, they are reported to be toxic to cells. However, in our study, both of the BNNS and BNNS-PEI complexes showed little cytotoxicity to human PBMCs up to a concentration of 100 μg/mL (Figure 3.5). This might be attributed mainly to the low molecular weight (600Da) PEI used in our experiment. Furthermore, many studies have shown that polycations such as PEI immobilized on the nanoparticles would decrease their cytotoxicity, because of the formation of a rigid molecular structure which reduced the density of cationic residues interacting with plasma membrances.[37] Therefore, BNNS-PEI complexes are safe as vehicles for drug delivery.

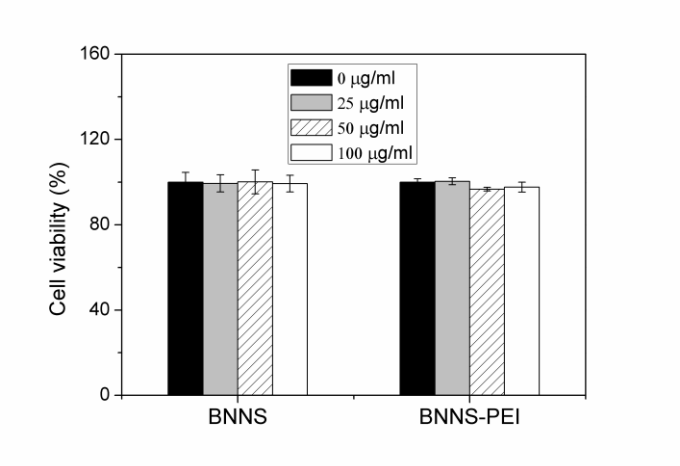

Figure 3.5 *In vitro* cytotoxicity assay. Relative cell viability of PBMCs incubated with increasing concentrations of BNNS or BNNS-PEI complexes measured by a water-soluble tetrazolium salt assay. Data are presented as mean ± SD (n = 5).

3.3.3 CpG ODNs loading

To study the ability of BNNS-PEI complexes as carrier for CpG ODNs delivery, BNNS-PEI complexes were incubated with CpG ODNs. Loading of CpG ODNs onto BNNS-PEI complexes was further confirmed by gel electrophoresis. The band of CpG ODNs from the supernatant became weaker when BNNS-PEI were mixed with CpG ODNs at higher weight ratio (BNNS-PEI/CpG ODNs), and disappeared from the ratio of 50 (Figure 3.6a). This indicates the electrostatic binding of the negatively charged CpG ODNs to the positively charged BNNS-PEI complexes, and all of the CpG ODNs could be bound by BNNS-PEI complexes at the weight ration of 50. Then we examined the loading capacity of the CpG ODNs on BNNS and BNNS-PEI complexes, which increased with the increase of the CpG ODNs concentrations and reached a plateau. As expected, BNNS-PEI complexes possessed a much higher ability to load CpG ODNs, calculated to be 24 μg/mg nanoparticles, about 8 times higher than that of BNNS (Figure 3.6b). This is attributed to the strong positive surface charge of the BNNS-PEI complexes, which enhanced the loading of the CpG ODNs through the electrostatic interactions. Release of the CpG ODNs from the BNNS-PEI/CpG ODNs complexes were further studied. However, no release of the CpG ODNs could be observed. This result suggests that the BNNS-PEI/CpG ODNs complexes are table and CpG ODNs could not be easily released from the BNNS-PEI complexes due to the strong binding.

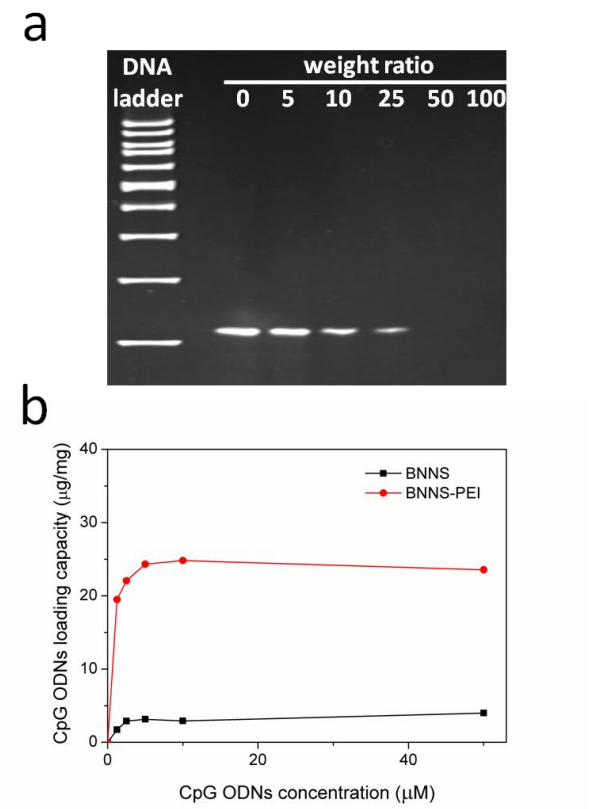

Figure 3.6 Loading of CpG ODNs on BNNS-PEI complexes. (a) Gel electrophoresis image of the supernatant after interaction of CpG ODNs with BNNS-PEI at increasing weight ratios. (b) Loading capacity of CpG ODNs on BNNS and BNNS-PEI complexes with increasing CpG ODNs concentrations, denoted as μg CpG ODNs loaded on 1 mg BNNS.

3.3.4 Intracellular uptake of the CpG ODNs

Delivery or transfection efficiency of the carrier is a critical criterion for a drug/gene delivery system. Although the improvement of the colloidal characteristics and CpG ODNs loading capacity of the BNNS-PEI complexes had been confirmed, still their ability to enhance the cellular uptake of the CpG ODNs needed investigation. For the cellular uptake study, FITC-labeled CpG ODNs was used to replace the regular CpG ODNs and loaded on BNNS and BNNS-PEI complexes, this produced complexes with green fluorescence when observed by CLSM. As shown in Figure 3.7, green fluorescence from the cells incubated with BNNS-PEI/FITC-CpG ODNs complexes was clearly observed, and much stronger than that in cells incubated with BNNS/FITC-CpG ODNs complexes. In contrast, no fluorescence could be observed when applying free FITC-labeled CpG ODNs to the cells, indicating the lower cellular uptake and the need of a

carrier for CpG ODNs delivery. These findings confirmed our hypothesis that intracellular delivery of CpG ODNs could be enhanced by BNNS-PEI complexes. After taken up by the cells, CpG ODNs localize mainly in endosomal compartments and activate the TLR 9. This initiates the induction of several cytokines and chemokines and further modulates the immune response.[10] Therefore, enhancement of cellular uptake of CpG ODNs by BNNS-PEI complexes is believed to strengthen the interaction of CpG ODNs with TLR 9 and trigger a better immune response.

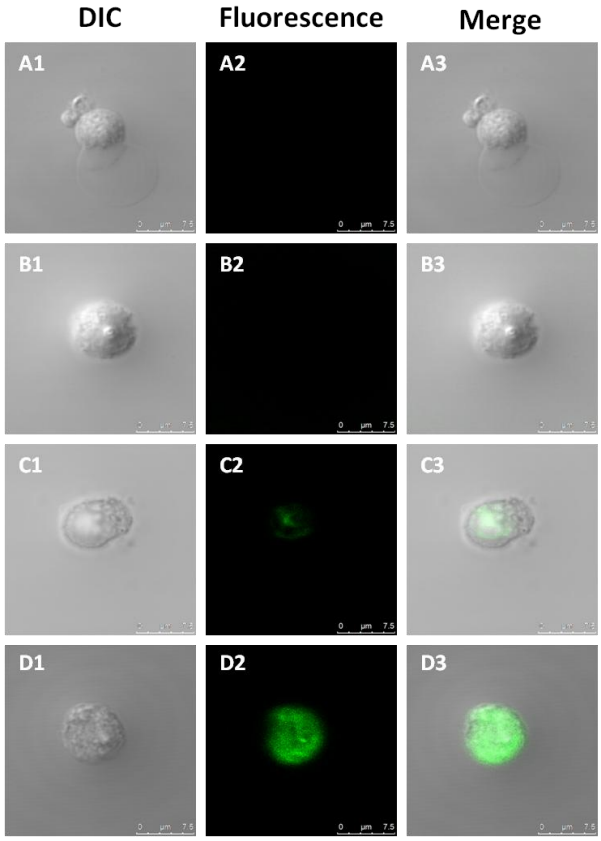

Figure 3.7 Confocal microscope images of PBMCs after 24 h of incubation with BNNS (A1-3), free CpG ODNs (B1-3), CpG ODNs loaded on BNNS (C1-3), CpG ODNs loaded on BNNS-PEI complexes (D1-3). CpG ODNs were labeled with FITC.

3.3.5 Cytokine induction *in vitro*

To test the efficacy of BNNS-PEI complexes as a carrier for CpG ODNs delivery, BNNS-PEI/CpG ODNs were incubated with PBMCs, and the resultant cytokines productions were determined by ELISA. As expected, PBMCs stimulated by BNNS-PEI/CpG ODNs complexes had the highest amount of IL-6 and TNF-α (Figure 3.8a, 3.8b), about 6 times higher than that of BNNS/CpG ODNs. Although PEI could be used

alone as a drug delivery carrier, BNNS-PEI complexes exhibited much higher efficiency and the BNNS-PEI/CpG ODNs complexes induced much more amount of the cytokines (Figure 3.8a, 3.8b). In contrast, without a carrier, free CpG ODNs could only induce a quite small amount. This suggests that higher cytokines production were due to the higher loading capacity and the enhanced cellular uptake of CpG ODNs attributed by positively charged BNNS-PEI complexes. Similar result was observed when we used a BNNS-binding peptide as a linker molecule for CpG ODNs delivery, which enhanced the CpG ODNs internalization by PBMCs.[38]

Although class-B CpG ODNs, which have a linear structure, can stimulate TLR 9 in B cells and induces IL-6 and TNF-α, they don't have the potential to induce IFN-α as class-A CpG ODNs do.[10,39-41] However, when we applied the CpG ODNs loaded electrostatically onto PEI functionalized BNNS or mixed with PEI to stimulate the PBMCs, they acquired the ability to induce the IFN-α (Figure 3.8c). In contrast, neither the free CpG ODNs nor the CpG ODNs loaded directly on BNNS could stimulate the IFN-α secretion. We also found that IFN-α induction was attributed to CpG ODNs molecules loaded on BNNS-PEI complexes but not free ones released from the BNNS-PEI/CpG ODNs complexes. Because we did not detect the release of CpG ODNs molecules form BNNS-PEI/CpG ODNs complexes under conditions that correspond to the physiological environment in the TLR 9-localized endolysosome. Although the mechanism why class-B CpG ODNs acquired the potential to induce IFN-α is not clear, it is reported that the physical form of the CpG ODNs may play important role.[17,42-43]

Studies showed that immunostimulatory effects of the CpG ODNs are dependent on not only their base sequence and structure, but also their physical form.[42] The greater ability of class A CpG ODNs to induce the IFN-α production is due to the formation of higher-order multimeric structure.[29] However, such structures are not observed in class B CpG ODNs, they form a linear structures.[44] Study has shown that an immune response similar to class A CpG ODNs could be obtained by artificially causing class B CpG ODNs to form multimeric structure using nanoparticles.[32,45] This suggests that the multimerization of CpG ODNs molecules is crucial for IFN-α induction. Therefore, when the class B CpG ODNs were loaded onto the positively charged BNNS-PEI complexes or mixed with PEI through electrostatic interaction, it was likely that they formed the higher-order multimeric structure similar to class A CpG ODNs, and acquired the ability to induce the IFN-α. In contrast, when class B CpG ODNs bound directly to negatively charged BNNS they

could not form multimeric structure because of the weak interactions, and like free class B CpG ODNs, so they could induce only the IL-6 and TNF-α but not IFN-α. However, the exact mechanism why class-B CpG ODNs acquire the ability to induce the IFN-α remains unclear and further investigation is under way.

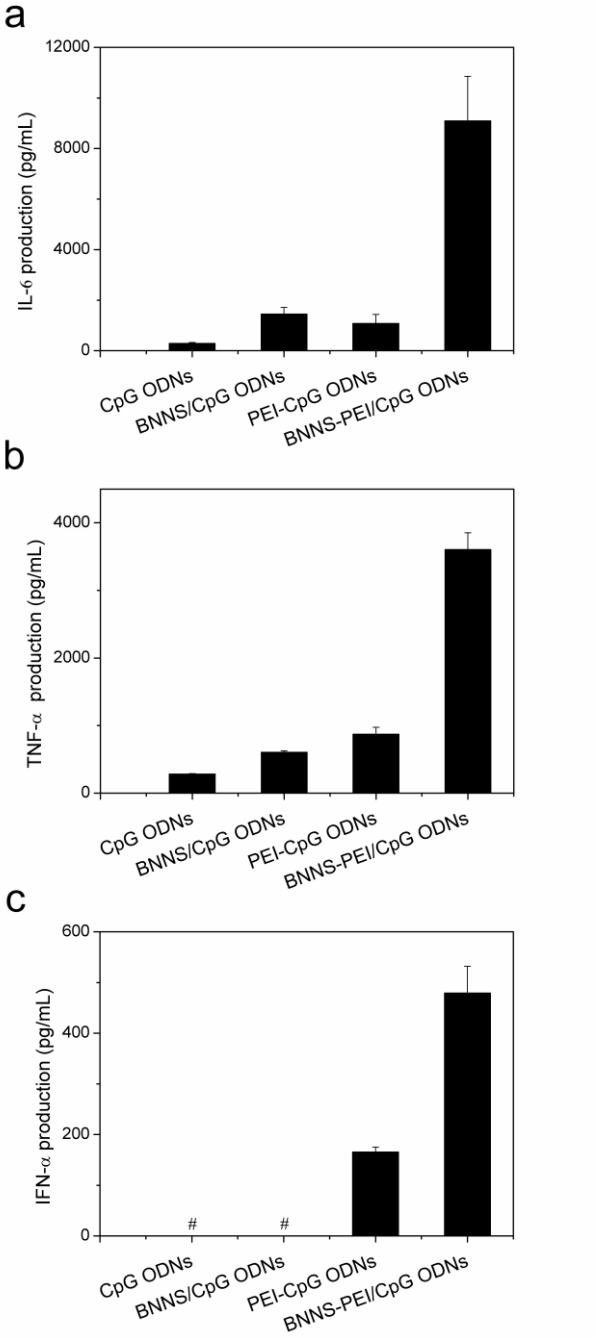

Figure 3.8 Cytokine induction from PBMCs stimulated by CpG ODNs loaded on BNNS and BNNS-PEI complexes. Loaded BNNS or BNNS/PEI complexes (50 μg/mL). (a) IL-6 production. (b) TNF-α production. (c) IFN-α production. Data are presented as mean ± SD (n = 3). The symbol # means not detectable (below detection limit).

3.4 Conclusion

In this chapter, we reported the use of PEI-functionalized BNNS as s nano-carrier for the intracellular delivery of CpG ODNs. PEI were coated on the surface of BNNS through noncovalent electrostatic interactions, the resultant BNNS/PEI complexes possessed strong positive charges and better dispersity and stability in aqueous solution. Furthermore, BNNS/PEI complexes are non-toxic to human PBMCs up to a concentration of 100 μg/mL. Due to their positive surface charge, BNNS/PEI complexes possess a superior ability to enhance the loading capacity and cellular uptake of CpG ODNs molecules. Using BNNS/PEI complexes as carrier for CpG ODNs delivery, cytokines such as IL-6 and TNF-α production from PBMCs were significantly enhanced compared to that of using BNNS or PEI as carrier. Most importantly, B class CpG ODNs loaded on BNNS/PEI complexes acquired the ability to induce IFN-α. It is thought that PEI coating changed the physical form of B class CpG ODNs on BNNS, further modulated their interaction with TLR 9 and induced the IFN-α. Therefore, our results highlight the promise of BNNS/PEI complexes as a novel nanocarrier for enhancing the delivery efficiency and immunostimulatory activity of CpG ODNs.

3.5 References

1. Krieg AM, Yi AK, Matson S, et al. CpG motifs in bacterial DNA trigger direct B-cell activation. *Nature.* 1995;374(6522):546-549.
2. Klinman DM. Immunotherapeutic uses of CpG oligodeoxynucleotides. *Nat. Rev. Immunol.* 2004;4(4):248-257.
3. Hemmi H, Takeuchi O, Kawai T, et al. A Toll-like receptor recognizes bacterial DNA. *Nature.* 2000;408(6813):740-745.
4. Wagner H. Bacterial CpG DNA activates immune cells to signal infectious danger. *Adv. Immunol.* 1999;73:329-368.
5. Akira S, Takeda K, Kaisho T. Toll-like receptors: critical proteins linking innate and acquired immunity. *Nat. Immunol.* 2001;2(8):675-680.
6. Klinman DM, Yi AK, Beaucage SL, Conover J, Krieg AM. CpG motifs present in bacterial DNA rapidly induce lymphocytes to secrete interleukin 6, interleukin 12, and interferon gamma. *Proc. Natl. Acad. Sci. U. S. A.* 1996;93(7):2879-2883.
7. Bauer S, Kirschning CJ, Häcker H, et al. Human TLR9 confers responsiveness to bacterial DNA via species-specific CpG motif recognition. *Proc. Natl. Acad. Sci. U. S. A.* 2001;98(16):9237-9242.
8. Stacey KJ, Sweet MJ, Hume DA. Macrophages ingest and are activated by bacterial DNA. *J. Immunol.* 1996;157(5):2116-2122.
9. Sun SQ, Zhang XH, Tough DF, Sprent J. Type I interferon-mediated stimulation of T cells by CgG DNA. *J. Exp. Med.* 1998;188(12):2335-2342.
10. Krieg AM. CpG motifs in bacterial DNA and their immune effects. *Annu. Rev. Immunol.* 2002;20:709-760.
11. Fonseca DE, Kline JN. Use of CpG oligonucleotides in treatment of asthma and allergic disease. *Adv. Drug Delivery. Rev.* 2009;61(3):256-262.
12. Klinman DM, Klaschik S, Sato T, Tross D. CpG oligonucleotides as adjuvants for vaccines targeting infectious diseases. *Adv. Drug Delivery. Rev.* 2009;61(3):248-255.
13. Krieg AM. Therapeutic potential of Toll-like receptor 9 activation. *Nat. Rev. Drug Discov.*

2006;5(6):471-484.

14. Murad YM, Clay TM. CpG oligodeoxynudeofides as TLR9 agonists: therapeutic applications in cancer. *BioDrugs.* 2009;23(6):361-375.

15. Mutwiri G, Littel-van Den Hurk SV, Babiuk LA. Approaches to enhancing immune responses stimulated by CpG oligodeoxynucleotides. *Adv. Drug Delivery. Rev.* 2009;61(3):226-232.

16. Mutwiri GK, Nichani AK, Babiuk S, Babiuk LA. Strategies for enhancing the immunostimulatory effects of CpG oligodeoxynucleotides. *J. Control. Release.* 2004;97(1):1-17.

17. Hanagata N. Structure-dependent immunostimulatory effect of CpG oligodeoxynucleotides and their delivery system. *Int. J. Nanomedicine.* 2012;7:2181-2195.

18. Sheehan JP, Lan HC. Phosphorothioate oligonucleotides inhibit the intrinsic tenase complex. *Blood.* 1998;92(5):1617-1625.

19. Henry SP, Beattie G, Yeh G, et al. Complement activation is responsible for acute toxicities in rhesus monkeys treated with a phosphorothioate oligodeoxynucleotide. *Int. Immunopharmacol.* 2002;2(12):1657-1666.

20. Chopra NG, Luyken RJ, Cherrey K, et al. Boron-nitride nanotubes. *Science.* 1995;269(5226):966-967.

21. Golberg D, Bando Y, Tang CC, Zhi CY. Boron nitride nanotubes. *Adv. Mater.* 2007;19(18):2413-2432.

22. Chen X, Wu P, Rousseas M, et al. Boron nitride nanotubes are noncytotoxic and can be functionalized for interaction with proteins and cells. *J. Am. Chem. Soc.* 2009;131(3):890-891.

23. Jonsson E, Simonsen L, Karlsson M, Larsson R. The hollow fiber model: A new method for in vivo-evaluation of antitumor effect, toxicity and pharmacokinetics of new anticancer drugs. *Ann. Oncol.* 1998;9:44-44.

24. Gao ZH, Zhi CY, Bando Y, Golberg D, Serizawa T. Isolation of individual boron nitride nanotubes via peptide wrapping. *J. Am. Chem. Soc.* 2010;132(14):4976-4977.

25. Ciofani G, Raffa V, Menciassi A, Cuschieri A. Boron nitride nanotubes: An innovative tool for nanomedicine. *Nano Today.* 2009;4(1):8-10.

26. Ciofani G, Danti S, Nitti S, Mazzolai B, Mattoli V, Giorgi M. Biocompatibility of boron nitride

nanotubes: An up-date of in vivo toxicological investigation. *Int. J. Pharm.* 2013;444(1-2):85-88.

27. Ciofani G, Danti S, Genchi GG, et al. Pilot in vivo toxicological investigation of boron nitride nanotubes. *Int. J. Nanomedicine.* 2012;7:19-24.

28. Zhi CY, Meng WJ, Yamazaki T, et al. BN nanospheres as CpG ODN carriers for activation of toll-like receptor 9. *J. Mater. Chem.* 2011;21(14):5219-5222.

29. Kerkmann M, Costa LT, Richter C, et al. Spontaneous formation of nucleic acid-based nanoparticles is responsible for high interferon-α induction by CpG-A in plasmacytoid dendritic cells. *J. Biol. Chem.* 2005;280(9):8086-8093.

30. Putnam D, Gentry CA, Pack DW, Langer R. Polymer-based gene delivery with low cytotoxicity by a unique balance of side-chain termini. *Proc. Natl. Acad. Sci. U. S. A.* 2001;98(3):1200-+.

31. Zhu JM, Tang AG, Law LP, et al. Amphiphilic core-shell nanoparticles with poly(ethylenimine) shells as potential gene delivery carriers. *Bioconjug. Chem.* 2005;16(1):139-146.

32. Manoharan Y, Ji QM, Yamazaki T, et al. Effect of molecular weight of polyethyleneimine on loading of CpG oligodeoxynucleotides onto flake-shell silica nanoparticles for enhanced TLR9-mediated induction of interferon-alpha. *Int. J. Nanomedicine.* 2012;7:3625-3635.

33. Meng WJ, Yamazaki T, Nishida Y, Hanagata N. Nuclease-resistant immunostimulatory phosphodiester CpG oligodeoxynucleotides as human Toll-like receptor 9 agonists. *BMC Biotechnol.* 2011;11:88.

34. Tang CC, Bando Y, Huang Y, Zhi CY, Golberg D. Synthetic routes and formation mechanisms of spherical boron nitride nanoparticles. *Adv. Funct. Mater.* 2008;18(22):3653-3661.

35. Yu RZ, Geary RS, Leeds JM, et al. Pharmacokinetics and tissue disposition in monkeys of an antisense oligonucleotide inhibitor of Ha-ras encapsulated in stealth liposomes. *Pharm. Res.* 1999;16(8):1309-1315.

36. Zhu YF, Ikoma T, Hanagata N, Kaskel S. Rattle-type Fe_3O_4@SiO_2 hollow mesoporous spheres as carriers for drug delivery. *Small.* 2010;6(3):471-478.

37. Feng LZ, Zhang SA, Liu ZA. Graphene based gene transfection. *Nanoscale.* 2011;3(3):1252-1257.

38. Zhang H, Yamazaki T, Zhi C, Hanagata N. Identification of a boron nitride nanosphere-binding peptide for the intracellular delivery of CpG oligodeoxynucleotides. *Nanoscale.*

2012;4(20):6343-6350.

39. Krug A, Towarowski A, Britsch S, et al. Toll-like receptor expression reveals CpG DNA as a unique microbial stimulus for plasmacytoid dendritic cells which synergizes with CD40 ligand to induce high amounts of IL-12. *Eur. J. Immunol.* 2001;31(10):3026-3037.

40. Hartmann G, Weeratna RD, Ballas ZK, et al. Delineation of a CpG phosphorothioate oligodeoxynucleotide for activating primate immune responses in vitro and in vivo. *J. Immunol.* 2000;164(3):1617-1624.

41. Hartmann G, Krieg AM. Mechanism and function of a newly identified CpG DNA moth in human primary B cells. *J. Immunol.* 2000;164(2):944-952.

42. Guiducci C, Ott G, Chan JH, et al. Properties regulating the nature of the plasmacytoid dendritic cell response to Toll-like receptor 9 activation. *J. Exp. Med.* 2006;203(8):1999-2008.

43. Honda K, Yanai H, Negishi H, et al. IRF-7 is the master regulator of type-I interferon-dependent immune responses. *Nature.* 2005;434(7034):772-777.

44. Klein DCG, Latz E, Espevik T, Stokke BT. Higher order structure of short immunostimulatory oligonucleotides studied by atomic force microscopy. *Ultramicroscopy.* 2010;110(6):689-693.

45. Chinnathambi S, Chen S, Ganesan S, Hanagata N. Binding mode of CpG oligodeoxynucleotides to nanoparticles regulates bifurcated cytokine induction via toll-like receptor 9. *Sci. Rep.* 2012;2:534.

Chapter 4 Chitosan coated BNNS for the enhanced CpG ODNs delivery and cytokines induction

4.1 Introduction

Recently, increasing attention has been paid to unmethylated CpG dinucleotides in immunotherapy.[1] These CpG motifs are found with high frequency in bacterial DNA, they stimulate the mammalian innate immune system *via* activation of the pattern-recognition receptor TLR 9.[1-6] Synthetic short, single-stranded ODNs that contain CpG motifs are similar to those found in bacterial DNA and stimulate a similar immune response.[2,7] The interaction of CpG ODNs with TLR 9 in antigen-presenting cells can activate two distinct signaling pathways, in which two transcription factors, NFκB and IRF-7, are translocated into the nucleus, leading to the induction of proinflammatory cytokines (such as IL-6 and IL-12) and/or type I interferons (such as IFN-α) respectively.[8] These two types of cytokines are reported to play important roles in the induction and maintenance of innate and adaptive immune responses.[9] Thus, CpG ODNs have a strong potential for improved vaccines as well as immunotherapies for allergy, cancer, and infectious diseases, which have been initiated in humans and numerous animal species.[10-13] However, natural CpG ODNs with only a phosphodiester backbone are not stable and prone to nuclease degradation in serum, and there are lots of evidence that the biologic activity of CpG ODNs is often transient.[14] This severely limits their potential immunotherapeutic applications. Therefore, great efforts have been taken in developing approaches to optimize the stimulatory activity of CpG ODNs. One of the most effective methods is chemical modification of the CpG ODNs.[14-16] Substituting the phosphodiester backbone with a phosphorothioate has been reported to possess a better immunostimulatory effect due to the increased resistance to nuclease degradation.[15-16] However, there is concern about several severe side effects caused by the modification of DNA backbone.[17] For example, repeated administration of backbone-modified CpG ODNs has been associated with reduced immune responses, organ enlargement, and lymphoid follicle destruction.[18] Recently, researchers have focused their eyes on searching for formulations and delivery systems to improve the stimulatory activity of CpG ODNs. Various particles, such as liposomes and inorganic nanoparticles have been used as carrier to

deliver unmodified CpG ODNs due to their ability to improve the stability and cellular uptake of CpG ODNs.[19-23]

BN has received increasing scientific interest recently due to its advantageous properties and analogous structure to carbon materials.[24-25] These make it a potential material for many applications ranging from composite materials to electrical and optical devices.[26-27] Besides, it has been revealed that BN has good biocompatibility, lower toxicity and easier cellular uptake than carbon.[28-29] Ciofani et al. investigated the cytocompatibility and magnetic properties of BNNT using neuroblastoma cells and demonstrated that BNNT are suitable as nanovectors for cell therapy, drug and gene delivery, and for other biomedical and clinical applications.[30] In our previous work, we used 150-nm BNNS as carrier for the delivery of unmodified CpG ODNs on activation of TLR 9.[31] BNNS showed no cytotoxicity and protected unmodified CpG ODNs from DNase degradation. Furthermore, BNNS taken up by cells were found in endolysosomes. This was particularity advantageous for a higher TLR 9 activity, as TLR 9 also localizes to endolysosomes. However, since CpG ODNs and BNNS are both negatively charged, the electrostatic repulsion between them is believed to lower the loading of CpG ODNs on BNNS. Therefore, the efficiency of CpG ODNs uptake was also limited and could not induce a robust cytokine response.

In this chapter, we prepared the chitosan coated BNNS, and used that as carrier for the delivery of CpG ODNs (Figure 4.1). CS is a naturally existing polysaccharide composed of glucosamine and N-acetylglucosamine residues derived from chitin.[32] CS is reported to have many beneficial properties, such as biocompatibility, biodegradability and low toxicity.[33] Besides, in contrast to other biodegradable polymer, CS is the only one exhibiting a cationic character, which allows electrostatic interactions with many negatively charged nucleic acids to form stable complexes.[34] Therefore, CS has been widely used in many drug and gene delivery systems. Wu et al developed a novel immunoadjuvant by enwrapping the CpG ODNs with CS nanoparticles (CpG-CNP) and demonstrated that CpG-CNP significantly promoted cellular and humoral immunity，and resistance of mice against *E.coli* infection.[35] Besides, CS are frequently utilized as coating agent to adjust the surface charge of the nanoparticles to bind negatively charged nucleic acid drugs.[36] Molecular weight (MW) is an important characteristic of CS that influences its physicochemical and biological properties. Therefore, MW of the CS is thought to play an important role in its complexation with

CpG ODNs and will affect the CpG ODNs-TLR 9 interaction. Thus, we used CS of three different MW to coat the surface of BNNS and examed the effect on CpG ODNs loading and the cytokines productions. It is hypothesized that CS coating on BNNS will enhance the loading capacity and cellular uptake of CpG ODNs, and further enhance their immunostimulatory effect.

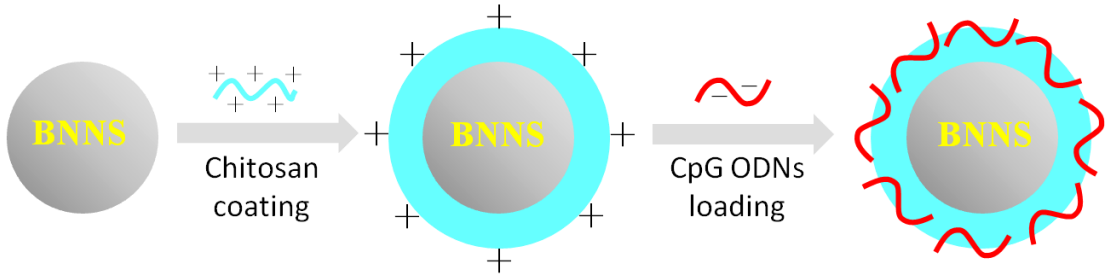

Figure 4.1 Scheme of preparation and application of the chitosan-coated BNNS for CpG ODNs delivery.

4.2 Materials and methods

4.2.1 Preparation of chitosan-coated BNNS (BNNS/CS)

Highly pure BNNS were synthesized by a chemical vapor deposition method as previously reported.[37] Chitosan with molecular weights of 60-120 kDa (named as CS-L), 110-150 kDa (CS-M), 140-220 kDa (CS-H) were purchased from Sigma-Aldrich (St. Louis, USA) and dissolved with 1% acetic acid solution to a concentration of 5 mg/mL prior to use. Working solution was prepared from the stock by dilution with Milli-Q water. BNNS (1 mg/mL) were suspended by sonication in Tris-HCl–buffered saline (50 mM HCl, 150 mM NaCl, pH 7.5) containing 0.1% Tween-20 (TBS-T). For surface coating, 500 μL BNNS solution was mixed with equal volume of 0.05 mg/mL CS solutions, the suspension was stirred at room temperature for 2 hours. The CS-coated BNNS were then collected by centrifugation at 12000 for 10 minutes, followed by five washes with Milli-Q water. The BNNS/CS complexes were finally resuspended in phosphate-buffered saline.

4.2.2 Characterization methods

TEM were performed by a 3000F high-resolution field emission transmission electron microscopy (JEOL, Japan) operated at an acceleration voltage of 300 kV. Fourier transform infrared (FTIR) spectra were carried out on a Spectrum GX spectrophotometer (Perkin Elmer, USA) at 4 cm^{-1} resolution with 32 scans.

Zeta potential measurements were conducted using a LEZA-600 electrophoresis zeta potential analyzer (Otsuka, Japan). Dynamic light scattering (DLS) measurements were obtained using a Photal DLS-6000DL instrument (Otsuka, Japan). Thermogravimetric analysis were conducted on an SII TG/DTA 6200 system using a heating rate of 5℃ per minute with an open alumina cell.

4.2.3 Cell culture

293XL-hTLR 9 cells stably expressing hTLR 9 were purchased from InvivoGen (CA, USA) and grown in Dulbecco's modified Eagle medium (DMEM) (Sigma-Aldrich, MO, USA) containing 10% (v/v) FBS, 50 units/mL penicillin, 50 mg/L streptomycin, 100 μg/mL normocin and 10 μg/mL blasticidin. Frozen PBMCs were purchased from Cellular Technology Limited (OH, USA) and thawed according to the manufacturer's protocol. Both cell lines were incubated at 37℃ with 5% CO_2.

4.2.4 *In vitro* cytotoxicity assay

The *in vitro* cytotoxicity of BNNS and the BNNS/CS complexes were investigated using a Cell Counting Kit-8 (CCK-8) (Dojindo, Japan). 5000 cells were seeded in a 96-well plate for 24 h to allow the cells to adhere and then exposed to serial dilutions of BNNS, BNNS/CS complexes, or medium (control). After a 24 h incubation at 37℃ with 5% CO_2, 10 μL of CCK-8 solution was added to each well and incubated for another 3 h. The absorbance at 450 nm was then measured using a microplate reader (MTP-880 Lab, Corona, Japan). Cytotoxicity was expressed as the percentage of cell viability compared to that of untreated control cells.

4.2.5 Preparation of CpG ODNs-loaded BNNS/CS (BNNS/CS/CpG ODNs)

Phosphodiester-based class-B CpG ODNs, referred to as CpG ODNs 2006x3-PD,[39] were purchased from Fasmac, Inc. (Kanagawa, Japan). CpG ODNs were diluted in sterile water at a concentration of 100 μM and stored at -20℃. To prepare the BNNS/CS/CpG ODNs complexes, 25 μL of CpG ODNs solution (20 μM) was incubated with equal volume of BNNS/CS solutions (2 mg/mL in PBS at pH 7.4) at room temperature with gentle shaking for 1 h. The mixture was then centrifuged at 15000 rpm for 15 minutes to collect the

BNNS/CS/CpG ODNs complexes. The loading capacity was calculated from the concentration of the unloaded CpG ODNs in the supernatant measured by a Nano Drop 2000 spectrophotometer (Thermo Scientific). The BNNS/CS/ CpG ODNs complexes were resuspended by adding 50 μL PBS and used for the following cytokine stimulation.

4.2.6 Cytokine assay

PBMCs were seeded in RPMI 1640 medium supplemented with 10% FBS, at a density of 5×10^6 cells/mL. Cells were immediately stimulated with CS/CpG ODNs, BNNS/CpG ODNs and BNNS/CS/CpG ODNs complexes. The final concentration of BNNS was about 50 μg/mL. For comparison, cells were also stimulated with Lipofectamine™ 2000-CpG ODNs complexes (Invitrogen , NY, USA). After 48 h and 8 h of incubation at 37℃ respectively, cell supernatants were collected for further analysis. The concentration of IL-6, IFN-α and TNF-α in the media was determined by ELISA using the Ready-SET-Go! Human IL-6, Human IFN-alpha-Module set (eBioscience, Vienna, Austria) and TNF-α kit (eBioscience, CA, USA), as per manufacturer's protocol.

4.2.7 Cellular uptake of BNNS/CS/CpG ODNs complexes

Fluorescein isothiocyanate-labeled CpG ODNs were loaded on BNNS and BNNS/CS respectively to form BNNS/CpG ODNs and BNNS/CS/CpG ODNs complexes. PBMCs (8×10^4) were seeded in a 35-mm petri dish with a glass bottom and incubated for 24 h at 37℃ with 5% CO_2. And then the prepared complexes were added to the dish. After incubation for 24 h, the cells were washed twice with PBS and fixed with 3.7% (v/v) paraformaldehyde. The fixed cells were visualized using an SP5 confocal laser scanning microscopy (CLSM, Leica, Germany).

4.2.8 Intracellular localization of CpG ODNs

293XL-hTLR 9 cells (8×10^4) were seeded in a 35-mm petri dish with a glass bottom and incubated for 24 h at 37℃ with 5% CO_2. BNNS/FITC-CpG ODNs and BNNS/CS/FITC-CpG ODNs complexes were then added to the dish at a final concentration of 50 μg/mL. After incubation for 24 h, the cells were washed twice with PBS and fixed with 3.7% (v/v) paraformaldehyde. Samples were then blocked for 1 h at room

temperature using 3% BSA in PBS and stained with anti-LAMP-1 antibody (Abcam, UK). The cells were visualized using the SP5 confocal laser scanning microscopy (CLSM, Leica, Germany), the images were acquired sequentially using separate laser excitation to avoid any cross-talk between the fluorophore signals.

4.2.9 Ethidium bromide (EB) displacement assay

The ethidium bromide (EB) displacement assay was used to determine the binding strength of the CpG ODNs to CS of different MW, by monitoring changes in fluorescence intensity of EB bound to CpG ODNs as a function of added CS concentrations. At room temperature, 100 μL CpG ODNs (10 μg/mL) was treated with 100 μL EB (1 μg/mL) for 10 min, then CS with different MW and series concentrations were added and incubated for 2 min, thereafter, the fluorescence intensity at 570 nm was measured on the microplate reader. The competitive binding constants (K) were calculated using the equation: $I = I_0 + K$ [CS], where I_0 and I are the fluorescence intensity in the absence and presence of the quencher CS, [CS] are the concentrations of the CS.

4.2.10 Statistical analysis

Statistical analysis was performed using Student's *t*-test. Data are presented as mean ± SD. Differences were considered statistically significant for $*p < 0.05$.

4.3 Results and discussion

4.3.1 Preparation and characterization of BNNS/CS complexes

BNNS were synthesized by a chemical vapor deposition method as previously reported, which have a ball-like shape and the average size is approximately 150 nm. To obtain the positively-charged surface and facilitate the attachment of CpG ODNs onto the BNNS, we used the chitosan to modify the BNNS, because CS is the only biodegradable and biocompatible polysaccharide that exhibiting a cationic character. Figure 4.2a shows the zeta potentials of BNNS and BNNS/CS complexes in PBS. It can be found that zeta potentials are changed after the coating of CS. Pure BNNS have the negative zeta potential of -5.98 ± 1.28 mV, while they are positive for BNNS/CS complexes. This suggests that the CS might have been coated on

the surface of BNNS and changed the zeta potential. Furthermore, the surface charge of the BNNS coating with CS exhibited a molecular weight (MW)-dependent manner, showing a higher positive charge density with the increase in MW of the CS. These results are thought to be due to the abundant amino groups in the CS of high MW. To further confirm the the coating of CS on BNNS, FTIR spectra was used. Figure 4.2b shows the FTIR spectra of low molecular weight CS, as well as the pure BNNS and CS-coated BNNS samples. 2927 cm^{-1} (C-H stretch) and 1644 cm^{-1} (amide I band, C=O stretch of acetyl group) are the characteristic stretching and bending vibration of CS.[40] BNNS present a strong band at around 1400 cm^{-1}, along with a less intense band at 780 cm^{-1}, which are assigned to the (B-N) and (B-N-B) vibrations respectively.[37] It can be observed that the BNNS/CS complexes clearly displays the peaks assigned to both BNNS and CS. These results demonstrate the presence of CS in the BNNS/CS complexes and confirm the success of the coating. Therefore, the negatively charged CpG ODNs were able to bind to positively charged BNNS/CS complexes through the electrostatic interaction.

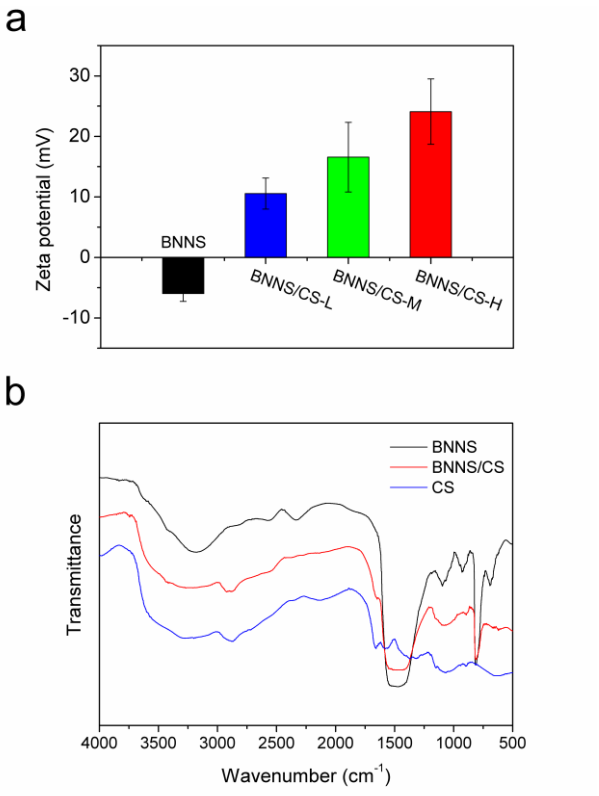

Figure 4.2 Characterizations of the BNNS/CS complexes. (a) Zeta potentials of BNNS and BNNS coated with CS of different molecular weights (MW) in PBS (pH 7.4). (b) FTIR spectra of BNNS, CS and BNNS/CS complexes.

It is reported that the size of the biomaterials could alter the TLR 9-mediated cytokine profiles as it affect their efficiency of cellular uptake, intracellular trafficking and so on.[9] Here, the size distributions of the BNNS with and without CS coating were measured using DLS. Compared to the pure BNNS, which has a average diameter of about 360 nm, coating with CS on the surface may have resulted in partial aggregation of the BNNS but have not greatly increased the size of the BNNS (Figure 4.3). This might be due to the relatively low concentration of CS included in the BNNS suspension. The dispersity and stability of nanoparticles are crucial characteristics for application as carrier in drug delivery system. In our experiment, we observed that CS coating notablely improved the dispersity and stability of BNNS in aqueous solution. Although the exact mechanism of these is not clear, the interaction of amino groups in CS with the BNNS surface is thought to play a important role. The amino functional groups from CS adsorbed onto the BNNS surface leads to good dispersion, CS molecules can also act as polycationic surfactant and improve the dispersion of the BNNS.[41-42] Furthermore, adsorption of the CS triggers a entropic repulsion among the CS-coated BNNS and stabilizes the dispersion, which is expected to be the most likely stabilization mechanism.[43] Therefore, CS coating made BNNS more suitable as carrier.

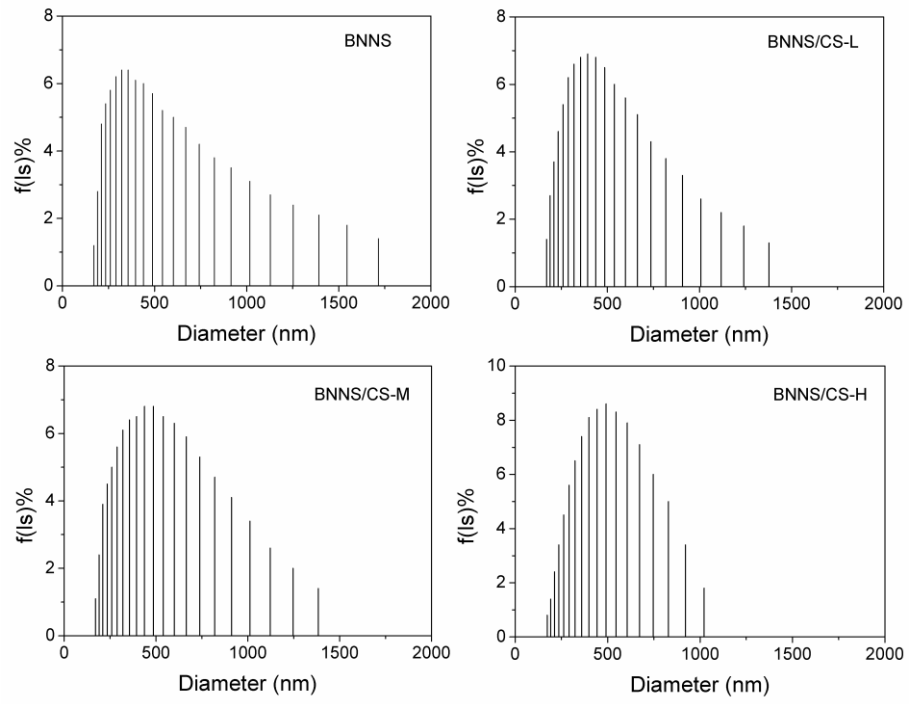

Figure 4.3 Size distributions of BNNS coated with CS of different molecular weights measured by DLS.

4.3.2 Cytotoxicity of the BNNS/CS complexes

Investigation on biological safety of drug delivery vehicles is a critical criterion for drug delivery system.[44] Although previous studies have demonstrated that BNNS and CS are biocompatible and suitable for drug delivery, it is still necessary to investigate the safety of the BNNS/CS complexes because in this study we used the acetic acid solution to dissolve the CS. Here, two types of cells, human PBMCs and 293XL-hTLR 9 cells, were used to study the *in vitro* cytotoxicity of BNNS/CS complexes measured by a water-soluble tetrazolium cell proliferation assay. Although CS with high MW are reported to be associated with potential cytotoxicity, BNNS coated with CS of three kinds of MW exhibited similar biocompatibility and showed no cytotoxicity to human PBMCs or 293XL-hTLR 9 cells up to a concentration of 100 μg/mL (Figure 4.4). These results suggests that the BNNS/CS complexes are safe and suitable as vehicles for drug delivery.

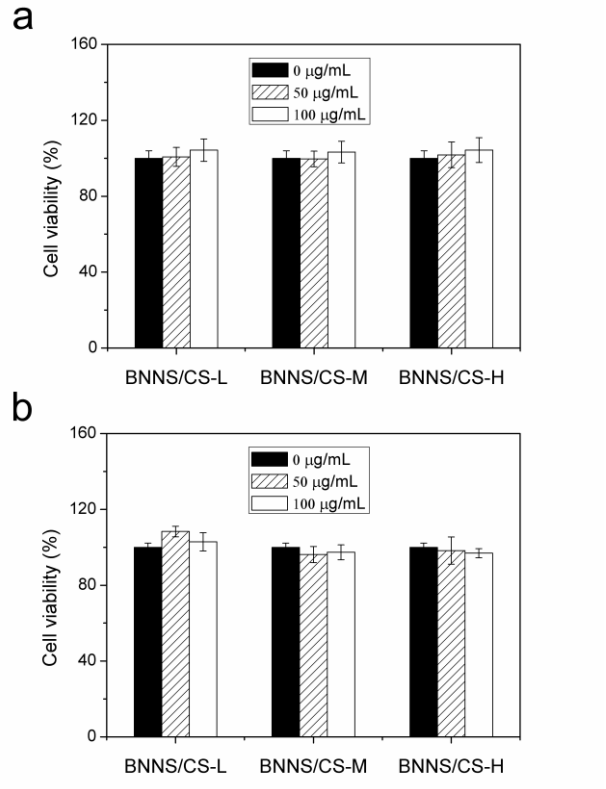

Figure 4.4 Cytotoxicity of BNNS coated with CS of different molecular weights to PBMCs and 293XL-hTLR 9 cells. (a) PBMCs. (b) 293XL-hTLR 9 cells. Cells were incubated with increasing concentrations of BNNS/CS complexes, and cell viability was measured by a water-soluble tetrazolium salt assay. Data are presented as mean ± SD (n = 5).

4.3.3 BNNS/CS complexes as carrier for the delivery of CpG ODNs

Next, we used the BNNS/CS to bind the CpG ODNs and yield BNNS/CS/CpG ODNs complexes. The negatively charged phosphate groups of the CpG ODNs backbone were thought to interact with the amine group of CS and result in CpG ODNs adsorption onto BNNS/CS. As expected, the maximum loading capacity of CpG ODNs was dramatically increased for BNNS/CS complexes, about 17.5, 21.4, and 27.2 μg CpG ODNs/mg nanoparticles for BNNS coated with CS-L, CS-M, and CS-H, respectively. These were more than 6 times higher than that of CpG ODNs loaded directly onto BNNS (Figure 4.5). This result is thought to be attributed to the positively charged BNNS surface after CS coating. Negatively charged CpG ODNs could easily bind to BNNS/CS complexes through the electrostatic interactions. Furthermore, the maximum capacity for loading CpG ODNs increased with the increase in the MW of CS (Figure 4.5), because the BNNS coated with CS of a higher MW had a higher positive charge density, which could bind more amount of negatively charged CpG ODNs.

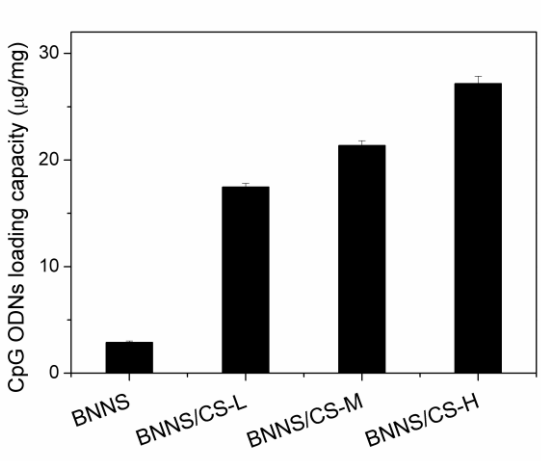

Figure 4.5 Loading capacity of CpG ODNs on BNNS and BNNS/CS complexes, denoted as μg CpG ODNs loaded on 1 mg BNNS. Data are presented as mean ± SD (n = 5).

The amounts of CS coated on the surface of BNNS were further determined by the TG analysis. The weight loss of the CS were estimated to be 8.5%, 9.1%, and 10.9% for CS-L, CS-M, and CS-H， respectively (Figure 4.6). Therefore, the ratio of CS on the BNNS surface and the loading capacity of CpG ODNs were similar for all of the three kinds of CS. This suggests that the CS/BNNS coverage ratio is not involved in the loading capacity of CpG ODNs. For this kind of electrostatic nanocomplexes, stability is critical for their

applications and has to be investigated. The stability of the BNNS/CS/CpG ODNs complexes is further studied by incubating the complexes under conditions that correspond to the physiological environment in the TLR 9-localized endolysosome. After 48 h, almost no release of CpG ODNs from the BNNS/CS complexes could be observed. This suggests that the BNNS/CS/CpG ODNs complexes are very stable and CpG ODNs could not be easily released from the BNNS/CS complexes because of the stronger binding of the CpG ODNs to BNNS/CS complexes.

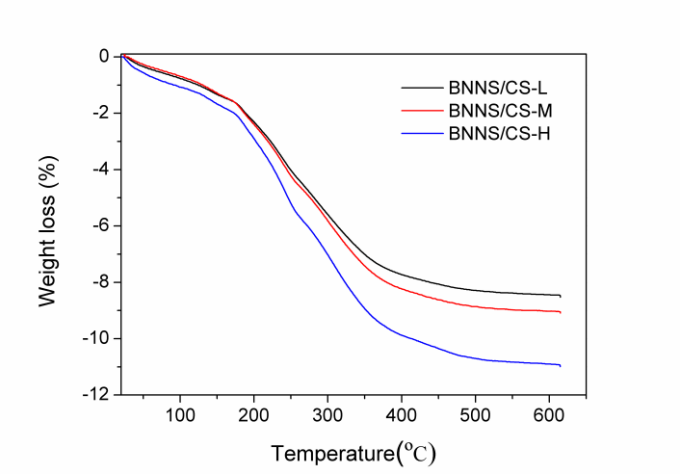

Figure 4.6 Thermogravimetric analysis curves of BNNS coated with CS.

Generally accepted that intracellular drug delivery significantly influences the efficiency of a drug delivery system.[14] After endocytosis, CpG ODNs in the endosome or lysosome can activate the TLR 9. This initiates the induction of multiple cytokines and chemokines, further modulates the immune response. Enhancement of cellular uptake of CpG ODNs is, therefore, vital for a better immune responses. To study the cellular uptake efficiency of CpG ODNs using BNNS/CS complexes as carriers, FITC-labeled CpG ODNs were loaded on BNNS and BNNS/CS respectively to form BNNS/CpG ODNs and BNNS/CS/CpG ODNs complexes. Then the complexes were incubated with PBMCs for 24 h and then investigated by CLSM observation. Green fluorescence from the BNNS/CpG ODNs and BNNS/CS/CpG ODNs were observed in the cells (Figure 4.7a). This implies that CpG ODNs were internalized into the cells after a 24 h incubation. Furthermore, at the same incubated condition, green fluorescence from the cells incubated with BNNS/CS/CpG ODNs complexes was much stronger than that in cells incubated with BNNS/CpG ODNs complexes. This indicates that more amount of CpG ODNs were internalized into the PBMCs when using BNNS/CS complexes as carriers. However, no fluorescence could be observed from the cells incubated with

free CpG ODNs, suggesting that lower cell uptake of free CpG ODNs, which made it difficult to observe the green fluorescence. Therefore, the BNNS/CS complexes seem to significantly enhance the efficiency of cellular uptake of CpG ODNs and are thought to facilitate the interaction of CpG ODNs with TLR 9. For CpG ODNs delivery, CpG ODNs should be delivered into endolysosomes where the TLR 9 localizes in.

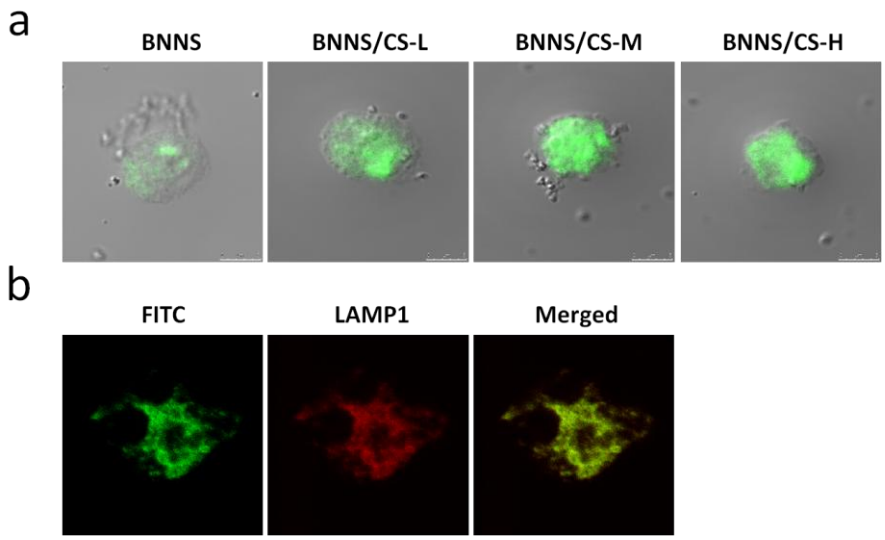

Figure 4.7 Cellular uptake and intracellular localization of the CpG ODNs. (a) Cellular uptake of CpG ODNs delivered by BNNS and BNNS coated with CS-L, CS-M and CS-H. (b) Intracellular Localization of CpG ODNs loaded on BNNS/CS complexes. CpG ODNs were labeled with FITC (Green). Cells were fixed, stained intracellularly with LAMP-1 antibodies (Red) and imaged by confocal microscopy.

We investigated the intracellular localization of CpG ODNs using BNNS/CS complexes as carriers. The lysosome-associated membrane protein-1 was chosen to identify the late endosomes endosomal vesicles in 293XL-hTLR 9 cells. Using confocal microscopy, we observed that CpG ODNs loaded on BNNS/CS complexes were localized in LAMP-1-positive late endosome (Figure 4.7b). Therefore, CpG ODNs were localized in late endosome after delivered into immune cells, and are thought to trigger several cell signaling pathways such as the NFκB, further result in the induction of proinflammatory cytokines. These results suggest that CS-coated BNNS are efficient carrier for the intracellular delivery of CpG ODNs.

4.3.4 Cytokine induction by BNNS/CS/CpG ODNs complexes

Figure 4.8 shows the cytokines induction in PBMCs stimulated by CpG ODNs delivered by BNNS and BNNS coated by CS with different MW. As expected, BNNS/CS/CpG ODNs complexes induced much

higher amount of IL-6 and TNF-α than that of CpG ODNs loaded directly on BNNS. This was mainly due to the the higher loading capacity and the enhanced cellular uptake of CpG ODNs using BNNS/CS complexes as carrier. In our previous work, when we used a BNNS-binding peptide as a linker molecule for CpG ODNs delivery, which improved the loading capacity of CpG ODNs on BNNS, the cytokines production were also significantly enhanced.[45] Furthermore, though CS itself is frequently reported as a polymeric carrier in many drug and gene delivery systems, in our study, BNNS/CS/CpG ODNs complexes induced about 2 times higher amount of cytokines than that of CS/CpG ODNs, because of the improved cellular uptake of CpG ODNs. Although the commercial transfection agents, Lipofectamine™ 2000, are reported to be with high transfection efficiency, here, in our study, BNNS/CS/CpG ODNs complexes induced higher amount of the cytokine than that of Lipofectamine-CpG ODNs complexes. Therefore, BNNS/CS/CpG ODNs complexes exhibited much better effect in cytokines production. Although maximum capacity for loading CpG ODNs increased with the increase in the MW of CS, BNNS coated with CS of low MW had the highest IL-6 and TNF-α productions, and both of the cytokines production decreased when the MW of CS increased. These results suggest that the MW of the CS coated on BNNS is a critical factor for cytokines induction by CpG ODNs. Surprisingly, different from PEI-functionalized BNNS, CpG ODNs loaded on BNNS/CS could not induce IFN-α production from PBMCs (Figure 4.8c). However, the mechanism remains unclear and further investigation is under way. To further investigate the cause of lower cytokines induction by CpG ODNs loaded onto BNNS coated with CS of higher MW, we analyzed the cellular uptake of FITC-labeled CpG ODNs loaded onto BNNS coated with CS of three kinds of MW. It was found that the cellular uptake of CpG ODNs loaded onto BNNS was not significantly affected by the MW of CS, all of them showed good cellular uptake behavior (Figure 4.7a). This suggests that the difference in cellular uptake is not the reason for the lower cytokines induction in BNNS coated with CS of high MW. Therefore, the MW of CS is thought to affect the cytokine induction. It has been reported that CS of low MW is more efficient for transfection than high MW CS.[46] In addition, MW of the CS is thought to play an important role in its complexation with CpG ODNs and thus affect the CpG ODNs-TLR 9 interaction. Ma et al reported that the binding strength and constant of CS with plasmid DNA were significantly influenced by MW of CS, which increased by almost an order of magnitude with an increase of the CS MW from 7 to 153 kDa.[47] Danielsen et al found that CS could compact plasmid DNA into various well-defined geometries, reflecting various CS-DNA interaction

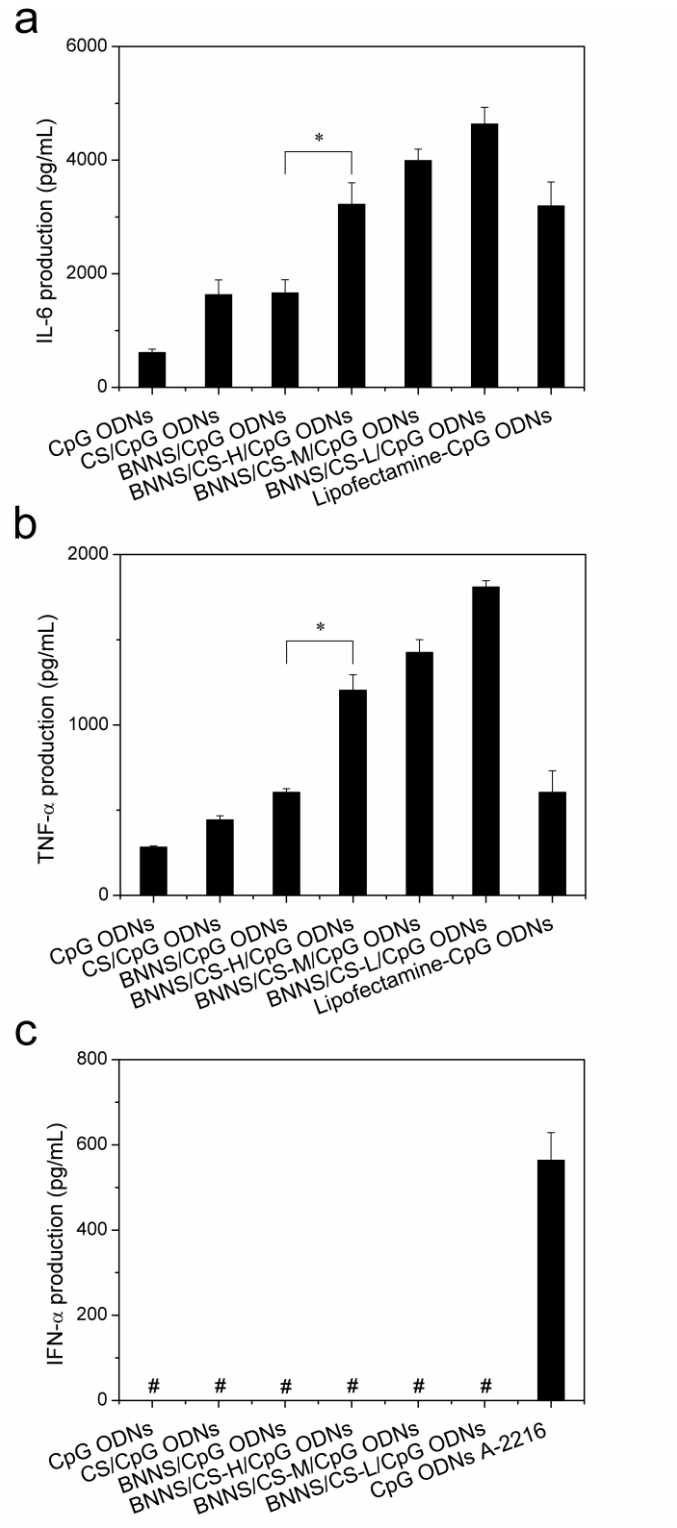

Figure 4.8 Cytokine induction in PBMCs stimulated by CpG ODNs loaded on BNNS and BNNS/CS complexes. Loaded BNNS or BNNS/CS complexes (50 μg/mL). (a) IL-6 production. (b) TNF-α production. (c) IFN-α production. Lipofectamine™ 2000 was used for comparison. Data are presented as mean ± SD (n = 3). The symbol # means not detectable (below detection limit). *$p < 0.05$.

strengths, which was strongly dependent on the MW of the CS.[48] We investigated the binding strength of CpG ODNs with CS of three different MW using the ethidium bromide (EB) displacement assay. The emission intensity of EB is known to be greatly enhanced when intercalatively binding to DNA.[49] Accordingly, adding a second DNA binding ligand would quench the EB emission through the replacement of the DNA-bound EB due to stronger binding affinity to DNA than EB.[50] As shown in Figure 4.9 , the emission of the DNA-bound EB was reduced upon the addition of CS. The competitive binding constants (*K*) were calculated to be ~ 10^5 M^{-1} and follow the order of CS-H > CS-M > CS-L (Table 4.1). This clearly indicates that CS of a higher MW has higher affinity and binds tightly to CpG ODNs. Therefore, the higher cytokines induction by BNNS coated with CS-L is thought to be caused by enhanced interaction of CpG ODNs with TLR 9, which attributed by the loose condensation of CpG ODNs. In contrast, CS-M and CS-H may complex CpG ODNs more tightly due to their higher positive charge density, making it difficult for CpG ODNs to interact with TLR 9.

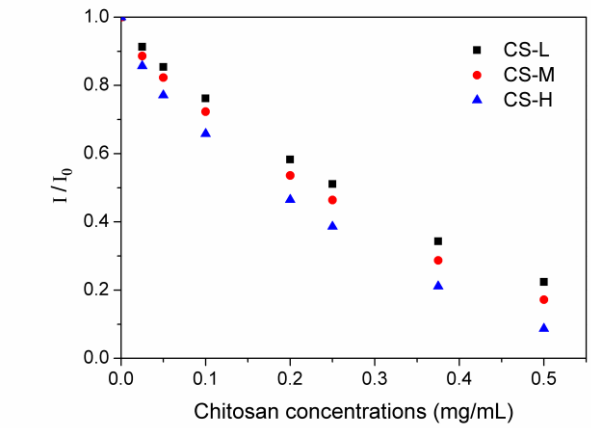

Figure 4.9 The plot of I/I_0 *vs.* [CS] for fluorescence quenching curves of CpG ODNs-EB by the CS of different MW. [CS], the concentrations of the chitosan. I_0, fluorescence intensity in the absence of CS, *I*, fluorescence intensity in the presence of CS.

Table 4.1 Competitive binding constants of chitosans to CpG ODNs calculated from the fluorescence quenching.

Chitosan	CS-L	CS-M	CS-H
K (M^{-1})	3.3×10^5	4.8×10^5	7.2×10^5

4.3.5 Suppressive effect of CS on IFN-α induction

In chapter 3, when we used PEI-functionalized BNNS as carrier for CpG ODNs, they induced the IFN-α from PBMCs. However, CpG ODNs loaded on CS-coated BNNS did not have this ability, though both of CS and PEI are cationic polymer that have similar properties. Recently, we found that CS inhibited the IFN-α production from PBMCs induced by class A CpG ODNs 2216, and this inhibitory effect showed a concentration-dependent manner (Figure 4.10). CS has also been reported to inhibit lipopolysaccharide -induced over-expression of IL-6 and TNF-α in RAW264.7 macrophage cells through blockade of MAPK and PI3K/Akt signaling pathways.[51] We hypothesized that some signaling pathways that leads to IFN-α secretion might be blocked by CS. However, the mechanism remains unclear and further investigation is under way.

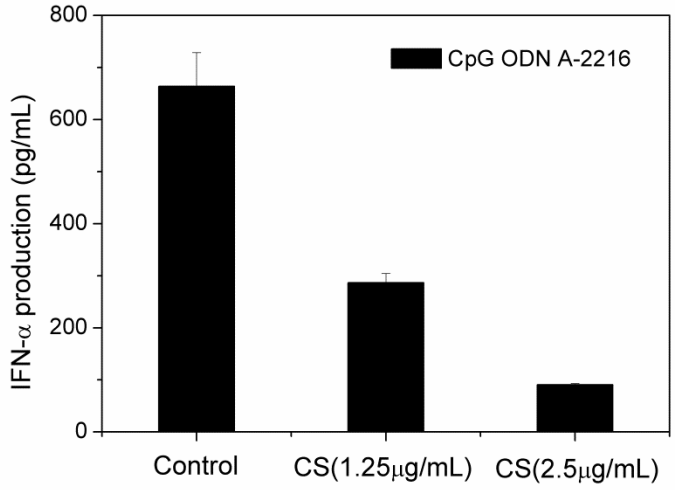

Figure 4.10 Suppressive effect of CS on IFN-α induction from PBMCs by class A CpG ODNs 2216. PBMCs were treated with CS for 4 h first, and then stimulated with class A CpG ODNs 2216. After 24 h, supernatants were collected and tested for IFN-α secretion by ELISA. Data are presented as mean ± SD (n = 3).

4.4 Conclusion

In this chapter, we prepared the CS-coated BNNS as carrier for the class B CpG ODNs delivery. CS coating shifted the surface zeta potential of BNNS from negative to positive in PBS. The BNNS/CS complexes exhibited a good dispersity and stability in aqueous solution due to the CS coating. Compared to

CpG ODNs directly loaded on BNNS, BNNS/CS complexes greatly improved the loading capacity and cellular uptake efficiency of CpG ODNs due to the their positive charge. The loading capacity of the CpG ODNs depended on the molecular weight (MW) of CS, which affected the positive charge density on the surface of BNNS. CpG ODNs loaded on BNNS/CS complexes were localized in LAMP-1-positive late endosome and significantly enhanced the IL-6 and TNF-α productions from PBMCs compared to that of CS/CpG ODNs complexes and CpG ODNs directly loaded on BNNS, even higher than that of using Lipofectamine™ 2000 as carrier. This was thought to be duo to a higher loading capacity and enhanced cellular uptake of CpG ODNs. Furthermore, MW of the CS used for BNNS coating affected the cytokines induction through varying the strength of the condensation of the CpG ODNs. Higher cytokines production was observed for CpG ODNs loaded on BNNS coated with CS of lower MW, though it showed the lowest loading capacity. We also found that CS had a suppressive effect on TLR 9 mediated IFN-α induction. However, the mechanism remains unknown. We anticipate that these findings will open a new avenue for the functionalization of BNNS as carrier in the delivery of nucleic acid therapies, such as CpG ODNs and small interfering RNA.

4.5 References

1. Klinman DM. Immunotherapeutic uses of CpG oligodeoxynucleotides. *Nat. Rev. Immunol.* 2004;4(4):248-257.
2. Krieg AM, Yi AK, Matson S, et al. CpG motifs in bacterial DNA trigger direct B-cell activation. *Nature.* 1995;374(6522):546-549.
3. Vollmer J, Krieg AM. Immunotherapeutic applications of CpG oligodeoxynucleotide TLR9 agonists. *Adv. Drug Delivery. Rev.* 2009;61(3):195-204.
4. Hemmi H, Takeuchi O, Kawai T, et al. A Toll-like receptor recognizes bacterial DNA. *Nature.* 2000;408(6813):740-745.
5. Wagner H. Bacterial CpG DNA activates immune cells to signal infectious danger. *Adv. Immunol.* 1999;73:329-368.
6. Bauer S, Kirschning CJ, Häcker H, et al. Human TLR9 confers responsiveness to bacterial DNA via species-specific CpG motif recognition. *Proc. Natl. Acad. Sci. U. S. A.* 2001;98(16):9237-9242.
7. Klinman DM, Yi AK, Beaucage SL, Conover J, Krieg AM. CpG motifs present in bacterial DNA rapidly induce lymphocytes to secrete interleukin 6, interleukin 12, and interferon gamma. *Proc. Natl. Acad. Sci. U. S. A.* 1996;93(7):2879-2883.
8. Akira S, Uematsu S, Takeuchi O. Pathogen recognition and innate immunity. *Cell.* 2006;124(4):783-801.
9. Chen HC, Sun B, Tran KK, Shen H. Effects of particle size on toll-like receptor 9-mediated cytokine profiles. *Biomaterials.* 2011;32(6):1731-1737.
10. Klinman DM, Klaschik S, Sato T, Tross D. CpG oligonucleotides as adjuvants for vaccines targeting infectious diseases. *Adv. Drug Delivery. Rev.* 2009;61(3):248-255.
11. Fonseca DE, Kline JN. Use of CpG oligonucleotides in treatment of asthma and allergic disease. *Adv. Drug Delivery. Rev.* 2009;61(3):256-262.
12. Murad YM, Clay TM. CpG Oligodeoxynudeofides as TLR9 Agonists Therapeutic Applications in Cancer. *BioDrugs.* 2009;23(6):361-375.
13. Krieg AM. Therapeutic potential of Toll-like receptor 9 activation. *Nat. Rev. Drug Discov.*

2006;5(6):471-484.

14. Mutwiri GK, Nichani AK, Babiuk S, Babiuk LA. Strategies for enhancing the immunostimulatory effects of CpG oligodeoxynucleotides. *J. Control. Release.* 2004;97(1):1-17.

15. Kurreck J. Antisense technologies - Improvement through novel chemical modifications. *Eur. J. Biochem.* 2003;270(8):1628-1644.

16. Agrawal S, Zhao QY. Antisense therapeutics. *Curr. Opin. Chem. Biol.* 1998;2(4):519-528.

17. Sheehan JP, Lan HC. Phosphorothioate oligonucleotides inhibit the intrinsic tenase complex. *Blood.* 1998;92(5):1617-1625.

18. Heikenwalder M, Polymenidou M, Junt T, et al. Lymphoid follicle destruction and immunosuppression after repeated CpG oligodeoxynucleotide administration. *Nat. Med.* 2004;10(2):187-192.

19. Zhu Y, Meng W, Li X, Gao H, Hanagata N. Design of mesoporous silica/cytosine−phosphodiester−guanine oligodeoxynucleotide complexes to enhance delivery efficiency. *J. Phys. Chem. C.* 2010;115(2):447-452.

20. Wilson KD, de Jong SD, Tam YK. Lipid-based delivery of CpG oligonucleotides enhances immunotherapeutic efficacy. *Adv. Drug Delivery. Rev.* 2009;61(3):233-242.

21. Bianco A, Hoebeke J, Godefroy S, et al. Cationic carbon nanotubes bind to CpG oligodeoxynucleotides and enhance their immunostimulatory properties. *J. Am. Chem. Soc.* 2004;127(1):58-59.

22. Rattanakiat S, Nishikawa M, Funabashi H, Luo D, Takakura Y. The assembly of a short linear natural cytosine-phosphate-guanine DNA into dendritic structures and its effect on immunostimulatory activity. *Biomaterials.* 2009;30(29):5701-5706.

23. Standley SM, Mende I, Goh SL, et al. Incorporation of CpG oligonucleotide ligand into protein-loaded particle vaccines promotes antigen-specific CD8 T-cell immunity. *Bioconjug. Chem.* 2006;18(1):77-83.

24. Chopra NG, Luyken RJ, Cherrey K, et al. Boron nitride nanotubes. *Science.* 1995;269(5226):966-967.

25. Zhi CY, Bando Y, Tang CC, Xie RG, Sekiguchi T, Golberg D. Perfectly dissolved boron nitride

nanotubes due to polymer wrapping. *J. Am. Chem. Soc.* 2005;127(46):15996-15997.

26. Gao ZH, Zhi CY, Bando Y, Golberg D, Serizawa T. Isolation of individual boron nitride nanotubes via peptide wrapping. *J. Am. Chem. Soc.* 2010;132(14):4976-4977.

27. Golberg D, Bando Y, Tang CC, Zhi CY. Boron nitride nanotubes. *Adv. Mater.* 2007;19(18):2413-2432.

28. Chen X, Wu P, Rousseas M, et al. Boron nitride nanotubes are noncytotoxic and can be functionalized for interaction with proteins and cells. *J. Am. Chem. Soc.* 2009;131(3):890-891.

29. Jonsson E, Simonsen L, Karlsson M, Larsson R. The hollow fiber model: A new method for in vivo-evaluation of antitumor effect, toxicity and pharmacokinetics of new anticancer drugs. *Ann. Oncol.* 1998;9(S2):44-44.

30. Ciofani G, Raffa V, Menciassi A, Cuschieri A. Boron nitride nanotubes: An innovative tool for nanomedicine. *Nano Today.* 2009;4(1):8-10.

31. Zhi CY, Meng WJ, Yamazaki T, et al. BN nanospheres as CpG ODN carriers for activation of toll-like receptor 9. *J. Mater. Chem.* 2011;21(14):5219-5222.

32. Agrawal P, Strijkers GJ, Nicolay K. Chitosan-based systems for molecular imaging. *Adv. Drug Delivery. Rev.* 2010;62(1):42-58.

33. Amidi M, Mastrobattista E, Jiskoot W, Hennink WE. Chitosan-based delivery systems for protein therapeutics and antigens. *Adv. Drug Delivery. Rev.* 2010;62(1):59-82.

34. Bernkop-Schnürch A, Dünnhaupt S. Chitosan-based drug delivery systems. *Eur. J. Pharm. Biopharm.* 2012;81(3):463-469.

35. Wu KY, Wu M, Fu ML, et al. A novel chitosan CpG nanoparticle regulates cellular and humoral immunity of mice. *Biomed. Environ. Sci.* 2006;19(2):87-95.

36. Ravi Kumar MNV, Bakowsky U, Lehr CM. Preparation and characterization of cationic PLGA nanospheres as DNA carriers. *Biomaterials.* 2004;25(10):1771-1777.

37. Tang CC, Bando Y, Huang Y, Zhi CY, Golberg D. Synthetic routes and formation mechanisms of spherical boron nitride nanoparticles. *Adv. Funct. Mater.* 2008;18(22):3653-3661.

38. Yu RZ, Geary RS, Leeds JM, et al. Pharmacokinetics and tissue disposition in monkeys of an antisense oligonucleotide inhibitor of Ha-ras encapsulated in stealth liposomes. *Pharm. Res.*

1999;16(8):1309-1315.

39. Meng WJ, Yamazaki T, Nishida Y, Hanagata N. Nuclease-resistant immunostimulatory phosphodiester CpG oligodeoxynucleotides as human Toll-like receptor 9 agonists. *BMC Biotechnol.* 2011;11:88.

40. Soares DCF, Ferreira TH, Ferreira CdA, Cardoso VN, de Sousa EMB. Boron nitride nanotubes radiolabeled with 99mTc: Preparation, physicochemical characterization, biodistribution study, and scintigraphic imaging in Swiss mice. *Int. J. Pharm.* 2012;423(2):489-495.

41. Yan LY, Poon YF, Chan-Park MB, Chen Y, Zhang Q. Individually dispersing single-walled carbon nanotubes with novel neutral pH water-soluble chitosan derivatives. *J. Phys. Chem. C.* 2008;112(20):7579-7587.

42. Ozarkar S, Jassal M, Agrawal AK. Improved dispersion of carbon nanotubes in chitosan. *Fibers and Polymers.* 2008;9(4):410-415.

43. Shvartzman-Cohen R, Levi-Kalisman Y, Nativ-Roth E, Yerushalmi-Rozen R. Generic approach for dispersing single-walled carbon nanotubes: The strength of a weak interaction. *Langmuir.* 2004;20(15):6085-6088.

44. Zhu YF, Ikoma T, Hanagata N, Kaskel S. Rattle-type Fe(3)O(4)@SiO(2) hollow mesoporous spheres as carriers for drug delivery. *Small.* 2010;6(3):471-478.

45. Zhang H, Yamazaki T, Zhi C, Hanagata N. Identification of a boron nitride nanosphere-binding peptide for the intracellular delivery of CpG oligodeoxynucleotides. *Nanoscale.* 2012;4(20):6343-6350.

46. Strand SP, Lelu S, Reitan NK, Davies CD, Artursson P, Varum KM. Molecular design of chitosan gene delivery systems with an optimized balance between polyplex stability and polyplex unpacking. *Biomaterials.* 2010;31(5):975-987.

47. Ma PL, Lavertu M, Winnik FM, Buschmann MD. New Insights into Chitosan-DNA Interactions Using Isothermal Titration Microcalorimetry. *Biomacromolecules.* 2009;10(6):1490-1499.

48. Danielsen S, Vårum KM, Stokke BT. Structural Analysis of Chitosan Mediated DNA Condensation by AFM: Influence of Chitosan Molecular Parameters. *Biomacromolecules.* 2004;5(3):928-936.

49. Karidi K, Garoufis A, Tsipis A, Hadjiliadis N, den Dulk H, Reedijk J. Synthesis, characterization, in

vitro antitumor activity, DNA-binding properties and electronic structure (DFT) of the new complex cis-(Cl,Cl) Ru(II)Cl2(NO+)(terpy) Cl. *Dalton Trans.* 2005(7):1176-1187.

50. Dhar S, Nethaji M, Chakravarty AR. Steric protection of a photosensitizer in a N,N-bis 2-(2-pyridyl)ethyl-2-phenylethylamine-copper(II) bowl that enhances red light-induced DNA cleavage activity. *Inorg. Chem.* 2005;44(24):8876-8883.

51. Ma P, Liu HT, Wei P, et al. Chitosan oligosaccharides inhibit LPS-induced over-expression of IL-6 and TNF-alpha in RAW264.7 macrophage cells through blockade of mitogen-activated protein kinase (MAPK) and PI3K/Akt signaling pathways. *Carbohyd Polym.* 2011;84(4):1391-1398.

Chapter 5 Summary

Bacterial and viral DNA containing unmethylated CpG dinucleotides stimulate the mammalian innate immune system. This process is mediated by the activation of TLR 9, a member of Toll-like receptor family. Synthetic ODNs containing unmethylated CpG motifs are like those found in bacterial DNA and possess similar immunostimulatory effects. The activation of TLR 9 initiates an immunostimulatory cascade that induce the maturation, differentiation, and proliferation of multiple immune cells including B and T lymphocytes, NK cells, and monocytes/macrophage. This further triggers cell signaling pathways including MAPKs and NFκB, subsequently results in the induction of multiple proinflammatory cytokines and chemokines that modulating the cellular inflammatory response. As such, CpG ODNs have potential for treatment of infectious diseases, allergies, and cancers. However, the immunostimulatory effects are often limited by the poor stability and cellular uptake of natural CpG ODNs. Therefore, there has been great interest in developing approaches to optimize the stimulatory activity of CpG ODNs. Chemical modification of CpG ODNs backbone is an effective technique to protect against degradation by nucleases. However, there is concern over several severe side effects. Since CpG ODNs are negatively charged, it is difficult for them to bind to the negatively charged cell surface. This electrostatic repulsion is believed to limit the efficiency of CpG ODNs uptake and their immunostimulatory effect. Evidence is accumulating indicates that both the stability and cellular uptake of natural CpG ODNs can be enhanced by using nanoparticles as carriers. Therefore, delivery of unmodified CpG ODNs using nanoparticles maybe an good approach to improve their immunostimulatory effect, and make it possible to use naturally occurring CpG ODNs in clinical applications.

In this regard, this dissertation focuses on development of novel delivery systems for natural CpG ODNs by using BNNS to enhance the immunostimulatory effect of CpG ODNs.

In chapter 1, a general introduction of this study was given, including the mechanism of human immune system, the interaction between TLR 9 and CpG ODNs, therapeutic potential of CpG ODNs, delivery systems for CpG ODNs, and the BNNS.

In chapter 2, a novel CpG ODNs delivery system based on a BNNS-binding peptide has been developed.

Firstly, a 12-amino acid peptide, designated as BP7, which had specific affinity for BNNS, was indentified using phage display technique. BNNS that bound BP7 (BNNS/BP7) were taken up into cells and showed no cytotoxicity. Using BP7 as a linker, the loading capacity of CpG ODNs on BNNS increased 5-fold compared to the direct binding of CpG ODNs to BNNS. Then we used the BP7–CpG ODNs conjugates–loaded BNNS to stimulate the PBMCs and measured the cytokine productions. BP7–CpG ODNs conjugates–loaded BNNS had a greater capacity to induce IL-6 and TNF-α production from PBMCs than that of CpG ODNs directly loaded on BNNS. However, it could not induce IFN-α from PBMCs. The higher amount of cytokine induction from BP7–CpG ODNs conjugates–loaded BNNS may be attributed to a higher loading capacity and stronger binding to BNNS with the linker BP7. Thus, the BNNS-binding peptide provide a promising strategy for enhancing the immunostimulatory effect of CpG ODNs.

In chapter 3, another CpG ODNs delivery system using cationic polymer-functionalized BNNS has been developed. PEI was coated on the surface of BNNS to achieve a positive surface charge, which facilitated the loading of negatively-charged CpG ODNs onto the BNNS. BNNS/PEI complexes greatly improved the cellular uptake efficiency of CpG ODNs. This further resulted in a enhanced IL-6 and TNF-α production from PBMCs compared to that of CpG ODNs directly loaded on BNNS. Most importantly, B class CpG ODNs loaded on BNNS/PEI complexes induced IFN-α, while neither free CpG ODNs nor CpG ODNs loaded directly on BNNS had this potential. It is thought that when the class B CpG ODNs were loaded onto the positively charged BNNS-PEI complexes, they formed the higher-order multimeric structure similar to class A CpG ODNs, and acquired the ability to induce the IFN-α.

In chapter 4, chitosan coated BNNS were used as carrier for the delivery of CpG ODNs. BNNS/CS complexes had positive zeta potential and exhibited a better dispersity and stability in aqueous solution than BNNS due to the CS coating. The BNNS/CS complexes greatly improved the loading capacity and cellular uptake efficiency of CpG ODNs due to their positive surface charge. The loading capacity of the CpG ODNs depend on the molecular weight (MW) of CS, which affected the positive charge density on the surface of BNNS. CpG ODNs loaded on BNNS/CS complexes significantly enhanced the IL-6 and TNF-α productions from PBMCs compared to that of CS/CpG ODNs complexes and CpG ODNs directly loaded on BNNS. We also found that molecular weight of the CS used for BNNS coating affected the cytokines induction through varying the strength of the condensation of the CpG ODNs. Surprisingly, different from PEI-functionalized

BNNS, CpG ODNs loaded on BNNS/CS could not induce IFN-α production from PBMCs. We also found that CS had a suppressive effect on TLR 9 mediated IFN-α induction. However, the mechanism remains unclear and further investigation is under way.

In conclusion, we have successfully developed several delivery systems for CpG ODNs based on BNNS, These delivery systems improved the loading capacity and cellular uptake of CpG ODNs, and are proved to be effective in enhancing the immunostimulatory effect of CpG ODNs. We also found that CS had a suppressive effect on TLR 9 mediated IFN-α induction. However, the mechanism remains unknown. Future work will be focused on the mechanisms of this effect and its possible therapeutic applications in immunological disorder diseases.

Publications

1. Papers published in journals

1 Zhang H, Yamazaki T, Zhi C, Hanagata N. Identification of a boron nitride nanosphere-binding peptide for the intracellular delivery of CpG oligodeoxynucleotides. *Nanoscale* **4**, 6343-6350 (2012).

2 Zhang H, Chen S, Zhi C, Yamazaki T, Hanagata N. Chitosan-coated boron nitride nanospheres enhance CpG oligodeoxynucleotide delivery and cytokine induction. *International Journal of Nanomedicine*, **8,** 1783-1793 (2013).

3 Chen S, Zhang H, Chinnathambi S, Hanagata N. Synthesis of novel chitosan-silica/CpG oligodeoxynucleotide nanohybrids with enhanced delivery efficiency. *Materials Science and Engineering C*. **33,** 3382–3388 (2013).

2. Presentations in conferences

1 Zhang H, Yamazaki T, Hanagata N. Screening of peptides selectively binding to boron nitride nanoparticles. 北海道大学生命科学院融合生命科学若手シンポジウム （平成 23 年 3 月，札幌）

2 Zhang H, Yamazaki T, Zhi C, Hanagata N. Identification of boron nitride nanospheres binding peptides. The Symposium on Micro/Nano Aspects of Biomaterials （平成 23 年 7 月，京都）

3 Zhang H, Yamazaki T, Zhi C, Hanagata N. Peptide with binding specificity for boron nitride nanospheres. The 9th World Biomaterials Congress (WBC2012) （平成 24 年 6 月，成都、中国 ）

4 Zhang H, Yamazaki T, Zhi C, Hanagata N. Identification of a specific binding peptide to boron nitride nanospheres for delivery of CpG oligodeoxynucleotides. 第 6 回ナノバイオメディカル学会大（平成 24 年 7 月，つくば）

Acknowledgements

I would like to express my gratitude to all those who helped me during my Ph.D. study.

My deepest gratitude goes first and foremost to my supervisor Professor Nobutaka Hanagata, for his constant encouragement, support, and scientific guidance during my Ph.D. study. He is a gentle teacher with profound knowledge and rigorous academic attitude. The successful accomplishment of the present thesis is mainly attributed to his guidance and support.

I would like to express my heartfelt gratitude to my supervisor, Associate Professor Tomohiko Yamazaki, for his constant support through my Ph.D. study. He gave me a lot of detailed advices during my study.

I am also grateful to Ms Akemi Hoshikawa, for her kindness in helping me solving all problems in my work and daily life.

I would like to express my gratitude to Dr. Chunyi Zhi for supplying the boron nitride nanospheres, as well as the support during my study.

I am grateful to Ms. Yuuki Nishida and Ms. Wei Wang for their guides in the phage display experiments at the very beginning.

I want to thank all the people in the Biosystem and Biomolecule Control Group for their constant help. Dr. Yoshihisa Kaizuka, Dr. Song Chen, Dr Wenjun Meng, Dr. Ling Zhang, Dr. Suwarti, Ms. Fei Zhuang, Mr. Chinnathambi Shanmugavel, Ms. Gabriela Furlan, Ms. Satomi Magae, Ms. Satomi Kohara, Ms. Bheema Deepthi, thank you all.

I would like to thank Dr. Takashi Minowa, Dr. Jie Li, Dr. Xianglan Li, Ms. Hiromi Morita, Ms. Shoko Kajiwara, Ms. Svetlana Chechetka from Nano Invitation Center of National Institute for Materials Science, for their support during my research.

In particular, thanks to my family for everything they have done for me, especially during my 23 years as a student. Their great love and continuous support are the source of power for me and will be appreciated forever.